The eye as a window to the brain

Balk, L.J.

2014

document version
Publisher's PDF, also known as Version of record

THE EYE AS A WINDOW TO THE BRAIN

Optical coherence tomography in MS

Lisanne Balk

The studies described in this dissertation were carried out at the department of Neurology, the Department of Ophthalmology and the department of Radiology of the VU University Medical Centre (VUmc) Amsterdam, the Netherlands. MS research at the VUmc is organised within the MS Centre Amsterdam. The author of this dissertation was financially supported by the Dutch MS Research foundation (grant number 09-358d).

Financial support for the printing of this dissertation was kindly provided by: the Dutch MS research foundation, Heidelberg Engineering, TEVA, Biogen Idec, Bayer B.V. and Novartis Pharma B.V..

Printing: Ridderprint BV, Ridderkerk, the Netherlands
Lay-out: Nikki Vermeulen, Ridderprint BV, Ridderkerk, the Netherlands
Cover: Nikki Vermeulen, Ridderprint BV, Ridderkerk, the Netherlands

ISBN: 978-90-5335-917-4

VRIJE UNIVERSITEIT

THE EYE AS A WINDOW TO THE BRAIN

Optical coherence tomography in MS

ACADEMISCH PROEFSCHRIFT

ter verkrijging van de graad Doctor aan
de Vrije Universiteit Amsterdam,
op gezag van de rector magnificus
prof.dr. F.A. van der Duyn Schouten,
in het openbaar te verdedigen
ten overstaan van de promotiecommissie
van de Faculteit der Geneeskunde
op vrijdag 24 oktober 2014 om 11.45 uur
in de aula van de universiteit,
De Boelelaan 1105

door

Lisanne Johanna Balk

geboren te Heemskerk

Promotoren: prof.dr. B.M.J. Uitdehaag
prof.dr. C.H. Polman

Copromotor: dr. A. Petzold

CONTENTS

Chapter 1

General introduction

Parts of the introduction have also been published in a recent review on OCT in MS.

LJ Balk, A Petzold

Current and future potential of retinal OCT in Multiple Sclerosis
with and without optic neuritis

Neurodegener Dis Manag. **2014;4:165-76**

INTRODUCTION

More than a century ago, one of the first neurologists who made extensive use of the just invented ophthalmoscope, John Hughlings Jackson (London, UK, 1835-1911), wrote; 'It is not too much to say that, without an extensive knowledge of ophthalmology, a methodological investigation of diseases of the nervous system is not merely difficult, but impossible'.[1] Precisely 140 years later, Steve Waxman (Yale, USA) predicted in a visionary Editorial that another invention just made, retinal optical coherence tomography (OCT) will finally permit to unravel the mechanisms of neuronal degeneration in vivo.[2] The fact inherent to both statements is that the eye can be perceived as 'a window to the brain'. The role of retinal OCT in investigating mechanisms of neurodegeneration in multiple sclerosis, is described and discussed in this thesis.

Multiple sclerosis

Multiple sclerosis (MS) is considered a neurodegenerative disorder, affecting more than 2 million people worldwide.[3] Until the turn of the century, MS was predominantly thought of as a mainly white matter disease, characterised by primarily inflammatory demyelination of the central nervous system (CNS). It was only through the work of several groups on post-mortem tissue, that the understanding of the pathogenesis of the disease fundamentally changed.[4] Besides the inflammatory part, neuroaxonal degeneration also plays an important role in the disease pathology.[5] The latter is the most important cause of irreversible disability in patients with MS.[6] To date, the exact aetiology of MS still remains unknown. Besides a certain genetic predisposition, multiple environmental factors have been suggested as influencing factors on the development of MS, such as birth country, previous infections, lack of sunlight, vitamin D deficiency or diet.[6]

The disease course in MS is very heterogeneous. A large proportion (about 80%) of patients experience a relapsing remitting (RR) onset of the disease (Figure 1), most often starting with an acute episode affecting one or more sites (clinically isolated syndrome, CIS). Females are more than twice as likely to have RRMS than men.[7] In time, around 50% of RR patients will enter the secondary progressive (SP) phase in which clinical relapses become less pronounced and slowly change into a gradual worsening of the disease. In around 10-15% of patients, the disease does not start with acute episodes of disability, but has a progressive onset (primary progressive MS, PPMS).[8] In both SP and PP MS, progression starts around the age of 40.[9] Compared with relapse-onset MS, people with PPMS are older at onset, show a larger degree of spinal cord atrophy and the incidence is similar in males and females.[8] The disease follows a relatively benign

course in 10% to 20% of patients. This benign form of MS was initially defined as having limited disability after at least 15 years of MS,[10] but other definitions have also been used. Although patients with benign MS experience relatively limited disability, they are not acquitted of disease progression in the future.[11,12] The clinical courses of all described disease types are shown in Figure 1.

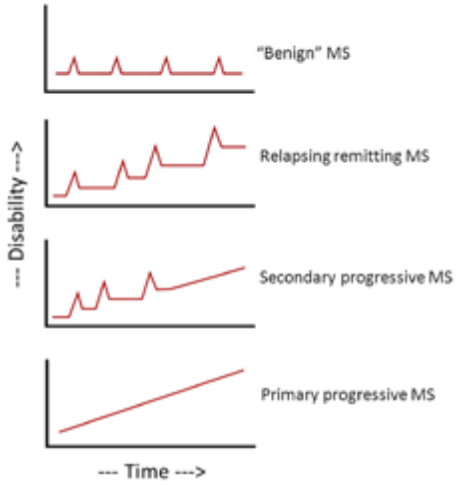

Figure 1. The clinical disease course differs between disease types. A benign MS course is characterised by limited disability, with complete recovery between relapses. Relapsing remitting (RR) MS is characterised by relapses, followed by full or partial recovery. RRMS can evolve into secondary progressive (SP) MS, in which clinical relapses become less pronounced and slowly change into gradually increasing disability. Patients with primary progressive (PP) MS experience a constant increase in disability over time, without clinical relapses.

Besides the disease course, the range of symptoms is also very heterogeneous. Symptoms can include involvement of motor, sensory, visual, and autonomic systems, dependent on the location of lesions in the CNS. Although the whole CNS is involved, the visual system is particularly often affected in MS. Approximately 20% of all MS patients present with an episode of optic neuritis (ON),[13] while in total, about 50% to 70% of patients will experience an episode of ON sooner or later in the disease course.[14] Symptoms of ON are unilateral loss of vision, developing over a period of a few days. This can include decreased contrast sensitivity, impaired color vision or visual field defects. An episode of ON typically starts to recover within 3 to 5 weeks after first complaints and usually, after several months visual acuity is largely or completely restored.[15]

Inflammation and neuroaxonal degeneration in MS

Trapp and colleagues al discovered in 1998 that transected axons were an important characteristic of MS lesions and that the frequency of axonal transection was related to the degree of inflammation within lesions.[5] These findings, among others, changed the initial believe of the etiology of the disease from a mainly white matter, demyelinating disease, to a situation in which axonal degeneration was considered an important pathological feature.

The exact interaction between inflammation and neuroaxonal degeneration (comprising both neuronal and axonal damage) is not yet clear. Many people have performed research with the hypothesis in mind that chronic inflammation or demyelination leads to degeneration of the axons.[16-18] More recent reports however have also considered the concept that MS is a primarily neuroaxonal degenerative disease with secondary inflammatory demyelination.[19]

Independent of the precise cause of the degenerative process, it was shown to be extensive in acute MS lesions. In the early stages of MS this is however not always associated with permanent disability.[20] It is therefore suggested, with the use of functional MRI studies, that this relative sparing of physical and cognitive functioning in the early phases of RRMS is due to the plasticity of the CNS, as this mechanism would compensate for the neuroaxonal degeneration.[21-25] When the compensatory ability of the human CNS can no longer compensate the accumulating damage, the patient will transit from a relapsing disease course, to a more progressive phase (SPMS).[26]

Assessment of neuroaxonal degeneration using OCT

Because neuroaxonal loss is not reversible and has a major impact on physical and cognitive functioning in MS patients, a validated monitoring tool is needed. Neuroaxonal degeneration remains difficult to assess. Although brain volumes, acquired with magnetic resonance imaging (MRI), can be used to determine axonal loss, MRI findings such as these may reflect something different than axonal loss, since brain atrophy according to MRI can also be caused by loss of non-neuronal cells.[27,28] This is further complicated by the methodological impasse to distinguish true atrophy (due to neuroaxonal loss), from pseudo-atrophy caused by resolution of inflammatory related oedema from active lesions.[27] Besides, a clear and well described dissociation exists between common neuro-radiological markers for inflammation, measured with MRI, and the degree of clinical disability in patients. This lack of agreement between the two is also referred to as "the clinical radiological paradox".[29]

Importantly, a relatively new method to quantify neuroaxonal degeneration in vivo, is retinal optical coherence tomography (OCT). Retinal OCT, first described in 1991 by Huang et al,[30] is a non-invasive technique that can generate a cross sectional image

of the retina by scanning the retina with a beam of light with a broad spectrum. The interference patterns of the back-scattered light are used to generate high resolution cross sectional or three dimensional images. In 1999, Parisi et al were the first to describe thinning of the retinal nerve fibre layer (RNFL, a layer consisting of axons which eventually form the optic nerve after leaving the eye at the lamina cribrosa), in MS, using a time-domain (TD) OCT device.[31] About ten years later, the more precise and reliable spectral-domain (SD) OCT was introduced.[32] Both TD and SD-OCT are currently available, although SD-OCT has major advantages over TD-OCT regarding precision and reliability, and has therefore become the preferred method in most recent studies. Figure 2 shows two examples of currently available SD-OCT machines.

Figure 2. Examples of the two most frequently used, commercially available SD-OCT machines. The machine to the left is manufactured by Heidelberg engineering and was used in the studies described in this thesis because of superior accuracy compared with the machine on the right (Carl Zeiss meditec). Since discovery of the method in 1991, a total of 36 commercially available OCT systems have entered the market.

Retinal OCT has the advantage of imaging the only part of the human CNS where non-myelinated axons and neurons are visible.[33] In the field of MS, the most often used scans are the peripapillary ring scans (Figure 3A) and the macular volume scan (Figure 3B).

Although most previous studies using SD-OCT were restricted to the use of the peripapillary RNFL (pRNFL) and complete macular volume, newer OCT segmentation algorithms allow quantification of more individual retinal layers (see Figure 3, right side). These developments in new software enable new possibilities for assessing damage in the neuronal cells (in the ganglion cell layer), axons (in the RNFL), but also bipolar cells (inner nuclear layer) and rods and cones (outer nuclear layer). This extension of possibilities allows for investigating the cascade of neuroaxonal degeneration in MS.[34]

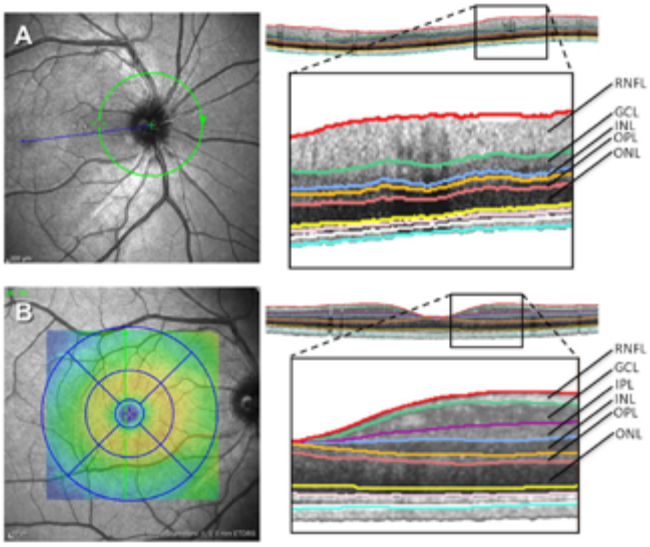

Figure 3. Example of scans and segmentation protocol for retinal OCT scans **(A)** Peripapillary ring scan of the right eye. **(B)** Macular volume scan (20 x 20 degrees field, 25 vertical Bscans) of the right eye. The coloured map represents a thickness map with a 1, 3 and 6 mm grid. On the right side, the segmented layers of the peripapillary ring scan (A) and macular volume scan (B) are depicted.
RNFL: retinal nerve fibre layer, GCL: ganglion cell layer, INL: inner nuclear layer, OPL: outer plexiform layer, ONL: outer nuclear layer, IPL: inner plexiform layer.

Key questions and outline of this thesis

The general aim of this thesis is to expand our understanding of neuroaxonal degeneration in longstanding MS by using OCT and to investigate the added value of OCT in management of the disease. As described above, neuroaxonal degeneration is a complex process, eventually leading to irreversible disability. An accurate measurement tool is therefore urgently needed. The retina is the only part of the human CNS where non-myelinated axons and neurons are visible, therewith offering a very promising structure to investigate the mechanisms underlying neuroaxonal degeneration in MS. The application of OCT in MS research as a biomarker for neuroaxonal degeneration is still relatively new, especially with the more recent use of SDOCT and new segmentation software. It is therefore of major importance that one knows how to produce scans of high quality in order to obtain reliable and reproducible data. The outline of this thesis is therefore divided in two main parts. The first part of this thesis (chapters 2 and 3) focuses on potential factors influencing the OCT measurements and essential quality control criteria that should be taken into account when using OCT.

The four key questions to be investigated in chapters 2 and 3 of this thesis are:

- What is the 'normal' physiological variation of retinal layer thickness?
- What physical factors may cause this physiological variation?
- Which technical and procedural aspects influence the accuracy of the OCT measurement?
- Could strict OCT quality control criteria increase scan quality and reliability?

These questions are addressed in the following chapters; *chapter 2.1* prospectively investigates the physiological variation of retinal layer thickness in healthy controls. Following up on this, *chapter 2.2* investigates whether the described physiological variation can be explained by hyperaemia, with the use of an algorithm which suppresses blood vessel artefacts. In *chapter 2.3*, the effect of oral hydration on OCT measurements was tested prospectively in an a small-scale randomised trial.

Next, *chapter 3.1* describes a simple sign by which OCT operators can identify an incorrect placement of the OCT measurement beam, which, if unrecognised, may lead to incorrect data at a magnitude far exceeding what is observed by physiological variation or neurodegeneration alone. Based on this and other published measurement artefacts, a comprehensive set of quality control criteria (OSCAR-IB criteria) was developed and validated. The developmental work is described in *chapter 3.2* and the international validation strategy in *chapter 3.3*.

The three main questions investigated in the second part of this thesis (chapter 4) are all focused on the clinical application of OCT in patients with longstanding MS:

- Can OCT distinguish between MS subtypes?
- Can OCT unravel the cascade of neuroaxonal degeneration in MS?
- To what extent does retinal layer atrophy reflect damage to the visual system and the global brain?

In more detail, *chapter 4.1* investigates the relationship between clinical heterogeneity and OCT. In *chapter 4.2*, a possible physiological barrier in the retina is described, which is suggested to prevent trans-synaptic spreading of neuroaxonal degeneration through the CNS. *Chapter 4.3* follows up on this by exploring the presence of retrograde and anterograde trans-synaptic degeneration in the visual system, and how damage of the visual system is associated with damage to the rest of the brain.

In the final section (*Chapter 5*), the results and methodological and clinical considerations of the previous chapters, as well as possible implications for future research are discussed.

REFERENCES

1. Jackson JH. Ophthalmology in its relation to general medicine. *BMJ* 1877;1:575-577.
2. Waxman SG, Black JA. Retinal involvement in multiple sclerosis. *Neurology* 2007;69:1562-3.
3. Milo R, Kahana E. Multiple sclerosis: geoepidemiology, genetics and the environment. *Autoimmun Rev* 2010;9:A387-A394.
4. Ferguson B, Matyszak MK, Esiri MM, Perry VH. Axonal damage in acute multiple sclerosis lesions. *Brain* 1997;120:393-9.
5. Trapp BD, Peterson J, Ransohoff RM, Rudick R, Mork S, Bo L. Axonal transection in the lesions of multiple sclerosis. *N Engl J Med* 1998;338:278-85.
6. Compston A, Coles A. Multiple sclerosis. *Lancet* 2008;372:1502-17.
7. Ebers GC. Environmental factors and multiple sclerosis. *Lancet Neurol* 2008;7:268-77.
8. Miller DH, Leary SM. Primary-progressive multiple sclerosis. *Lancet Neurol* 2007;6:903-12.
9. Confavreux C, Vukusic S. The clinical epidemiology of multiple sclerosis. *Neuroimaging Clin N Am* 2008;18:589-x.
10. Lublin FD, Reingold SC. Defining the clinical course of multiple sclerosis: results of an international survey. National Multiple Sclerosis Society (USA) Advisory Committee on Clinical Trials of New Agents in Multiple Sclerosis. *Neurology* 1996;46:907-11.
11. Hawkins SA, McDonnell GV. Benign multiple sclerosis? Clinical course, long term follow up, and assessment of prognostic factors. *J Neurol Neurosurg Psychiatry* 1999;67:148-52.
12. Sayao AL, Devonshire V, Tremlett H. Longitudinal follow-up of "benign" multiple sclerosis at 20 years. *Neurology* 2007;68:496-500.
13. Miller D, Barkhof F, Montalban X, Thompson A, Filippi M. Clinically isolated syndromes suggestive of multiple sclerosis, part I: natural history, pathogenesis, diagnosis, and prognosis. *Lancet Neurol* 2005;4:281-8.
14. Balcer LJ. Clinical practice. Optic neuritis. *N Engl J Med* 2006;354:1273-80.
15. Hickman SJ, Dalton CM, Miller DH, Plant GT. Management of acute optic neuritis. *Lancet* 2002;360:1953-62.
16. Bjartmar C, Kidd G, Mork S, Rudick R, Trapp BD. Neurological disability correlates with spinal cord axonal loss and reduced N-acetyl aspartate in chronic multiple sclerosis patients. *Ann Neurol* 2000;48:893-901.
17. Lovas G, Szilagyi N, Majtenyi K, Palkovits M, Komoly S. Axonal changes in chronic demyelinated cervical spinal cord plaques. *Brain* 2000;123:308-17.
18. Dutta R, McDonough J, Yin X et al. Mitochondrial dysfunction as a cause of axonal degeneration in multiple sclerosis patients. *Ann Neurol* 2006;59:478-89.
19. Trapp BD, Nave KA. Multiple sclerosis: an immune or neurodegenerative disorder? *Annu Rev Neurosci* 2008;31:247-69.
20. Confavreux C, Vukusic S. Natural history of multiple sclerosis: a unifying concept. *Brain* 2006;129:60616.
21. Reddy H, Narayanan S, Arnoutelis R et al. Evidence for adaptive functional changes in the cerebral cortex with axonal injury from multiple sclerosis. *Brain* 2000;123:2314-20.
22. Pantano P, Iannetti GD, Caramia F et al. Cortical motor reorganization after a single clinical attack of multiple sclerosis. *Brain* 2002;125:1607-15.
23. Parry AM, Scott RB, Palace J, Smith S, Matthews PM. Potentially adaptive functional changes in cognitive processing for patients with multiple sclerosis and their acute modulation by rivastigmine. *Brain* 2003;126:2750-60.
24. Rocca MA, Mezzapesa DM, Falini A et al. Evidence for axonal pathology and adaptive cortical reorganization in patients at presentation with clinically isolated syndromes suggestive of multiple sclerosis. *Neuroimage* 2003;18:847-55.
25. Morgen K, Sammer G, Courtney SM et al. Distinct mechanisms of altered brain activation in patients with multiple sclerosis. *Neuroimage* 2007;37:937-46.
26. Trapp BD, Ransohoff R, Rudick R. Axonal pathology in multiple sclerosis: relationship to neurologic disability. *Curr Opin Neurol* 1999;12:295-302.
27. Khoury S, Bakshi R. Cerebral pseudoatrophy or real atrophy after therapy in multiple sclerosis. *Ann Neurol* 2010;68:778-9.

28. Barkhof F, Calabresi PA, Miller DH, Reingold SC. Imaging outcomes for neuroprotection and repair in multiple sclerosis trials. *Nat Rev Neurol* 2009;5:256-66.

29. Barkhof F. The clinico-radiological paradox in multiple sclerosis revisited. *Curr Opin Neurol* 2002;15:239-45.

30. Huang D, Swanson EA, Lin CP et al. Optical coherence tomography. *Science* 1991;254:1178-81.

31. Parisi V, Manni G, Spadaro M et al. Correlation between morphological and functional retinal impairment in multiple sclerosis patients. *Invest Ophthalmol Vis Sci* 1999;40:2520-7.

32. de Boer JF, Cense B, Park BH, Pierce MC, Tearney GJ, Bouma BE. Improved signal-to-noise ratio in spectral-domain compared with time-domain optical coherence tomography. *Opt Lett* 2003;28:20679.

33. Petzold A, de Boer JF, Schippling S et al. Optical coherence tomography in multiple sclerosis: a systematic review and meta-analysis. *Lancet Neurol* 2010;9:921-32.

34. Balk LJ, Twisk JWR, Steenwijk MS et al. A dam for retrograde axonal degeneration in Multiple Sclerosis? *J Neurol Neurosurg Psychiatry*. 2014;85:7829.

Chapter 2

Optical coherence tomography: reliability and influencing factors

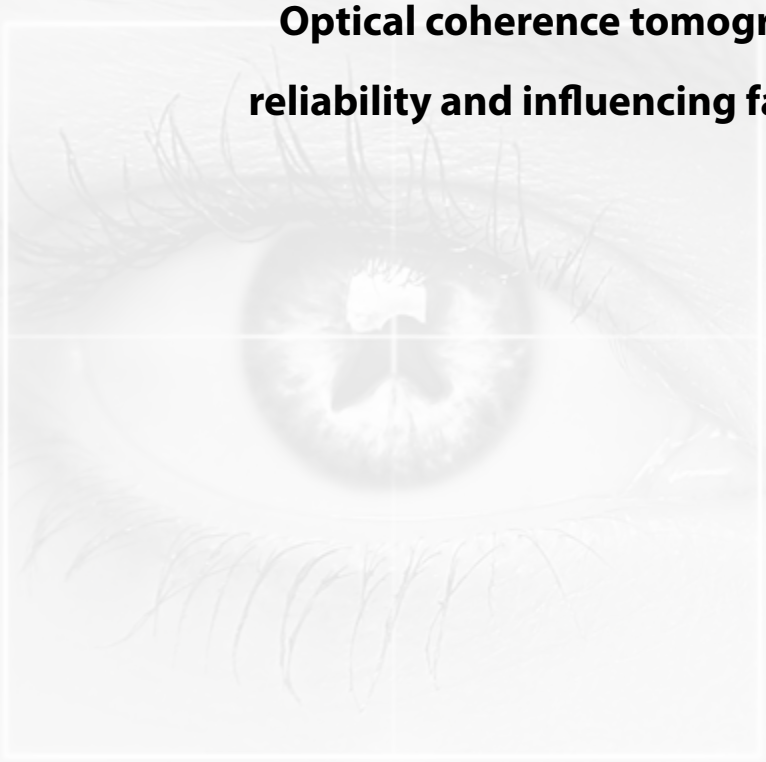

Chapter 2.1

The physiological variation of the retinal nerve fibre layer thickness and macular volume in humans as assessed by spectral-domain optical coherence tomography

LJ Balk, JM Sonder, EMM Strijbis, JWR Twisk, J Killestein, BMJ Uitdehaag, CH Polman, A Petzold

***Invest Ophthalmol Vis Sci*. 2012;53:1251-7**

ABSTRACT

Purpose With the introduction of spectral domain optical coherence tomography (SD-OCT), changes in the retinal nerve fibre layer (RNFL) thickness and macular volume (MV) can be detected with a high precision. This study aimed to determine whether there is a physiological quantifiable degree of variation of these structures in humans.

Methods This study took place during a 10 km charity run at VU University Amsterdam. Weight, height, hydration status, RNFL thickness (ring scan,12 degrees around the optic nerve head) and MV (20x20 degrees) were assessed in 69 subjects (44 runners, 25 controls) using the Heidelberg Spectralis with eye-tracking function. The SD-OCT scans were assessed before running (normal status), after running (more dehydrated status) and 1-1,5 hours after finishing the run (rehydrated status). Controls were measured at the same time intervals as the runners, but did not participate in the running event. Changes over time were assessed by general linear models (GLM), correcting for repeated measurements.

Results In runners, a significant increase of both the RNFL thickness (94.4 µm (baseline) to 95.2 µm (rehydration), $p=0.04$) and MV (288.9 µm (baseline) to 291.0 µm (rehydration), $p<0.001$) over time was observed. Controls did not show significant changes over time. Anatomically, the physiological change of RNFL thickness was most marked in the nasal sectors.

Conclusion This prospective study demonstrated a significant physiological variation of the RNFL thickness and MV at a proportion which, on an individual patient level, may be relevant for longitudinal studies in neurodegenerative diseases.

INTRODUCTION

Neurodegeneration is a major problem for a range of neurological diseases and there is a lack of techniques that can readily quantify the process. Recently there has been wide interest in the hypothesis that analysis of the retinal nerve fibre layer (RNFL) could act as a marker for neurodegenerative processes in de central nervous system.[1-4] Research in this field was largely driven by the use of time-domain OCT (TD-OCT) in patients with optic neuritis (ON) and multiple sclerosis (MS).[5,6] A consistent finding is that loss of RNFL occurs in the range of 20 µm following ON and 7 µm in MS without ON.[6] The estimated annual loss of RNFL thickness in MS patients without ON is about 2 µm compared to 0.1 µm in controls.[7]

OCT is a non-invasive technique that can generate a cross sectional image of the RNFL by scanning the retina with a beam of light. The interference patterns of the back-scattered light are used to generate a high resolution image.[8,9] Besides the RNFL thickness, which measures unmyelinated retinal axons that are continuous with the optic nerve, OCT technology allows for volume scans which provide information about both the axons and their ganglion cell bodies.[2,10] In the macula, the ganglion cell bodies account for about 34% of the total macular volume (MV). As yet, OCT has been successfully used to monitor retinal ganglion cell axon loss in a number of ophthalmological diseases,[11-16] but more and more recent reports emphasise the usefulness of this technique in neurology.[2,4,17-21] This is partly due to some advantages OCT has in a routine clinical setting; it is relatively easy to perform, time-efficient and less resource demanding than magnetic resonance imaging (MRI) based assessments of brain atrophy.[22]

High-resolution SD-OCT technology makes it possible to detect changes in the RNFL thickness with high accuracy (1.14-2.39 µm)[23]. For comparison, the diameter of retinal ganglion cells is about 15 µm.[24] It may, therefore, be possible to reliably detect changes in RNFL thickness related to physiological factors at a cellular level.

Consequently, it is important to assess this effect, because physiological variation in the range of the anticipated annual change of RNFL thickness (0.1-2 µm) may influence data interpretation from longitudinal studies on neurodegeneration.

Hence, the objective of this explorative study was to determine whether physiological variation can cause changes of the RNFL thickness and MV, detectable by SD-OCT.

METHODS

This study was approved by the medical ethical committee (protocol number 2010/336) and the scientific research committee (protocol number CWO/10-22E) of the of the VU University Medical Centre in Amsterdam, the Netherlands.

Study design

The study design was prospective with longitudinal data assessment. The study took place at the VU University Medical Centre Amsterdam on the 23rd of November 2010. The setting was a 10 km. charity run to support MS research. The over 800 participants of the charity run were informed about the possibility to participate in this study at time of subscription. Included subjects were measured three times and were first scanned before the start of the charity run, which represented a 'normal' situation. Thereafter, the subject started his/her 10 km run, and within 5 to 10 minutes after the subject had finished the second scan was performed. All subjects were advised to refrain from drinking during the race and before the 2nd scan to attain a more dehydrated status. Afterwards, the subjects were advised to drink water and sports-drinks to re-hydrate again. The third and last scan was performed 1.5 hours after rehydration. Control subjects were also measured three times, at the same time intervals as the runners, but did not participate in the running event and did not perform any other strenuous exercise on the day of scanning.

Subjects

All subject included were of good general health. There were 44 participants of the charity run and 25 controls included. Due to limited scanning time at the day of the event, only one eye of all runners and only 6 controls were scanned on the day of the charity run. Of the remaining 19 controls, one eye was scanned on subsequent days, although strictly adhering to the predefined time intervals. Both runners and controls were eligible for inclusion in this study if they were 18-60 years of age. Exclusion criteria were any ophthalmologic or neurological conditions or myopia of more than -6.0 diopters. The study adhered to the tenets of the Declaration of Helsinki and informed written consent was obtained from all included runners and controls before study entry.

Optical Coherence Tomography

OCT images were acquired with SD-OCT (Spectralis software version 1.1.6.3; Heidelberg Engineering Inc., Heidelberg, Germany) using dual beam simultaneous imaging, with the eye tracking function enabled. Baseline and follow-up scans were co-registered to allow for optimal anatomical alignment of the retina.

The accuracy for repeated RNFL thickness measurements of the Heidelberg Spectralis used in this study is excellent (coefficients of variation 0.42%-1.45%; intraclass correlation coefficients above 0.95).[3,23,25,26] Likewise, the reproducibility of MV measurements gives a coefficients of variation below 0.5% and ICC of 0.96.[27-29]

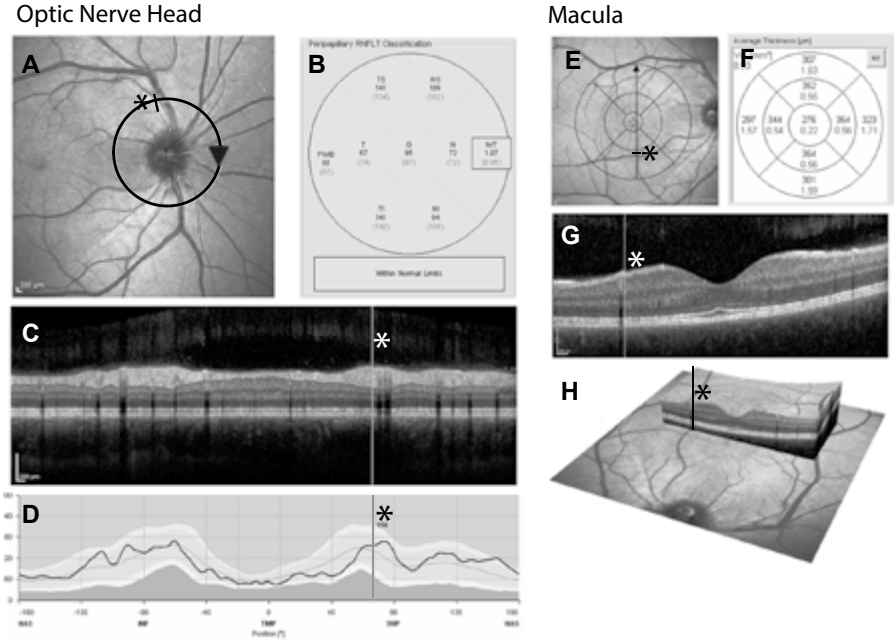

Figure 1. The two scan sequences used in this study. **(A)** A circular scan centred on the optic nerve head. The ring scan starts at the arrow head seen to the right of the circular line (nasal sector). For orientation a small black line is inserted (asterisk). **(B)** The data is expressed in µm RNFL thickness for each retinal sector and the papillo-macula bundle (PMB). **(C)** Cross sectional image of RNFL (B-scan, averaged from about 200 A-scans). The vertical grey line corresponds to the position of the asterisk shown in (A) next to the superior temporal retinal artery and vein. **(D)** The RNFL thickness is measured across 768 locations. The baseline data is shown by a closed black line . The normative data is given in shades of grey, where the whitish layer in the centre corresponds to the 95% normal range, the dark and lighter grey areas represent values outside the 99% confidence interval of the normal distribution, indicating outside normal limits. The vertical grey line corresponds to the position of the asterisk shown in (A) and (C). **(E)** A volume scan, centred on the macula. The scan consists of multiple aligned scans of which the black arrow indicates one. For orientation a small black line is inserted (asterisk). **(F)** Circular lines on the plots represent 1-, 3-, and 6-mm scan diameter. The innermost circle defines the fovea, an area with few retinal ganglion cells. The data in the inner sector and inner and outer quadrants is expressed in macular thickness (µm) and macular volume (mm^3). **(G)** A cross sectional image of macula in which the vertical grey line corresponds to the position of the asterisk shown in (E). **(H)** A three-dimensional image of the macula, visualising the retinal layers. The black line corresponds to the position of the asterisk shown in (E) and (G).

A circular scan with a 3.4-mm-diameter circle (12 degrees) was used. The ring scan was centred manually on the optic nerve head (ONH) after activating the eye tracking function in each subject. Likewise, the MV scan (20 x 20 degrees, 25 sections) was manually centred over the macula after activation of the eye tracking function.

The following quantitative OCT data was collected: the global mean RNFL thickness around the ONH as well as sector specific RNFL thickness (temporal, temporal/inferior, temporal/superior, nasal, nasal/inferior, nasal/superior and papillo-macula bundle, figure 1B). The volume scan provides both volume data (mm^3, in grey) and mean retinal thickness (µm, in black) per quadrant of the macular area of the retina (figure 1F). In this study the global mean of the circle scan and the average thickness in µm of the inner area of the volume scan were included in the analyses, thus avoiding interpolation from the data. Fixation control during retinal OCT scanning was achieved using an internal fixation point. All OCT scans at the charity run were performed by one trained observer (AP) to minimise the analytical error.

Quality control

All OCT scans underwent consensus quality control by two trained observers (LB, AP). Criteria for scan rejection were as published[30]: (1) poor quality (signal strength < 15 dB) (2) algorithm line failures, (3) decentration artefacts and (4) boundary line errors. Scans failing quality control were excluded from the analyses.

Physiological parameters

Demographic data (ethnicity, age, sex), and physiological data (weight, height, hydration status) were collected. For ethical reasons the subjects hydration status was assessed non-invasively (AP) using validated clinical signs (dryness of the tongue or mucosa, skin turgor, capillary refill time)[31] and by calculating the change of weight (Δ weight = weight pre run – weight post run). All runners were asked to go to the toilet before the first weight assessment the to ensure that any weight loss before and after the run was caused by perspiration.

Statistical analyses

The Body Mass Index (BMI) was calculated as weight in kilograms divided by height in meters squared (kg/m^2). It was planned to dichotomise the subjects into normally hydrated and dehydrated based on the clinical signs (dryness of the tongue or mucosa, skin turgor, capillary refill time)[31] and loss of weight.

Baseline characteristics were compared between runners and controls using independent-samples t-tests (continuous variables) and χ^2 tests (dichotomous variables). Since the RNFL thickness and MV were measured three times within every subject, longitudinal data analyses methods were used since these methods take into account the fact that the repeated observations of each subject are correlated. To assess if there was a difference in RNFL thickness and MV between the three longitudinal measurements and to see if these changes over time were different between the

runners and controls, a General Linear Model (GLM) for repeated measures was used. In figures, the data for the runners and controls was normalised to baseline (100%) for ease of visual comparison. The mean relative changes of the groups were based on means of individual changes which were, for the circular scan, calculated for each of the 768 A-scans.

In addition to the analyses where the global mean of the circular scan was used to describe changes over time, further analyses were performed with use of extended data of the circular scan. Instead of using sector specific RNFL thickness values, all individual scan points were used. A circular scan consists of 768 consecutive scan points, together forming a circle around the ONH, as shown in figure 1A (grey circle). Analysing all scan points might give a more detailed depiction of the anatomical location where changes in RNFL thickness occur and makes it possible to relate these changes to the underlying anatomy. All 768 scan points were equally divided in 12 clockwise sectors. Subsequently, linear multi-level analyses were performed, including interactions on sector level, to determine differences between runners and controls for every retinal sector.

Moreover, assuming weight loss as a measure for hydration status, the effect of hydration status was explored more in detail. To determine the impact of weight loss due to perspiration and evaporation, sensitivity analyses were performed. Therefore, all analyses were repeated after excluding subjects in the lowest tertile of weight change to see whether this changed results.

Statistical analyses were performed using SPSS 17.0, except the multi-level analyses, which were done using MLwiN 2.22 (University of Bristol, Center for Multilevel Modeling, Bristol, UK). A significance level of 5% (two-sided) was assumed.

RESULTS

Of all subjects assessed for eligibility (both runners and controls, N=91), 18 were excluded prior to the first scan because of eye-disease (N=3), age > 60 (N=9) or only showing up after the run had already started (N=6). All included runners finished the 10 km charity run. None of the runners was however, dehydrated. In fact, skin turgor and capillary refill time were suggestive of an hyperaemic state. Runners lost on average 1.03 kg during running (range 0.4-2.4 kg).

Of all scanned subjects (N=73), 4 were excluded as their scans failed quality control because of decentration artefacts (N=1) or algorithm line failure (N=3). Figure 2 summarises the the flow of subject in- and exclusion.

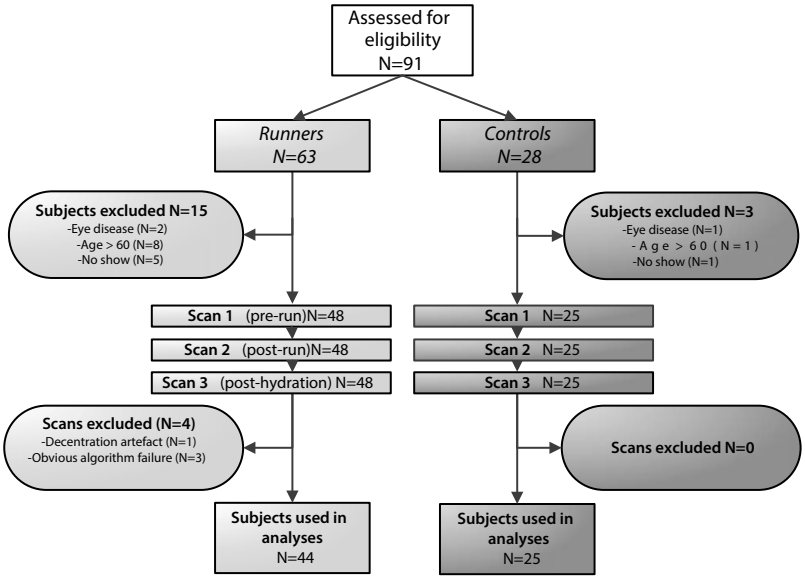

Figure 2. Flowchart of subjects recruited in this study. On the left side the in- and exclusion of subjects and scans are depicted, as at the right side the same aspects are shown for controls. In total, 44 runners and 25 controls were included for statistical analyses.

Changes over time and difference between runners and controls

Table 1 shows the baseline characteristics of the runners and controls. The groups were matched for age, height, weight and BMI ($p>0.05$ for all comparisons). There were more males in the runners group compared to the control group ($p=0.01$). The mean RNFL thickness and MV between both groups were comparable at baseline ($p>0.05$ for both comparisons).

Table 1 Physiological characteristics of all subjects at baseline. The percentage, mean and standard deviation (SD) are shown.

	Runners (N=44)	Controls (N=25)	p-value
Sex (% male)	77%	44%	0.01
Age (years)	42.3 (10.6)	38.1 (13.3)	0.19
Height (m)	1.80 (0.1)	1.74 (0.2)	0.07
Weight (kg)	78.5 (12.7)	75.3 (11.2)	0.30
BMI	24.0 (2.8)	23.8 (3.5)	0.77
Mean RNFL thickness (µm) Baseline scan	94.4 (10.2)	96.9 (9.7)	0.40
Inner macular volume (µm) Baseline scan	288.9 (20.1)	279.6 (17.1)	0.06

There was a significant change from the baseline RNFL thickness (p=0.04) and MV (p=0.00001) in the runners, but not in the controls (table 2). Of note, the significant physiological change of the MV in the runners occurred mainly after oral re-hydration.
In addition to the group specific changes over time on absolute data presented in table 2, the comparisons in relative development over time between runners and controls are shown in figures 3A (circle scan) and 3B (volume scan). To this purpose, individual scans were normalised to baseline (100%) with physiological deviation from baseline expressed as relative values. Each subject was taken as her/his own control.
There was no significant difference of the relative ring scan data *between* the two groups (figure 3A, p=0.17), despite the significant increase *over time* in runners (figure 3A, p=0.04). The significant physiological change *over time* in the runners was further highlighted by the clear increase of RNFL thickness above the published measurement noise (coefficient of variation) of 0.42%[3] (figure 3A, gray shaded area).
The physiological changes became even more noticeable by analysing relative volume data. There were significant differences between the runner and controls for the MV data (figure 3B, p=0.003). As before, the physiological changes of the runners' MV was clearly above the published measurement noise level (0.45% [27-29] figure 3B, gray shaded area).

Table 2 Physiological change of RNFL thickness and macular volume following exercise (scans 1 & 2) and oral rehydration (scans 2 & 3), presented as mean (SD)

	Scan 1 (pre-run)	Scan 2 (post-run)	Scan 3 (post-hydration)	p-value*
Runners				
Mean RNFL thickness (µm)	94.4 (10.2)	94.9 (10.5)	95.2 (10.4)	0.04
Inner macular volume (µm)	288.9 (20.1)	289.1 (19.9)	291.0 (20.3)	0.00001
Controls				
Mean RNFL thickness (µm)	96.9 (9.7)	97.1 (9.9)	97.1 (9.7)	0.56
Inner macular volume (µm)	279.6 (17.1)	279.4 (16.5)	279.4 (16.8)	0.94

Values shown are mean (SD).
* General linear model correcting for repeated measures.

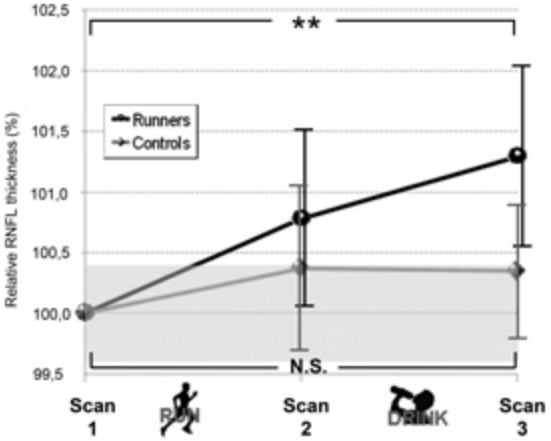

Figure 3. (A) The relative physiological change of the RNFL thickness over time. The individual scans were normalised to the baseline value (100%). Changes over time were presented as relative to the individual baseline value (for absolute data and standard deviations see Tables 1&2). The range of expected noise between repeated OCT measurement was expressed as the measurement accuracy (also referred to as the coefficient of variation) above and below the 100% mark (gray shaded area). The vertical black and grey bars represent the (scan specific) 95% confidence intervals. In the control group repeated measurements remain within the noise level (gray shade area) and did not change significantly over time (N.S., p=0.56). In contrast, for the runners there was a significant (p=0.04) increase of the RNFL thickness over time which was clearly above the level of measurement noise.

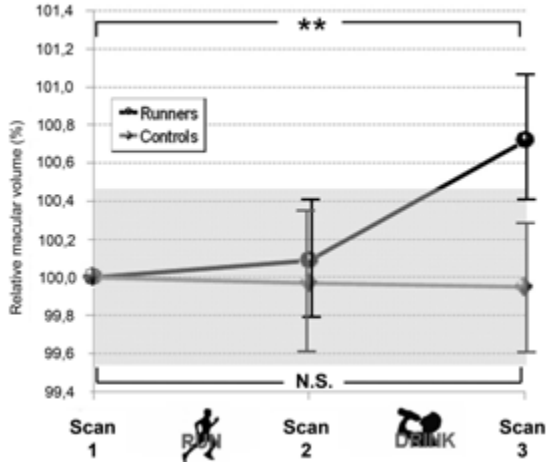

Figure 3. (B) The relative physiological change of the macular volume over time. Individual scans were normalised to the baseline value (100%). Changes over time were presented as relative to the individual baseline value (for absolute data and standard deviations see Tables 1&2). The range of expected noise between repeated OCT measurement was expressed as the measurement accuracy (also referred to as the coefficient of variation) above and below the 100% mark (gray shaded area). The vertical black and grey bars represent the (scan specific) 95% confidence intervals. In the runners group a significant increase of the RNFL thickness over time (p=0.00001) was observed, clearly above the noise level at scan 3. In contrast, for the controls there was no significant change over time (p=0.94) and values remained within the noise level.

The anatomical presentation of the physiological RNFL thickness changes at the ONH

The changes of the RNFL thickness of the 768 A-scans around the ONH were related to the underlying anatomy. Multi-level analyses over the *entire observation period* (±3 hours) demonstrated that the differences between runners and controls were not the same for all 12 sectors (figure 4A). Significant differences between the two groups were observed only for the nasal sectors (sectors 3 to 5 in figure 4A) and for sector 12. The relationship with the underlying anatomy was illustrated by figure 4B. As can be appreciated from the standard deviations in figures 3A&B these changes were not significant on a shorter time-intervals, but only over the entire observation period.

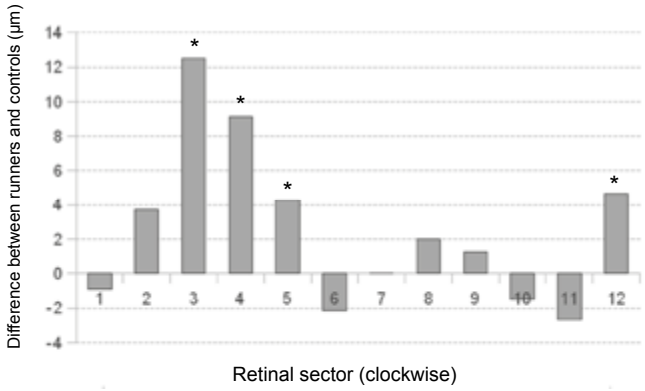

Figure 4. **(A)** The absolute difference between runners and controls (µm), averaged over the entire observation period, is shown across 12 retinal sectors around the ONH. Significant differences are marked with an asterisk, which indicates a p-value <0.05. A positive value means higher RNFL thickness for controls.

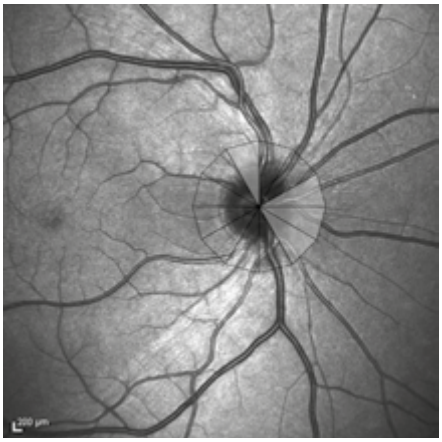

Figure 4. (B) For orientation the 12 positions of a clock are projected on the ONH. The sectors are labelled clockwise. Sectors in which the difference between runners and controls was significant are shaded in grey. The sectors 3-5 ($p<0.05$) correspond to the well vascularised nasal area of the retina. Sector 12 ($p<0.05$) is located superiorly, adjacent to the superior temporal retinal artery and vein.

Sensitivity analysis

Assuming that subjects who lost more weight had more changes in hydration status, subjects in the lowest tertile of weight loss were excluded from the following analyses. Consequently, 30 runners remained.

The previously reported differences between runners and controls (figures 3A and 3B) both slightly changed (RNFL thickness p=0.63, MV p=0.02), while the significance of the results of the extended circular scan data did not change (data not shown).

DISCUSSION

Changes of the RNFL thickness and MV over time are firmly established as a robust measure for disease progression for glaucoma, macular degeneration and an increasing number of other ophtalmological disorders. Subsequently, it has been proposed to use the RNFL thickness around the ONH and MV also as biomarkers for neuro-axonal degeneration in neurological disorders in general and for MS in particular.[4,32,33] Because an increasing number of clinical trials include the RNFL thickness and inner MV as a secondary outcome measure it seemed timely to investigate the range of physiological variation in these eloquent areas *in vivo*. The present study examined whether physiological variation could cause detectable changes in RNFL thickness and MV in healthy human subjects as measured by SD-OCT.

The results of this prospective, longitudinal study clearly demonstrated that for the runners, both the RNFL thickness at the ONH and the inner MV changed under physiological conditions (table 1&2). For controls, neither the circular nor the volume scan showed significant changes over time. To add further weight to this argument, the observed physiological change in the runners were clearly above the published measurement noise level (figure 3A&B, gray shaded area). This strongly suggests that the findings of this study were not only statistically significant, but also biologically relevant. The results of the analyses with extended RNFL thickness data give an indication of the anatomical presentation of the observed changes in RNFL thickness. These results should however be interpreted with caution, since the analyses were performed using absolute data and there is considerable inter-subject variability of RNFL thickness.

The significant change in RNFL thickness in runners, as a consequence of physiological variation, was on average 1.6 µm. This change is small, but over 10-times larger than the estimated annual RNFL thickness loss in healthy controls (0.1 µm)[7]. Given the high accuracy of the SD-OCT device, (CV=0.42%)[3], the observed change is most unlikely to be caused by a measurement error. Furthermore, the data of a 2-year longitudinal

multiple sclerosis cohort study of the RNFL thickness showed a change over time well within the range of physiological variation reported it the present study.[34] It could be possible that the paradoxical finding of an increase of the RNFL thickness over time in patients with secondary progressive multiple sclerosis who did not suffer from optic neuritis (see empty triangles in figure 1 in reference [34]) may be due to physiological variation.

How can the observed physiological change of the RNFL thickness and MV be explained? Because this study was designed within the constraints of a public charity run there is no hard physiological data relying on invasive physiological or laboratory measures. It is therefore only possible to speculate on feasible mechanisms such as change in re-hydration related change of cellular volume which may be dependent on the runners electrolyte status.[35] Alternatively, the exercise induced hyperaemic state may be relevant. Future studies including blood and urine laboratory measures as well as experiments designed to induced controlled hypercapnia may be informative.

Of note, Kinkelder *et al*[36] have reported a measurement artefact that was not controlled for in this study. Heartbeat induced axial motion during OCT volume scanning of the retina can affect RNFL measurements. This artefact is likely to increase noise rather than to introduce a bias and is therefore an unlikely explanation for the here reported physiological changes. Additionally, the detailed anatomical analyses in the present study did not show that the change of RNFL thickness was confined to the retinal branch arteries and veins around the ONH. Finally, it may be that the measurement accuracy of the SD-OCT ring scan was lowest were the start and end-point of the scan met, which in this experiment was nasally. This issue may be addressed by programming the OCT software such that it permits for selection of ring-scan start point for future studies.

The reproducibility of the OCT device used in this study (Spectralis, Heidelberg) is excellent.[3,23,29] This is most likely due to the systems eye tracking function (TruTrack) during the scanning process as well as automatic recognition of the exact same scan location for follow up examination. Using these features minimises extrinsic factors, such as the patients' ability to fixate and measurements are therefore less sensitive to subjective operator judgement.[29] Moreover, Jo *et al* observed diurnal variation in retinal thickness, measured with time-domain OCT (TD-OCT), but not with SD-OCT.[37] They stated that the difference was likely due to the good reproducibility of SD-OCT, in contrast with the TD-OCT. Consequently, the observed changes in RNFL thickness and macular volume in the present study were unlikely to represent a measurement error and strongly suggest relevant physiological variation.

In conclusion, this study showed for the first time that the physiological variation on RNFL thickness and MV not only exceeded the estimated measurement error of the SD-OCT device, but most importantly occurred at a proportion which, on an individual

patient level was about 10 times above the estimated annual change. These findings are therefore relevant for the design and data interpretation of longitudinal studies which use the RNFL and MV as a biomarker in humans.

REFERENCES

1. Serbecic N, Beutelspacher SC, Kircher K, Reitner A, Schmidt-Erfurth U. Interpretation of RNFLT values in multiple sclerosis associated acute optic neuritis using high-resolution SD-OCT device. *Acta Ophthalmol.* 2012;90:540-5.
2. Barkhof F, Calabresi PA, Miller DH, Reingold SC. Imaging outcomes for neuroprotection and repair in multiple sclerosis trials. *Nat Rev Neurol.* 2009;5:256-266.
3. Serbecic N, Beutelspacher SC, Aboul-Enein FC, Kircher K, Reitner A, Schmidt-Erfurth U. Reproducibility of high-resolution optical coherence tomography measurements of the nerve fibre layer with the new Heidelberg Spectralis optical coherence tomography. *Br J Ophthalmol.* 2011;95:804-810.
4. Jindahra P, Hedges TR, Mendoza-Santiesteban CE, Plant GT. Optical coherence tomography of the retina: applications in neurology. *Curr Opin Neurol.* 2010;23:16-23.
5. Costello F, Hodge W, Pan YI, Eggenberger E, Freedman MS. Using retinal architecture to help characterize multiple sclerosis patients. *Can J Ophthalmol.* 2010;45:520-526.
6. Petzold A, de Boer JF, Schippling S et al. Optical coherence tomography in multiple sclerosis: a systematic review and meta-analysis. *Lancet Neurol.* 2010;9:921-932.
7. Talman LS, Bisker ER, Sackel DJ et al. Longitudinal study of vision and retinal nerve fiber layer thickness in multiple sclerosis. *Ann Neurol.* 2010;67:749-760.
8. Huang D, Swanson EA, Lin CP et al. Optical coherence tomography. *Science.* 1991;254:1178-1181.
9. Jaffe GJ, Caprioli J. Optical coherence tomography to detect and manage retinal disease and glaucoma. *Am J Ophthalmol.* 2004;137:156-169.
10. Burkholder BM, Osborne B, Loguidice MJ et al. Macular volume determined by optical coherence tomography as a measure of neuronal loss in multiple sclerosis. *Arch Neurol.* 2009;66:1366-1372.
11. Costello F, Coupland S, Hodge W et al. Quantifying axonal loss after optic neuritis with optical coherence tomography. *Ann Neurol.* 2006;59:963-969.
12. Kanamori A, Nakamura M, Escano MFT, Seya R, Maeda H, Negi A. Evaluation of the glaucomatous damage on retinal nerve fiber layer thickness measured by optical coherence tomography. *Am J Ophthalmol.* 2003;135:513-520.
13. Massin P, Girach A, Erginay A, Gaudric A. Optical coherence tomography: a key to the future management of patients with diabetic macular oedema. *Acta Ophthalmol Scand.* 2006;84:466-474.
14. Medeiros FA, Zangwill LM, Bowd C, Weinreb RN. Comparison of the GDx VCC scanning laser polarimeter, HRT II confocal scanning laser ophthalmoscope, and stratus OCT optical coherence tomograph for the detection of glaucoma. *Arch Ophthalmol.* 2004;122:827-837.
15. Medeiros FA, Moura FC, Vessani RM, Susanna RJ. Axonal loss after traumatic optic neuropathy documented by optical coherence tomography. *Am J Ophthalmol.* 2003;135:406-408.
16. Trip SA, Schlottmann PG, Jones SJ et al. Retinal nerve fiber layer axonal loss and visual dysfunction in optic neuritis. *Ann Neurol.* 2005;58:383-391.
17. Albrecht P, Frohlich R, Hartung HP, Kieseier BC, Methner A. Optical coherence tomography measures axonal loss in multiple sclerosis independently of optic neuritis. *J Neurol.* 2007;254:1595-1596.
18. Henderson APD, Trip SA, Schlottmann PG et al. A preliminary longitudinal study of the retinal nerve fiber layer in progressive multiple sclerosis. *J Neurol.* 2010;257:1083-1091.
19. Kallenbach K, Frederiksen J. Optical coherence tomography in optic neuritis and multiple sclerosis: a review. *Eur J Neurol.* 2007;14:841-849.
20. Pula JH, Reder AT. Multiple sclerosis. Part I: neuro-ophthalmic manifestations. *Curr Opin Ophthalmol.* 2009;20:467-475.
21. Sergott RC, Frohman E, Glanzman R, Al-Sabbagh A. The role of optical coherence tomography in multiple sclerosis: expert panel consensus. *J Neurol Sci.* 2007;263:3-14.

22. Siepman TAM, Bettink-Remeijer MW, Hintzen RQ. Retinal nerve fiber layer thickness in subgroups of multiple sclerosis, measured by optical coherence tomography and scanning laser polarimetry. *J Neurol.* 2010;257:1654-1660.

23. Wu H, de Boer J, Chen T. Reproducibility of retinal nerve fiber layer thickness measurements using spectral domain optical coherence tomography. *J Glaucoma.* 2011;20:470-6.

24. Dacey DM, Petersen MR. Dendritic field size and morphology of midget and parasol ganglion cells of the human retina. *Proc Natl Acad Sci U S A*. 1992;89:9666-9670.

25. Arthur SN, Smith SD, Wright MM et al. Reproducibility and agreement in evaluating retinal nerve fibre layer thickness between Stratus and Spectralis OCT. *Eye (Lond)*. 2011;25:192-200.

26. Serbecic N, Beutelspacher S, Aboul-Enein F, Kircher K, Reitner A, Schmidt-Erfurth U. Reproducibility of high-resolution optical coherence tomography measurements of the nerve fibre layer with the new Heidelberg Spectralis optical coherence tomography. *Br J Ophthalmol.* 2011;95:804-10.

27. Menke MN, Dabov S, Knecht P, Sturm V. Reproducibility of retinal thickness measurements in healthy subjects using spectralis optical coherence tomography. *Am J Ophthalmol*. 2009;147:467-472.

28. Pierro L, Giatsidis SM, Mantovani E, Gagliardi M. Macular thickness interoperator and intraoperator reproducibility in healthy eyes using 7 optical coherence tomography instruments. *Am J Ophthalmol.* 2010;150:199-204.

29. Wolf-Schnurrbusch UEK, Ceklic L, Brinkmann CK et al. Macular thickness measurements in healthy eyes using six different optical coherence tomography instruments. *Invest Ophthalmol Vis Sci*. 2009;50:3432-3437.

30. Domalpally A, Danis RP, Zhang B, Myers D, Kruse CN. Quality issues in interpretation of optical coherence tomograms in macular diseases. *Retina.* 2009;29:775-781.

31. Steiner MJ, DeWalt DA, Byerley JS. Is this child dehydrated? *JAMA.* 2004;291:2746-2754.

32. Frohman EM, Fujimoto JG, Frohman TC, Calabresi PA, Cutter G, Balcer LJ. Optical coherence tomography: a window into the mechanisms of multiple sclerosis. *Nat Clin Pract Neurol.* 2008;4:664-675.

33. Galetta KM, Calabresi PA, Frohman EM, Balcer LJ. Optical coherence tomography (OCT): imaging the visual pathway as a model for neurodegeneration. *Neurotherapeutics.* 2011;8:117-132.

34. Serbecic N, Aboul-Enein F, Beutelspacher SC et al. High resolution spectral domain optical coherence tomography (SD-OCT) in multiple sclerosis: the first follow up study over two years. *PLoS One*. 2011;6:e19843.

35. Petzold A, Keir G, Appleby I. Marathon related death due to brainstem herniation in rehydration-related hyponatraemia: a case report. *J Med Case Reports*. 2007;1:186

36. de Kinkelder R, Kalkman J, Faber DJ et al. Heartbeat-induced axial motion artefacts in optical coherence tomography measurements of the retina. *Invest Ophthalmol Vis Sci.* 2011;52:3908-3913.

37. Jo Y, Heo D, Shin Y, Kim J. Diurnal variation of retina thickness measured with time domain and spectral domain optical coherence tomography in normal subjects. *Invest Ophthalmol Vis Sci.* 2011;17;52:6497-500.

Chapter 2.2

Retinal hyperaemia-related blood vessel artefacts are relevant to automated OCT layer segmentation

LJ Balk, M Mayer, BMJ Uitdehaag, A Petzold

J Neurol. **2014;261:511-7**

ABSTRACT

Background A frequently observed local measurement artefact with spectral domain OCT is caused by the void signal of the retinal vasculature. This study investigated the effect of suppression of blood vessel artefacts with and without retinal hyperaemia.

Methods Spectral domain OCT scans, centred on the optic nerve head, were performed in 46 healthy subjects (92 eyes). Baseline scans were made during rest, while for the follow-up scan, 23 subjects (50 %) performed strenuous physical exercise. Systemic and retinal hyperaemia were quantified. Quantification of retinal nerve fibre layer (RNFL) thickness was performed with and without suppression of retinal blood vessel artefacts. The potential systematic effect on RNFL thickness measurements was analysed using Bland-Altman plots.

Results At baseline (no retinal hyperaemia), there was a systematic difference in RNFL thickness (3.4 µm, limits of agreement -0.9 to 7.7) with higher values if blood vessel artefacts were not suppressed.
There was significant retinal hyperaemia in the exercise group ($p<0.0001$). Baseline thickness increased from 93.18 to 93.83 µm ($p<0.05$) in the exercise group using the algorithm with blood vessel artefact suppression, but no significant changes were observed using the algorithm without blood vessel artefact suppression.

Conclusion Retinal hyperaemia leads to blood vessel artefacts which are relevant to the precision of OCT layer segmentation algorithms. The two algorithms investigated in this study can not be used interchangeably. The algorithm with blood vessel artefact suppression was more sensitive in detecting small changes in RNFL thickness. This may be relevant for the use of OCT in a range of neurodegenerative diseases where only a small degree of retinal layer atrophy has been found so far.

INTRODUCTION

Peripapillary retinal nerve fibre layer (RNFL) thickness, measured by optical coherence tomography (OCT), has been proposed as a marker for neurodegenerative processes in the central nervous system. The annual rate of RNFL loss in healthy subjects is estimated at 0.1 µm using time domain OCT and about 2 µm in patients with multiple sclerosis who did not have optic neuritis.[1] Likewise, in other neurodegenerative diseases such as Alzheimer's disease, Parkinson's disease or Wilson's disease RNFL thinning is very small on not yet reproducibly found by all groups.[2-10] Compared to time-domain OCT the measurement accuracy has considerably increased with spectral domain OCT to 0.42-1.45 % (coefficient of variation, CV).[11,12] Therefore, the published RNFL thickness changes are well in the range of what commercially available spectral domain OCT machines can capture.

There is evidence for physiological and diurnal variation of the RNFL thickness and macular volume.[13-16] We previously reported the range of physiological RNFL thickness variation for the ring scan to be about 0.8 µm after physical exercise.[16] At the time we speculated that this degree of physiological variation may have been caused by exercise related changes of retinal haemodynamics which enhance a well recognised measurement artifact.[17] This artifact also causes localised algorithm failures due to a void signal in the vicinity of retinal blood vessels (Figure 1A, white arrows). Whether suppression of this localised void signal (Figure 1B) allows for correction of the observed physiological variation in RNFL thickness is not known. Anatomically, the highest co-localisation between retinal blood vessels and RNFL occurs in a circle around the optic disc. Therefore, a 3.4 mm peripapillary ring-scan provides the ideal model to investigate the potential influence of blood vessel void signal artifacts on automated RNFL layer segmentation. To answer this question we compared two different software algorithms with (Figure 1A) and without (Figure 1B) suppression of the localised blood vessel void signal in a group of athletes with recognised physiological changes in a pre-/post exercise setting.[16]

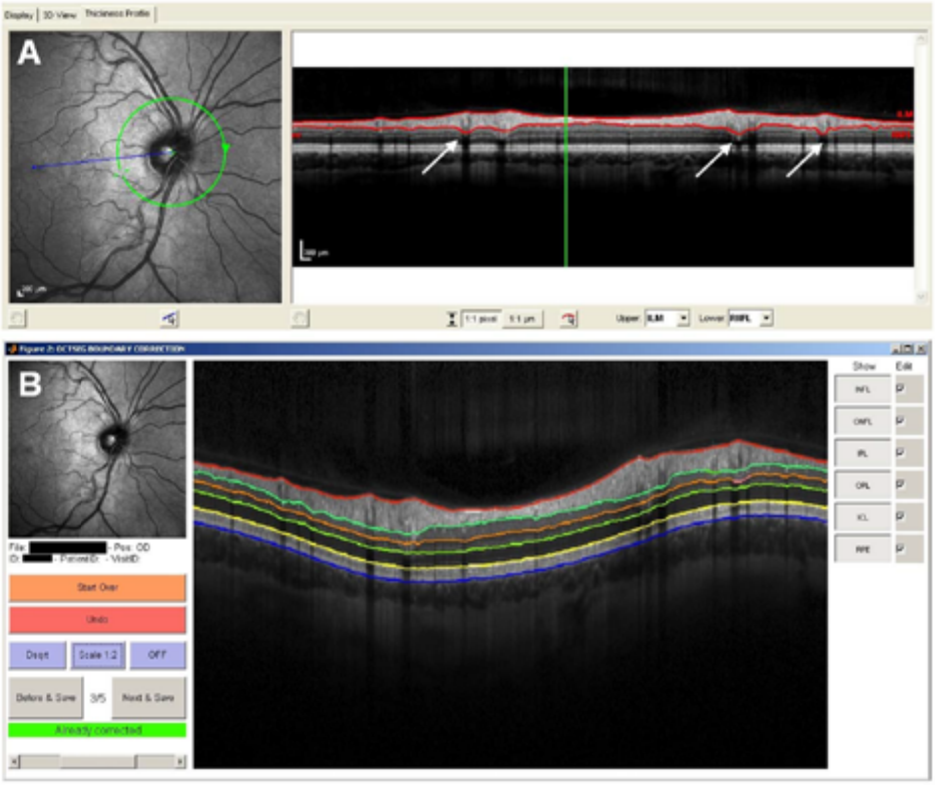

Figure 1. Screenshot of **(A)** a typical localised algorithm disturbance at sites of retinal blood vessel void signals using commercial software (HE). **(B)** Suppression of this measurement artifact using the manual segmentation correction tool of OCTSEG.

METHODS

This study was approved by the medical ethical committee and the scientific research committee of the VU University Medical Centre in Amsterdam, the Netherlands. We certify that all applicable institutional and governmental regulations concerning the ethical use of human volunteers were followed during this research.

Study population

In total, 46 (92 eyes) of 73 subjects from a previous report,[16] had an OCT scan of sufficient inter-layer contrast to qualify for the OCTSEG algorithm. The study protocol has been described in detail before.[16] In brief, two OCT scans were obtained in all subjects. After the first scan, 23 (50 %) participants performed strenuous physical exercise whilst the

other half rested for about 1 h. Runners were allowed to rehydrate during the exercise. In contrast, controls did not have any fluid intake during the exercise. Subsequently, the second OCT scan was performed in both groups. Hydration was assessed by validated clinical signs (skin turgor, capillary refill time and mucosa moisture).[18] In addition, retinal hyperaemia was assessed by measurement of the blood vessel diameter, pre- and post-exercise for the superior temporal and nasal retinal arteries of the scanning laser image as co-registered to the OCT ringscan (see below).

Retinal OCT

OCT images were acquired with an SD-OCT (Spectralis, Heidelberg Engineering Inc, Heidelberg, Germany. Software version 1.1.6.3), using dual beam simultaneous imaging, with the eye-tracking function enabled.[12] Baseline and follow-up scans were co-registered to allow for optimal anatomical alignment of the retina. All scans were recorded by one qualified operator using the ring scan (diameter 12° or 2.4 cm) at the optic nerve head (ONH). Fixation control during retinal OCT scanning was achieved using an internal fixation point. The RNFL thickness was obtained using two different types of segmentation software retrospectively; the Heidelberg Spectralis (HE) and the Erlangen (OCTSEG) algorithms. The intra-session variability for the global average ringscan with the eye-tracking function enabled for the RNFL thickness had a intraclass correlation coefficient (ICC) of 0.96. The HE algorithm is the standard, commercial software used on the Spectralis SD-OCT machine.

The OCTSEG algorithm is a new freely available segmentation algorithm (http://www5.informatik.uni-erlangen.de/research/software/octseg), which was developed to allow a reliable retinal layer segmentation on scans of both normal subjects and glaucoma patients. Specifically, OCTSEG quantified the RNFL thickness in between segmented boundaries for blood vessels which were determined by adaptive thresholding.[19] The automated segmentation of the RNFL was followed by careful revision and manual correction was not necessary for either algorithm. The excellent performance for the high-contrast RNFL contrasted with the poorer performance of either algorithm for the deeper retinal layers we have reported previously.[16]

Statistical analyses

Bland-Altman plots were used for comparison of RNFL thickness data obtained from the different algorithms. The scatter of data and the systematic difference were shown in these plots. Mean RNFL thickness values were compared with linear regression analyses and paired t tests with correction for repeated (n = 2) measurements. Proportions were compared using the Chi Square test. The average

change of the retinal blood vessel diameter was calculated per group with an increase

from baseline indicating retinal hyperaemia. The Shapiro-Wilk test was used to test for normality. Normally distributed data was compared using the Student t test and the Wilcoxon two-sample test for paired samples which were non-Gaussian. In order to make group comparisons with both baseline and repeated measurements of non-Gaussian data, a general linear model (GLM) for repeated measures was used, taking the correlations between repeated measurement into account. Subgroup analyses were performed considering gender as a co-variate. Statistical analyses were performed using IBM SPSS 20.0 and SAS (V9.3). A significance level of 0.05 (two-sided) was assumed.

RESULTS

All subjects completed the study. The demographic baseline data are summarised in Table 1. The two groups were of comparable age. In the exercise group there were more male subjects (p = 0.005, Chi Square test). For both algorithms the groups (exercise and control) showed comparable RNFL thickness values on baseline (p>0.05 for both HE and OCTSEG software). All included scans fulfilled rigorous OCT quality control criteria.[19]

Table 1 Subject characteristics at baseline.

	Exercise group	Control group	p-value
N	23	23	
Age (y)	37.5 (±13.6)	43.1 (±8.8)	ns
Sex (% male)	87%	44%	0.005
Hyperaemia	0%	0%	ns
Retinal vasculature diameter (µm)	95.6 ± 19.5	98.1 ± 18.3	ns
HE RNFL thickness (µm)	96.7±7.9	97.6±8.6	ns*
OCTSEG RNFL thickness (µm)	93.2±8.1	94.3±9.6	ns*

The mean (± SD) and percentages are presented
*Global average value for the peripapillary ring scan. There was no significant difference between groups (p>0.05) either for a direct comparison or a comparison with correction for age.

Post-exercise hyperaemia

Following exercise and at acquisition of the second scan, all subjects from the strenuous exercise group showed systemic and retinal signs of hyperaemia (Table 2).

Table 2 Signs for hyperaemia post-exercise

	Exercise group	Control group	p-value
Systemic hyperaemia	100%	0%	<0.0001
Retinal vasculature diameter (µm)	108.7 ± 21.2	93.5 ± 18.1	<0.0001
Δ diameter change from baseline	+13.1 ± 19.5	-4.6 ± 7.7	<0.0001

Retinal hyperaemia (averaged diameter of the superior temporal and nasal retinal arteries). The Student t test was used for normally distributed data

Algorithm comparison

The Bland-Altman plot of the baseline data, where all subjects were at rest, shows substantial scatter of the individual A-scans (Figure 2A). There was a systematic difference between the methods, with the commercial algorithm (HE) giving higher values compared to the OCTSEG method averaging at +3.4 µm (limits of agreement -22.5 to 29.3). The dispersion of the data increases with higher mean values of RNFL thickness, which frequently coincide with areas of high vascularisation.[19] The difference between the measurements increased with RNFL thickness according to the formula (linear regression): Y = 0.09X - 5.4 where Y is defined as □□HE (µm) - OCTSEG (µm)'□ and X as □□[HE (µm) + OCTSEG (µm)/2]". Because the large number of individual measurements does not allow one to visually assess the size of the error, the mean difference and standard deviation for each measurement were plotted as well (Figure 2B). This plot highlights that the size of the measurement error exceeds 10 µm (closed horizontal reference lines in Figure 2B) for an averaged RNFL thickness of less than 40 µm or more than 130 µm (dotted vertical reference lines in Figure 2B).

Effect of retinal haemodynamics

The HE segmentation software, which does not suppress the diffuse signal due to retinal vasculature, did not show a significant change of RNFL thickness between the first and second scan in either group (ΔRNFL 0.41 µm in exercise group, -0.33 µm in control group). In contrast, the OCTSEG algorithm, which in fact does suppress the diffuse signal, showed a small but significant increase in runners (ΔRNFL 0.65 µm, p = 0.047) and a significant decrease in controls between the first and second scan (ΔRNFL - 0.72 µm, p = 0.037). When the changes between the first and second scan were compared between the exercise and control group using GLM (within group) analyses, only the OCTSEG software showed a significant difference (p<0.01). Significance remained after considering gender as co-variate. The Bland-Altman plots comparing both methods for the second scan are shown in Figure 3A (exercise group) and 3B (control group). The scatter of data and the systematic differences between the methods are comparable

for both groups [3.2 µm (LoA -23.5 to 29.9 µm) for HE versus 3.7 µm (LoA -21.2 to 28.6 µm) for OCTSEG.

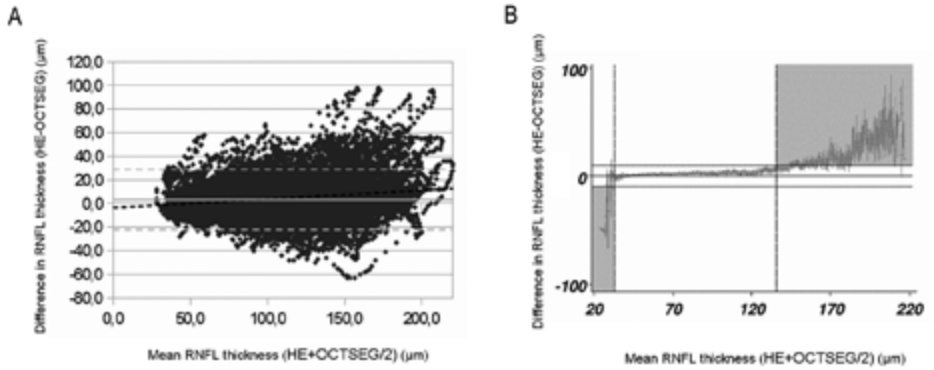

Figure 2. (A) Bland-Altman plot comparing the RNFL thickness of both types of segmentation software. For every subject, all 768 A-scans were used. The plot shows that there was a systematic difference between the two algorithms averaging at 3.4 µm (limits of agreement -22.5 to 29.3), indicating systematic higher values for the HE software. **(B)** The difference scores between the two algorithms on the y-axis (mean ± SD) shows that the OCTSEG algorithm relative overestimates the RNFL thickness below 40 µm (dotted vertical reference line to the left) and relative underestimates the RNFL above 130 µm (dotted vertical reference line to the right) compared to the HE algorithm. The grey shaded areas indicate where the difference between both methods exceed 10 µm from the mean (closed horizontal reference lines).

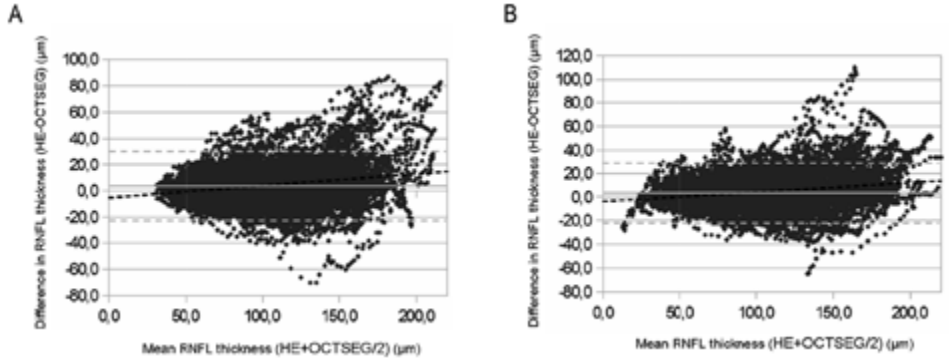

Figure 3. (A) Bland-Altman plot of exercise group with induced hyperaemia. The systematic difference between the two algorithms is 3.2 µm (LoA -23.5 to 29.9),which is comparable to the systematic difference of 3.7 µm (LoA -21.2 to 28.6) in the non-hyperaemic, control group **(B)**

RNFL layer thickness accuracy improves with number of averaged A-scans

There was no significant difference for the averaged measurement error (CV = SD/ mean * 100) for the individual A-scans of all individuals, either at baseline or follow-up. Although hyperaemia was clearly present in the exercise group during the second scan, the measurement error did not decrease when suppression of the void signal of retinal

vessel was used. Clearly, the CV can be reduced by averaging the number of A-scans (Supplementary Figure 1). A CV of <1 % can be achieved by averaged data of the upper and lower half of the retina (two analysed sectors) or the global mean (A-scans averaged to one sector). The respective Bland-Altman plot for the global average alone is shown in supplementary Figure 2. Overall for a large number of A-scans the CV for OCTSEG is lower compared to the CV for the HE algorithm. The CV of the OCTSEG equals the CV of the HE algorithm for evaluation of less than six sectors (Supplementary Figure 1). Importantly, this gain of measurement accuracy is at the price of loss of anatomical information.

DISCUSSION

First, the effect of retinal hyperaemia on the precision of automated retinal layer segmentation was performed, comparing two types of segmentation software. Second, this study extends on previous data on the physiological change of the RNFL thickness,[16] now using a refined algorithm (OCTSEG) that suppresses a well-recognised artifact, which we had discussed as an important weakness of the previous study.[19-21] The main finding is that the in-house developed OCTSEG algorithm confirmed the previously reported data on a significant increase of RNFL thickness in the group of athletes,[22] possibly related to true cellular volume shifts. Interestingly, the OCTSEG algorithm also permitted us to reveal a small decrease of the RNFL thickness in the control group, which may be related to a small degree of physiological dehydration. In contrast to previous studies that compared different OCT devices,[23] there is a lack in the literature comparing the effect of retinal hyperaemia on retinal layer segmentation under controlled conditions on the same device. Performing these comparisons within the same device is relevant to avoid the possibility that inter-device variation may, at least in part, be the cause for subsequent differences in post-image processing.

The two algorithms were compared in order to assess if they could be used interchangeably. The Bland-Altman plots clearly show that a systematic difference exists between the two algorithms (Figure 2A). The scatter of data is largest for higher values (above 130 µm) of RNFL thickness (Figure 2A, B). After physical exercise with induced hyperaemia, the systematic difference between the two algorithms is 3.2 µm (LoA -23.5 to 29.9) (Figure 3A), which is comparable to the systematic difference of 3.7 µm (LoA -21.2 to 28.6) in the non-hyperaemic control group. Although hyperaemia clearly has no large effect on the systematic difference, the difference between the two algorithms is not consistent with RNFL thickness, as illustrated by the slope of the regression lines in Figures 2A and 3A, B. Importantly, the OCTSEG algorithm relatively overestimates

the RNFL thickness in the lower RNFL thickness regions (below 40 µm) and relatively underestimates the RNFL thickness in higher regions (above 130 µm) compared to the HE algorithm. This makes comparing values of both methods even more complicated.
This argument is further strengthened by the revision of measurement accuracy in relationship to the number of averaged A-scans as shown in Supplementary Figure 1. This figure essentially shows that the effect of suppression of the vascular void signal artifact for small anatomical regions is such that there is no agreement between the two algorithms on physiological thickness changes. This level of disagreement can gradually be averaged out, such that the CV for the global ring-scans is just below 10%. In contrast, for a higher anatomical resolution with more than 12 clockwise sectors the CV is over 35% which is unacceptably high. A number of recent studies have compared different algorithms and devices.[24-29] Notably, this data was based on the global average only. These data were consistent with the Bland-Altman plots shown for the global average in this study (Supplementary Figure 2). It would be interesting to test how these data compare for a higher anatomical resolution as discussed here.
In order to determine the effect of retinal hyperaemia on RNFL thickness, serial OCT scans were performed in control subjects and in subjects before and after induction of systemic physiological hyperaemia. Although all subjects in the exercise group showed significant signs of systemic and retinal hyperaemia, the scans using the HE software, which include measurement artifacts caused by
the retinal vasculature, did not show a significant increase of RNFL thickness in the hyperaemic group compared to the control group. In contrast, the OCTSEG algorithm, which did suppress the localised void signal of the retinal vasculature, detected a larger and significant increase in the exercise group ($p<0.05$). Because the OCTSEG algorithm excludes artifacts caused by retinal vessels, one would not expect a larger increase to be observed, compared to the HE algorithm. Therefore, the data suggest that the observed changes in RNFL thickness were physiological in nature and that the OCTSEG algorithm is the more sensitive method to detect these. In line with this argument is that there was a small, but significant, decrease of the RNFL in control subjects, likely related to dehydration during the event. We would be hesitant to suggest that the improved noise-reduction due to blood vessel void signal suppression should be seen as a limitation of the method.
Taken together, the change of RNFL thickness in this cohort cannot be explained by a measurement artifact caused by a hyperaemia-related localised void signal of the retinal vasculature and may be related to change of the cellular volume in the retina of as yet to be determined cause.
Given the overall excellent CV of the global averaged ring-scan and the unlikely scenario of exercise-induced hyperaemia in severely disabled neurological patients,

the potential added analytical accuracy may only be minimal, but, as said above, this comes at the cost of loss of anatomical resolution.
Given the retinotopic projections it would be desirable to make use of individual OCT A-scan data in a longitudinal, multimodal imaging study. Particularly, one may want to correlate possible atrophy of the posterior optic pathways and visual cortex as assessed by structural magnetic resonance imaging (MRI) with localised retinal layer atrophy. Design of such studies might be advised to consider that the precision of current automated retinal layer segmentation decreases if more than 12 clockwise sectors are considered (Supplementary Figure 1).
We are unable to tell from our data if future automated algorithms with vessel void artifact suppression may be superior in a clinical trial setting to the present algorithms. One argument to the contrary not discussed earlier could also be that perivascular pathology recognised in some diseases may be missed. Because, by definition, all forms of automated RNFL quantification are image-post-processing procedures, an optional function of this suppression may open avenues to test this in different settings. Such an option would also overcome the limitation that, at present, two different software versions instead of one single software are required. This also highlights another limitation of this study. All data were acquired in healthy controls. Therefore, we are unable to extrapolate from the present data on the effect of hyperaemia in patients with disease-related changes in RNFL thickness.
In summary, the physical exercise caused only small changes in retinal haemodynamics and RNFL thickness measurements. These changes were physiological in nature and not related to measurement artifacts caused by a localised void signal of the retinal vasculature. The two algorithms investigated in this study cannot be used interchangeably, but the OCTSEG algorithm is more sensitive in detecting small changes in RNFL thickness. This may be relevant for the application of OCT in a range of neurodegenerative conditions were only a small degree of retinal layer atrophy can be expected.

SUPPLEMENTARY MATERIAL

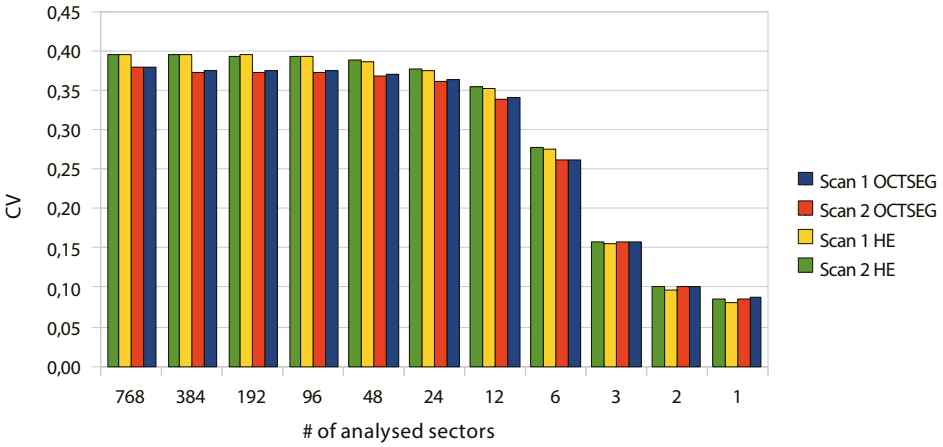

Supplementary Figure 1. The precision (coefficient of variation, CV) of the RNFL thickness (scan 1 and 2 of exercise group) clearly increases with the amount of averaged A-scans. The global mean RNFL thickness is indicated by n=1, twelve clock-wise sectors by n=12 and the full set of all 768 A-scans by n=768. The change in CV between the baseline (scan 1) and second scan (scan 2) in the exercise group is comparable for the two types of software (HE and OCTSEG).

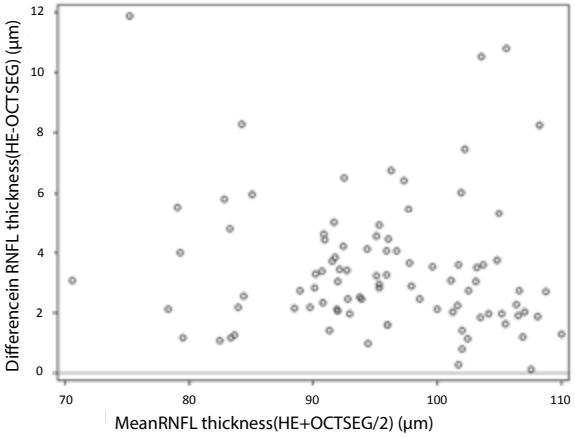

Supplementary Figure 2. Bland-Altman plot comparing the RNFL thickness of both types of segmentation software. For every subject the global average data were used. The plot demonstrates a systematic difference between the two algorithms with consistently higher values for the HE software.

REFERENCES

1. Talman LS, Bisker ER, Sackel DJ, et al. Longitudinal study of vision and retinal nerve fiber layer thickness in multiple sclerosis. *Ann Neurol* 2010;67:749-760.
2. Parisi V, Restuccia R, Fattapposta F, Mina C, Bucci MG, Pierelli F. Morphological and functional retinal impairment in Alzheimer's disease patients. *Clin Neurophysiol* 2001;112:1860-1867.
3. Paquet C, Boissonnot M, Roger F, Dighiero P, Gil R, Hugon J. Abnormal retinal thickness in patients with mild cognitive impairment and Alzheimer's disease. *Neurosci Lett* 2007;420:97-99.
4. Altintas O, Iseri P, Ozkan B, Caglar Y. Correlation between retinal morphological and functional findings and clinical severity in Parkinson's disease. *Doc Ophthalmol* 2008;116:137-146.
5. Brandt AU, Zimmermann H, Kaufhold F, et al. Patterns of retinal damage facilitate differential diagnosis between Susac syndrome and MS. *PLoS One* 2012;7:e38741.
6. Garcia-Martin E, Satue M, Fuertes I, et al. Ability and reproducibility of Fourier-domain optical coherence tomography to detect retinal nerve fiber layer atrophy in Parkinson's disease. *Ophthalmology* 2012;119:2161-2167.
7. He X-F, Liu Y-T, Peng C, Zhang F, Zhuang S, Zhang J-S. Optical coherence tomography assessed retinal nerve fiber layer thickness in patients with Alzheimer's disease: a meta-analysis. *Int J Ophthalmol* 2012;5:401-405.
8. Albrecht P, Muller A-K, Ringelstein M, et al. Retinal neurodegeneration in Wilson's disease revealed by spectral domain optical coherence tomography. *PLoS One* 2012;7:e49825.
9. Kirbas S, Turkyilmaz K, Tufekci A, Durmus M. Retinal nerve fiber layer thickness in Parkinson disease. *J Neuroophthalmol* 2013;33:62-65.
10. Marziani E, Pomati S, Ramolfo P, et al. Evaluation of retinal nerve fiber layer and ganglion cell layer thickness in Alzheimer's disease using spectral-domain optical coherence tomography. *Invest Ophthalmol Vis Sci* 2013;54:5953-5958.
11. Arthur SN, Smith SD, Wright MM, et al. Reproducibility and agreement in evaluating retinal nerve fibre layer thickness between Stratus and Spectralis OCT. *Eye (London)* 2011;25:192-200.
12. Balk LJ, Petzold A. Influence of the eye-tracking-based follow-up function in retinal nerve fiber layer thickness using fourier-domain optical coherence tomography. *Invest Ophthalmol Vis Sci* 2013;54:3045.
13. Jo Y-J, Heo D-W, Shin Y-I, Kim J-Y. Diurnal variation of retina thickness measured with time domain and spectral domain optical coherence tomography in healthy subjects. *Invest Ophthalmol Vis Sci* 2011;52:6497-6500.
14. Read SA, Collins MJ, Alonso-Caneiro D. Diurnal variation of retinal thickness with spectral domain OCT. Optom Vis Sci 2012;89:611-619
15. Tan CS, Ouyang Y, Ruiz H, Sadda SR. Diurnal variation of choroidal thickness in normal, healthy subjects measured by spectral domain optical coherence tomography. *Invest Ophthalmol Vis Sci* 2012;53:261-266.
16. Balk L, Mayer M, Uitdehaag BMJ, Petzold A. Physiological variation of segmented OCT retinal layer thicknesses is short-lasting. *J Neurol* 2013;260:3109-3114.
17. de Kinkelder R, Kalkman J, Faber DJ, et al. Heartbeat-induced axial motion artifacts in optical coherence tomography measurements of the retina. *Invest Ophthalmol Vis Sci* 2011;52:3908-3913.
18. Steiner MJ, DeWalt DA, Byerley JS. Is this child dehydrated? *JAMA* 2004;291:2746-2754.
19. Tewarie P, Balk L, Costello F, et al. The OSCAR-IB consensus criteria for retinal OCT quality assessment. *PLoS One* 20127:e34823.
20. Wolf-Schnurrbusch UEK, Ceklic L, Brinkmann CK, et al. Macular thickness measurements in healthy eyes using six different optical coherence tomography instruments. *Invest Ophthalmol Vis Sci* 2009;50:3432-3437.
21. Foo LL, Perera SA, Cheung CY, et al. Comparison of scanning laser ophthalmoscopy and high-definition optical coherence tomography measurements of optic disc parameters. *Br J Ophthalmol* 2012;96:576-580.
22. Balk LJ, Sonder JM, Strijbis EMM, et al. The physiological variation of the retinal nerve fiber layer thickness and macular volume in humans as assessed by spectral domain-optical coherence tomography. *Invest Ophthalmol Vis Sci* 2012;53:1251-1257.

23. Buchser NM, Wollstein G, Ishikawa H, et al. Comparison of retinal nerve fiber layer thickness measurement bias and imprecision across three spectral-domain optical coherence tomography devices. *Invest Ophthalmol Vis Sci* 2012;53:3742-3747.

24. Kiernan DF, Mieler WF, Hariprasad SM. Spectral-domain optical coherence tomography: a comparison of modern highresolution retinal imaging systems. *Am J Ophthalmol* 2010;149:18-31.

25. Savini G, Carbonelli M, Barboni P. Retinal nerve fiber layer thickness measurement by Fourier-domain optical coherence tomography: a comparison between cirrus-HD OCT and RTVue in healthy eyes. *J Glaucoma* 2010;19:369-372.

26. Sull AC, Vuong LN, Price LL, et al. Comparison of spectral/Fourier domain optical coherence tomography instruments for assessment of normal macular thickness. *Retina* 2010;30:235-245.

27. Watson GM, Keltner JL, Chin EK, Harvey D, Nguyen A, Park SS. Comparison of retinal nerve fiber layer and central macular thickness measurements among five different optical coherence tomography instruments in patients with multiple sclerosis and optic neuritis. *J Neuroophthalmol* 2011;31:110-116.

28. Lammer J, Scholda C, Prunte C, Benesch T, Schmidt-Erfurth U, Bolz M. Retinal thickness and volume measurements in diabetic macular edema: a comparison of four optical coherence tomography systems. *Retina* 2011;31:48-55.

29. Tatrai E, Ranganathan S, Ferencz M, DeBuc DC, Somfai GM. Comparison of retinal thickness by Fourier-domain optical coherence tomography and OCT retinal image analysis software segmentation analysis derived from Stratus optical coherence tomography images. *J Biomed Opt* 2011;16:056004.

Chapter 2.3

Physiological variation of retinal layer thickness is not caused by hydration: A randomised trial

LJ Balk, T Oberwahrenbrock, BMJ Uitdehaag, A Petzold

J Neurol Sci. **2014 Jun 30. [Epub ahead of print]**

ABSTRACT

Purpose There is evidence for physiological variation of retinal thicknesses as determined by optical coherence tomography (OCT). We tested if such changes could be explained by hydration and would exceed what may be expected from normal ageing.

Methods Subjects (N=26) of a previous study were re-assessed and were randomized to 3 groups of a hydration escalation trial (no hydration, 1x hydration, 2 hydration). Automated retinal layer segmentations were performed for the macular retinal nerve fibre layer (RNFL), ganglion cell layer (GCL), inner plexiform layer (IPL), inner nuclear layer (INL), outer plexiform layer (OPL) and outer nuclear layer (ONL). The averaged volumes were calculated for the central foveola, 3 mm and 6 mm circles of the ETDRS grid.

Results Following oral hydration there were no significant differences of retinal layer thicknesses between the three randomised groups in any of the ETDRS regions at any time-point. Ageing related changes were significant over an 18 month period for the GCL.

Conclusions The negative outcome of this trial implies that, until the causes for the observed variation are resolved, investigators may need to accept, and include into trial power calculations, a small degree of variation (< 1%) of quantitative SD-OCT imaging either due to human physiology or instrument/software related factors.

INTRODUCTION

A significant degree of variability of retinal layer thicknesses has been observed by several groups under physiological and pathological conditions.[1-7] These data are relevant to clinical studies employing optical coherence tomography (OCT) as biomarker for neurodegeneration because typically, only small changes are observed. The cause for the observed retinal layer thickness changes remains however unknown. Several hypotheses have been put forward. First, relying on measurement of the diurnal variation (8 am, 6 pm, 52 eyes) methodological limitations of time domain optical coherence tomography (TD-OCT) were held responsible for the variability of the entire retinal thickness.[2] However, others and we have also observed physiological variation of the entire retinal thickness and individually segmented retinal layers using spectral domain optical coherence tomography (SD-OCT).[1,3-5] Second, also relying on measurements of diurnal variation, it was suggested that this may be due to changes in blood pressure, retinal metabolism, and standing position.[7] Third, one may attribute disease related factors to the observed changes in some studies,[6-8] but this would not explain the variation observed in healthy control subjects.[1-5] Importantly, three studies using SD-OCT found variation of individual retinal layers in healthy control subjects.[1,3-5] A limitation of studies on the diurnal variation is that the interpretation of causative factors remains retrospective and speculative. In contrast, prospective assessment of these changes in an experimental and control group under well controlled conditions permits to document such factors. For this reason we had recorded several physiological factors and quantified retinal layer thicknesses at strenuous exercise (experimental group) and at rest (control group) under time-matched diurnal conditions.[1] At the time we discussed the possible influence of the haemodynamic factors and the hydration state.[1] Re-analysis of our data, excluding retinal blood vessel related segmentation artefacts, suggested that these masked rather then caused physiological changes.[9] Individual layer related thickness changes were of such short duration (1-2 h) that rapid water volume shifts seemed as a more likely explanation.[10]

This study had two objectives: first, to evaluate the effect of hydration on individual retinal layer thicknesses (hydration escalation trial); second, to assess the age-related change on individual retinal layer thicknesses (longitudinal study). We therefore contacted the same subjects participating in our original study[1] again eighteen months after the event.

METHODS

Ethical approval, institutional board review (IRB) and written informed consent from all subjects were obtained.

Study design

The study designs for the hydration trial and the longitudinal observational study are summarised in Figure 1. Twenty-six of the 69 healthy subjects participating in the original study[1] agreed to be followed-up. The follow-up took place 18 months after the charity run of the original study. All re-assessed 26 subjects underwent three subsequent SD-OCT scans. A hydration escalation protocol was used to test for a possible plateau effect. For hydration, 500 mL of an isotonic sport drink was used for every time point (Figure 1A). For all subjects who participated in the hydration trial, 18 month longitudinal data for only one eye was available (Figure 1B).

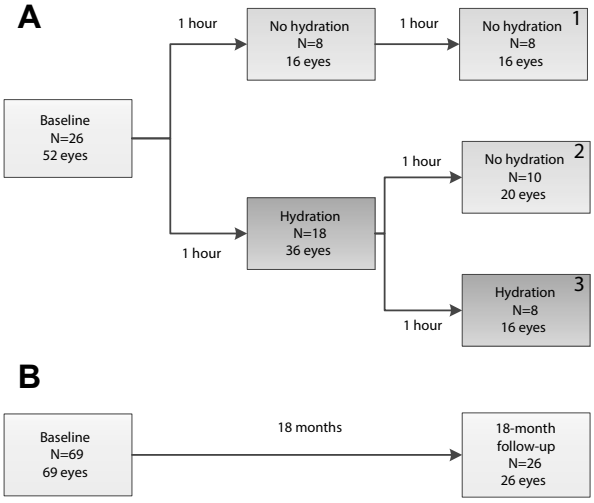

Figure 1. Flow chart of the study design. (A) The hydration trial tested if there were changes of retinal layer thicknesses related to hydration. (B) The longitudinal study tested if there were changes of retinal layer thicknesses related to ageing. Retinal SD-OCT scans were acquired at the time points indicated by boxes.

SD-OCT

In the hydration trial, a macular volume scan (20x20°) was performed at three time points. All images were obtained with a SD-OCT (Heidelberg Spectralis, software version 1.1.6.3) with the eye tracking function (EBF) enabled which, in our experience, provides the best accuracy.[11] Image co-registration was used to allow for optimal anatomical alignment.

Automated retinal layer segmentation

Automated segmentation of the individual retinal layers was performed with validated beta-software provided by Heidelberg Engineering (Heidelberg, Germany) [Oberwahrenbrock et al. Multicenter Inter-rater Reliability of Retinal Layer Segmentation Using Spectral domain OCT, submitted]. The intra-class correlation coefficients were 0.98 (RNFL), 0.90 (GCL), 0.7 (IPL), 0.98 (GCIP), 0.99 (INL), 0.91 (OPL) and 0.94 (ONL). Macular layer thickness maps were created in MATLAB 2012b (Mathworks, Ismaning, Germany) as previously described.[12] Figure 2 shows the regions of the EDTRS grid used for statistical analyses and the segmented layers.

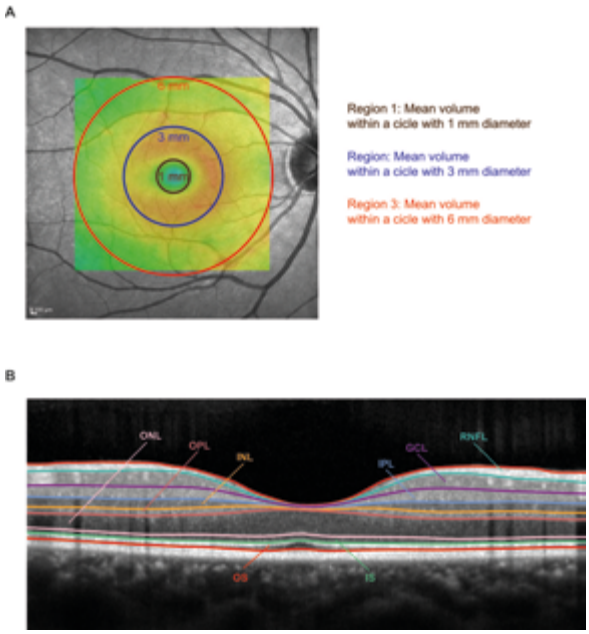

Figure 2. The (A) ETDRS grid regions and (B) retinal layers used for statistical analyses are shown.

Theory/calculation

SAS software (version 9.3) was used for statistical analysis and preparation of figures. Subjects were randomised to three hydration groups using SAS. Group 1 consisted of subjects receiving no hydration at all, group 2 of subjects receiving hydration only after the first OCT measurement and group 3 of subjects receiving hydration after the first and second OCT measurement. The change of retinal layer thicknesses for the four measurement points was calculated as before: follow-up data were normalised to baseline (100%).[1] Non-Gaussian data were presented as median, interquartile range (IQR). The non-parametric Wilcoxon two-sample test was used for comparison of two

and general linear models (GLM) for repeated measures for comparison of more than two variables as in our previous analyses.[1,10] Analyses were adjusted for age and for each subject both eyes were considered as outlined in Figure 1. The chi-square test was used for categorical data analysis. Level of significance was set to alpha 0.05. The Bonferroni method was used to correct for multiple testing.

RESULTS

The baseline characteristics of the subjects were summarised in Table 1. There were no significant differences for age, weight, height or BMI between the three groups.

Table 1 Subjects' characteristics. The median and interquartile range (IQR) are shown.

	Group 1 (no hydration)	***Group 2 (1x hydration)***	***Group 3 (2x hydration)***	***Total (pooled data)***
Subjects	8	10	8	26
Eyes	16	20	16	52
Age (years)	45 (35-52)	44 (29-54)	30 (27-51)	41 (29-52)
Gender (m:f)	6:2	6:4	6:2	18:8
Weight (kg)	72 (67-90)	76 (71-86)	79 (67-94)	74 (68-89)
Height (m)	1.80 (1.76-1.85)	1.78 (1.73-1.83)	1.82 (1.77-1.87)	1.80 (1.77-1.84)
BMI	22.8 (21.7-26.6)	23.6 (21.9-25.5)	25.2 (21.2-29.0)	23.5 (21.7-25.6)

Hydration trial

All subjects completed the hydration trial (Figure 1A). A small (<1%) degree of layer thickness variation was observed between the three measurement points (Figure 3, not significant). There was no statistically significant relationship whatsoever between changes of retinal layer thicknesses in any of the three ETDRS regions tested at any time-point. Particularly data for the RNFL, GCL and INL showed only a small degree of scatter over time. Data for the IPL, OPL, ONL, IS and OS were more noisy.

Longitudinal study

There were significant changes in the longitudinal study (Figure 1B). Significant thinning was observed for the GCL. The median decrease for the GCL was 1.9% within the 3 mm (Figure 4, $p<0.01$) and 1.2% within the 6 mm ETDRS circles ($p<0.01$). Significant thickening was observed for the ONL. The median increase for the ONL was 1.9% within the 3 mm ($p<0.01$) and 2.5% within the 6 mm ETDRS circles ($p<0.001$). Figure 3 also suggested a trend for increased layer thicknesses for the RNFL and INL, but statistical significance was missed after Bonferroni correction for multiple comparisons (corrected p-value = 0.016).

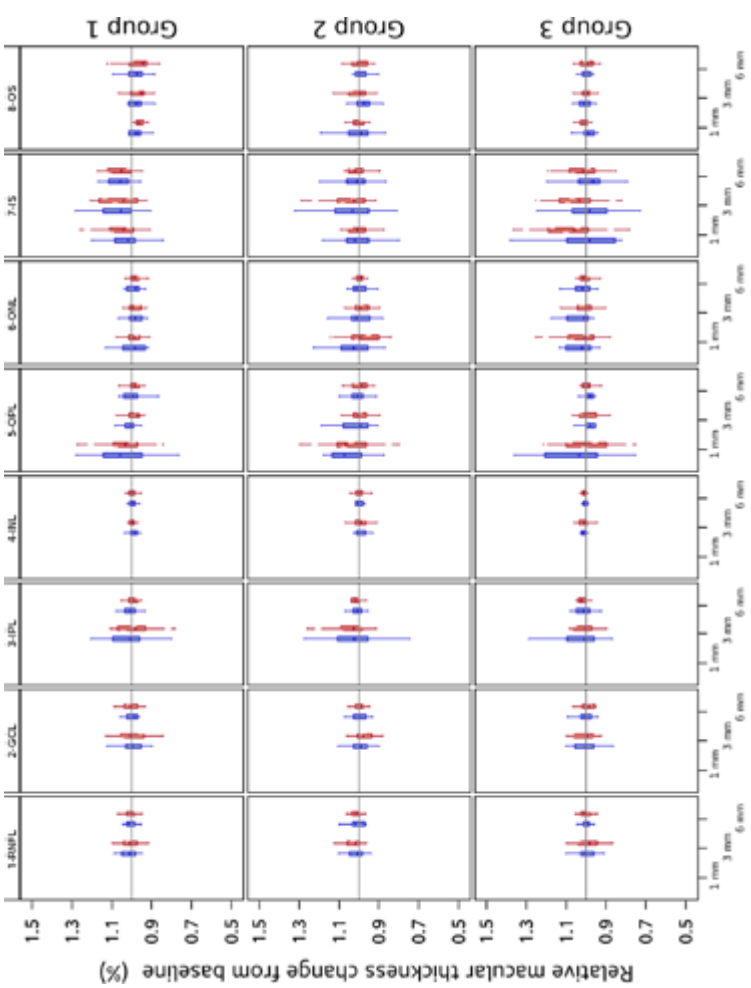

Figure 3. Oral hydration does not affect retinal layer thicknesses. The relative changes from baseline (horizontal grey line) are shown after 1 h (blue, first box-and-whisker) and 2 h (red, second box-and-whisker). Subjects receiving no hydration (group 1) are shown on the top, subjects receiving one drink (group 2) in the middle and subjects receiving two drinks (group 3) at the bottom. Data were presented for three regions of the ETDRS grid; foveola = 1 mm, 3 mm and 6 mm. There were no significant differences between the groups for any of the retinal layers in any ETDRS region at any time point.
The relative macular thickness changes were normalised to the baseline values of the hydration escalation trial. The horizontal grey line represents the normalised baseline data (100%). Data above the grey line indicates retinal layer thickness increase and data below the grey line indicates retinal layer thickness decrease. Data for retinal layers were only reported where anatomically present. Therefore no data were reported in the foveola for the RNFL, GCL, INL and IPL.

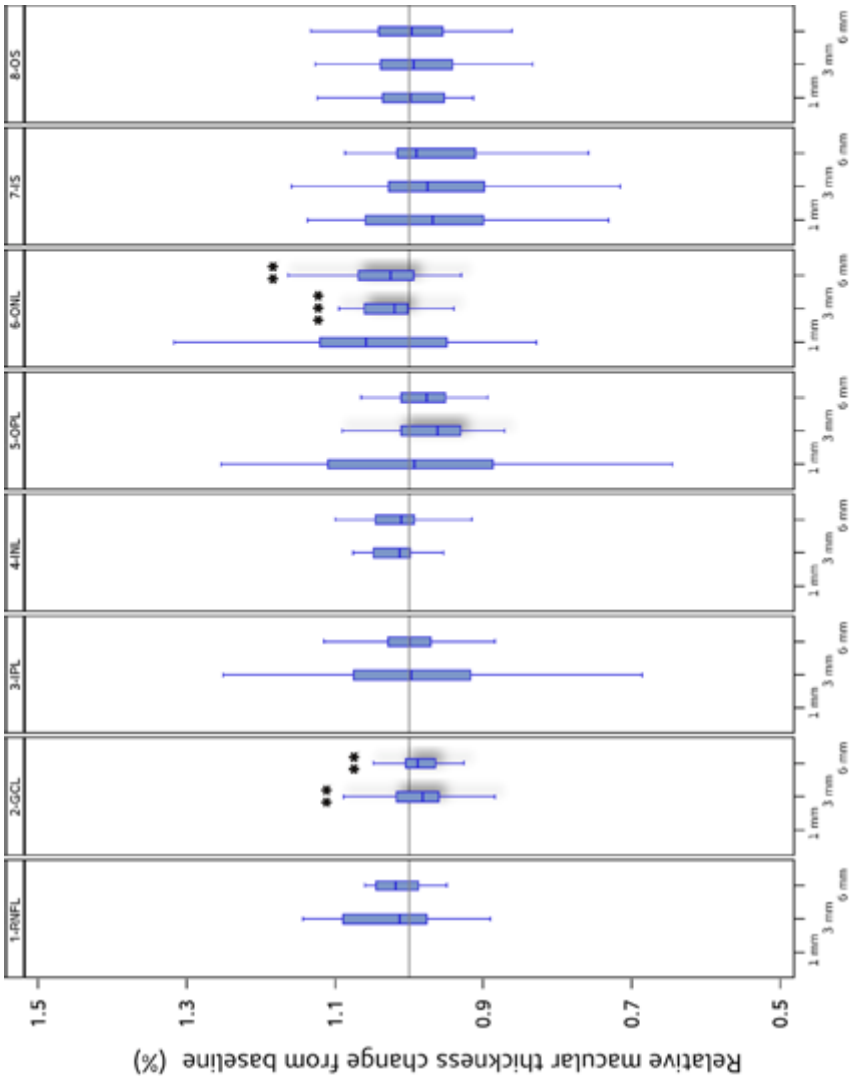

Figure 4. Ageing related changes of retinal layer thicknesses over an 18 month period. Regions for the ETDRS grid were as in Figure 3 and axes were scaled to the same size. The Bonferroni corrected p-value for a predefined alpha of 0.05 calculates to 0.016, ** = p<0.01, *** = p<0.001.

DISCUSSION

This study investigated if oral hydration might be a factor to consider for longitudinal retinal OCT studies. The paradigm was tested prospectively in a randomised trial setting. The negative data of the study suggests that oral hydration is not responsible for the observed physiological variation of retinal layer thicknesses.[1-7]

The study also suggests that there is a significant loss of retinal ganglion cells in the macular region (1.9%) which can be observed within an 18 month period. But we caution against extrapolation from this data, because the observed rate of atrophy is more than what one would expect for healthy control subjects.

Whilst this study was under review Narayanan et al. reported a -0.88 µm/year decrease of the combined GCL/IPL in patients with one single episode of optic neuritis and a -0.49 µm/year decrease in patients with multiple sclerosis without MS.[12] From their Table 1, the percentage loss for the entire macular region in the latter group calculates to 0.55% per year, or 0.81% over an 18 month period. A notable limitation of this study was the range of the OCT follow-up from two months to 3.8 years.[12]

Interestingly, on a group levels, there was also a 1.9% increase of the ONL, in the 3 mm ETDRS circle. This increase in outer retinal layer thickness is not well understood, but has also been observed in a cross-sectional study in patients with multiple sclerosis who never had optic neuritis if compared to healthy control subjects.[13] Whilst it will remain a speculation to suggest compensatory mechanisms for these observations, the point can be made that total retinal thickness measurements (a sum of the inner and outer retinal layers) are unlikely to provide a reliable surrogate outcome for neurodegeneration. Likewise, for the larger 6 mm ETDRS circle a 1.2% loss of GCL was observed. The corresponding increase of the ONL was larger with 2.5%. There are yet no longitudinal studies in healthy control subjects which permit to compare these segmented layer data. The age range was too narrow (22-57 years) and study was underpowered to analyse if there was a relationship between GCL atrophy and age.

Paradoxically, given the significant decrease of the GCL, there was a trend for an increase of the RNFL over the 18 month observation period. Although statistical significance was narrowly missed for the 6 mm ETDRS circle ($p=0.02$) after Bonferroni correction (the corrected p-value for alpha 0.05 is <0.016), this was clearly due to the limited power of the study. Careful observation of Figure 3 did not reveal similar short term changes within the 6 mm ETDRS circle for the RNFL in either of the three groups. From the present data we are unable to tell whether these changes in macular RNFL thickness are more likely to be physiological in nature or related to ganglion cell dropout.

Limitations of this study include the accuracy of individual layer segmentation. Particularly, the low contrast between the GCL and IPL remains a challenge. Therefore,

mild degrees of GCL thickness changes following hydration might be masked by measurement noise. On the other side of the argument one needs to be cautious with regard to possible measurement artefacts due to the challenges of the GCL/IPL differentiation. The algorithm used in this present study was not able to suppress blood vessel artefacts which were found to be relevant in a previous study.[9] Likewise, the external limiting membrane which discriminates between the ONL and IS is not always clearly visible for each of the OCT B-scans comprising a comprehensive macular volume scan. Consequently, possible ONL thickness changes remain to be interpreted with caution. Taken together, the factors relevant to explain the frequently reported physiological and diurnal variation of retinal layer thicknesses remain unknown.[1-7] Phantom eye data suggests that instrument/software related factors may also be relevant.[14] These authors suggest a variation of (non quality controlled) vertical thickness measurements between two different Heidelberg Spectralis instruments in the range of 4 µm (184 µm versus 188 µm) which calculates to 2.1% (Table 2 in reference 14). This exceeds our and others' experience with this instrument , if rigorous quality control criteria are applied.[11,15,16] Still, the topic of normal thickness variability needs to be solved because the degree of normal variation is relevant for the small changes observed with neurodegeneration but the related causes remain unknown.

Conclusions

First, this study provides prospective, longitudinal evidence for a significant degree of ganglion cell loss in healthy control subjects over an 18 month period which exceeds the short term physiological variation of the GCL. Second, the negative outcome of the oral hydration trial is of practical relevance because patients should be allowed to consume fluids as they please as this does not interfere with subsequent measurements. Third, unless the issue of normal variation is resolved, clinical investigators may have to consider a small degree of variation (<1%, Figure 3) for clinical trials. More specifically, this information will need to be included in power calculations for trials designed to observe only very small degrees of retinal layer thickness changes.

REFERENCES

1. Balk LJ, Sonder JM, Strijbis EMM, et al. The physiological variation of the retinal nerve fiber layer thickness and macular volume in humans as assessed by spectral domain-optical coherence tomography. *Invest Ophthalmol Vis Sci* 2012;53:1251-1257.
2. Jo YJ, Heo DW, Shin YI, and Kim JY. Diurnal variation of retina thickness measured with time domain and spectral domain optical coherence tomography in healthy subjects. *Invest Ophthalmol Vis Sci* 2011;52:6497-6500.
3. Read SA, Collins MJ, and Alonso-Caneiro D. Diurnal Variation of Retinal Thickness with Spectral Domain OCT. *Optom Vis Sci* 2012;89:611-619.
4. Usui S, Ikuno Y, Akiba M, et al. Circadian changes in subfoveal choroidal thickness and the relationship with circulatory factors in healthy subjects. *Invest Ophthalmol Vis Sci* 2012;53:2300-2307.
5. Tan CS, Ouyang Y, Ruiz H, and Sadda SR. Diurnal variation of choroidal thickness in normal, healthy subjects measured by spectral domain optical coherence tomography. *Invest Ophthalmol Vis Sci* 2012;53:261-266.
6. Frank RN, Schulz L, Abe K, and Iezzi R. Temporal variation in diabetic macular edema measured by optical coherence tomography. *Ophthalmology* 2004;111:211-217.
7. Gupta B, Grewal J, Adewoyin T, Pelosini L, and Williamson TH. Diurnal variation of macular oedema in CRVO: prospective study. *Graefes Arch Clin Exp Ophthalmol* 2009;247:593-596.
8. Diabetic Retinopathy Clinical Research Network, Danis RP, Glassman AR, et al. Diurnal variation in retinal thickening measurement by optical coherence tomography in center-involved diabetic macular edema. *Arch Ophthalmol* 2006;124:1701-1707.
9. Balk L, Mayer M, Uitdehaag B, and Petzold A. Retinal hyperaemia related blood vessel artifacts are relevant to automated OCT layer segmentation. *J Neurol* 2014;261:511-7.
10. Balk L, Mayer M, Uitdehaag BMJ, and Petzold A. Physiological variation of segmented OCT retinal layer thicknesses is short-lasting. *J Neurol* 2013;260:3109-3114.
11. Balk LJ and Petzold A. Influence of the eye-tracking-based follow-up function in retinal nerve fiber layer thickness using fourier-domain optical coherence tomography. *Invest Ophthalmol Vis Sci* 2013;54:3045.
12. Narayanan D, Cheng H, Bonem KN, Saenz R, Tang RA and Frishman LJ. Tracking changes over time in retinal nerve fiber layer and ganglion cell-inner plexiform layer thickness in multiple sclerosis. *Mult Scler* 2014 Mar 17. [Epub ahead of print]
13. Balk LJ, Twisk JWR, Steenwijk MD, Daams M, Tewarie P, Killestein J, et al. A dam for retrograde axonal degeneration in multiple sclerosis?, *J Neurol Neurosurg Psychiatry* 2014,85:782-789
14. Folgar FA, Yuan EL, Farsiu S, and Toth CA. Lateral and axial measurement differences between spectral-domain optical coherence tomography systems. *J Biomed Opt* 2014;19:16014.
15. Tewarie P, Balk L, Costello F, et al. The OSCAR-IB Consensus Criteria for Retinal OCT Quality Assessment. *PLoS One* 2012;7:e34823.
16. Wolf-Schnurrbusch UEK, Ceklic L, Brinkmann CK, et al. Macular thickness measurements in healthy eyes using six different optical coherence tomography instruments. *Invest Ophthalmol Vis Sci* 2009;50:3432-3437.

Chapter 3

OSCAR-IB criteria

Chapter 3.1

A simple sign for recognising off-axis OCT measurement beam placement in the context of multicentre studies

LJ Balk, WAEJ de Vries-Knoppert, A Petzold

***PLoS One*. 2012;7:e48222**

ABSTRACT

Purpose Optical coherence tomography (OCT) allows quantification of the thickness of the retinal nerve fibre layer (RNFL) thickness, a potential biomarker for neurodegeneration. The estimated annual RNFL loss in multiple sclerosis amounts to 2 µm using time domain OCT. The recognition of measurement artefacts exceeding this limit is relevant for the successful use of OCT as a secondary outcome measure in clinical trials.

Methods Prospective study design. An exploratory pilot study (ring and volume scans) followed by a cohort study (1,980 OCT ring scans). The OCT measurement beam was placed off-axis to the left, right, top and bottom of the subjects pupil and RNFL thickness of these scans were compared to the centrally placed reference scans.

Results Off-axis placement of the OCT measurement beam resulted in significant artefacts in RNFL thickness measurements (95%CI ± 9 µm, maximal size of error 42 µm). Off-axis placement gave characteristic patterns of the OCT live images which are not necessarily saved for review. Off-axis placement also causes regional inhomogeneity of reflectivity in the outer nuclear (ONL) and outer plexiform layers (OPL) which remains visible on scans saved for review.

Conclusion Off-axis beam placement introduces measurement artefacts at a magnitude which may mask recognition of RNFL loss due to neurodegeneration in multiple sclerosis. The resulting pattern in the OCT live image can only be recognised by the technician capturing the scans. Once the averaged scans have been aligned this pattern is lost. Retrospective identification of this artefact is however possible by presence of regional inhomogeneity of ONL/OPL reflectivity. This simple and robust sign may be considered for quality control criteria in the setting of multicentre OCT studies. The practical advice of this study is to keep the OCT image in the acquisition window horizontally aligned whenever possible.

INTRODUCTION

Accurate assessment of neurodegeneration is important for prognosis and evaluation of neuroprotective treatment strategies. Spectral-domain (SD) optical coherence tomography (OCT) allows to quantify RNFL thickness changes with a precision in the range of 1.14-2.39 μm.[1] It has been proposed that OCT measurements of the retina may provide promising primary outcome measures for neuroprotective treatment trials in multiple sclerosis (MS).[2,3]

The estimated annual loss of RNFL thickness in MS is about 1-2 μm.[4] Longitudinal, observational studies are underway to validate these findings with the newer, high resolution SD-OCT technology. As with other imaging studies of neurodegeneration,[2] qualified assessment of the OCT will become a requirement for high quality multicentre studies. At present there are no validated reading centre criteria available for the assessment of OCT scans in MS. A review of the literature shows that the most frequently reported errors are related to boundary line errors, poor signal strength or bad placement of the ring scan at the optic nerve head (ONH).[5] To the best of our knowledge, the potential artefact introduced by off-axis placement of the measurement beam is not known and is therefore investigated in this study.

METHODS

This study was approved by the medical ethical committee (protocol number 2010/336) and the scientific research committee (protocol number CWO/10-22E) of the of the VU University Medical Centre in Amsterdam, the Netherlands. The individuals in video S1 have given written informed consent (as outlined in PLOS consent form) to publish the video material.

This study consists of a video documented pilot and a main study. In both studies all scans were recorded by one qualified operator, using SD-OCT (Heidelberg Spectralis, Software version 1.1.6.3) with the eye tracking function enabled. In the pilot study, all scans were obtained in the right eye (0 dpt, both with dilated (Tropicamide 0.5%) and undilated pupil) of one subject. Four OCT scans were performed: (1) a ring scan (diameter 12° or 2.4 cm, 20-25 ART) at the ONH, (2) a macular volume scan (20 x 20°, 49 ART, 25 sections), (3) a papillomacular bundle (PMB) volume scan set at a 7° angle at the macular of 20° length and 4° width (105 sections) and (4) an ONH volume scan (15 x 15°, 24 ART, 73 sections). The first of each scan was set as reference. The automated follow-up option was used for repeat scans. The OCT measurement beam was placed

about 2 mm off-axis temporal, nasal, superior and inferior from the subjects pupil centre. Locations were changed randomly. A total of 10 measurements were taken per location.

For the main study, all measurements were taken in a dimmed room and pupil size was measured. Pharmacological pupil dilatation was not performed. The same ring scan at the ONH was assessed in both eyes of 11 subjects at 9 locations. The first location was with central beam placement and defined as the reference scan. As for the pilot study, the eye-tracking function was enabled and the very first scan used as reference for automated placement of the ring-scan for the following scans. The second location was a small degree of superior off-axis placement (about 1/3 of the individual pupil size), resulting in a live image slightly deviating from a straight horizontal OCT image. The third location was a larger (about 2/3 of the individual pupil size) superior displacement. The fourth and fifth location were respective small and large temporal displacements. The sixth and seventh location were respective small and large inferior displacements. The eighth and ninth location were respective small and large nasal displacements. In addition, all subjects underwent formal automated perimetry using 30-2 threshold test (SITA-Standard strategy) on the Humphrey field analyser (Carl Zeiss Meditec, Dublin, CA, USA). Refractive errors were corrected using wide angle lenses. Visual field data was reported as the overall field mean deviation as derived from control data provided by the manufacturer.

All statistical analyses were performed using SAS software (V9.2). The mean ± standard deviation (SD) are presented. The Kruskal-Wallis test was used for comparison of multiple groups within each retinal sector. Two types of analyses were performed. First, the absolute values of the RNFL thickness were compared for each eye separately in each subject in order to test whether off-axis beam placement may matter on an individual subject basis. Second, a group comparison was performed. In order to compare the RNFL values the absolute size of the error in µm was calculated. Because equal sized errors in different directions (e.g. +x µm and -x µm) average each other statistically, $|x|$ was used to indicate the size of the measurement error for descriptive data analysis.

RESULTS

Pilot study

The video (video 1, supplementary data) gives a live coverage of the effect of off-axis measurement beam placement.

To illustrate the problem the effect of nasal and temporal off-axis measurement beam placement on RNFL thickness data is shown (Figure 1 A-E). With temporal/nasal off-axis

placement the path-length for light reflected from the nasal and temporal proportion of the ONH differ such that the OCT live B-scan appears to be tilted in opposite directions (Figure 1 B&C). This tilt is not anymore seen on the averaged summary image (Figure 1 D&E). The resulting measurement artefacts in per sector ranged from -5 µm for the PMB in the temporal sector to +7 µm (nasal sector) (Figure 1 D&E).

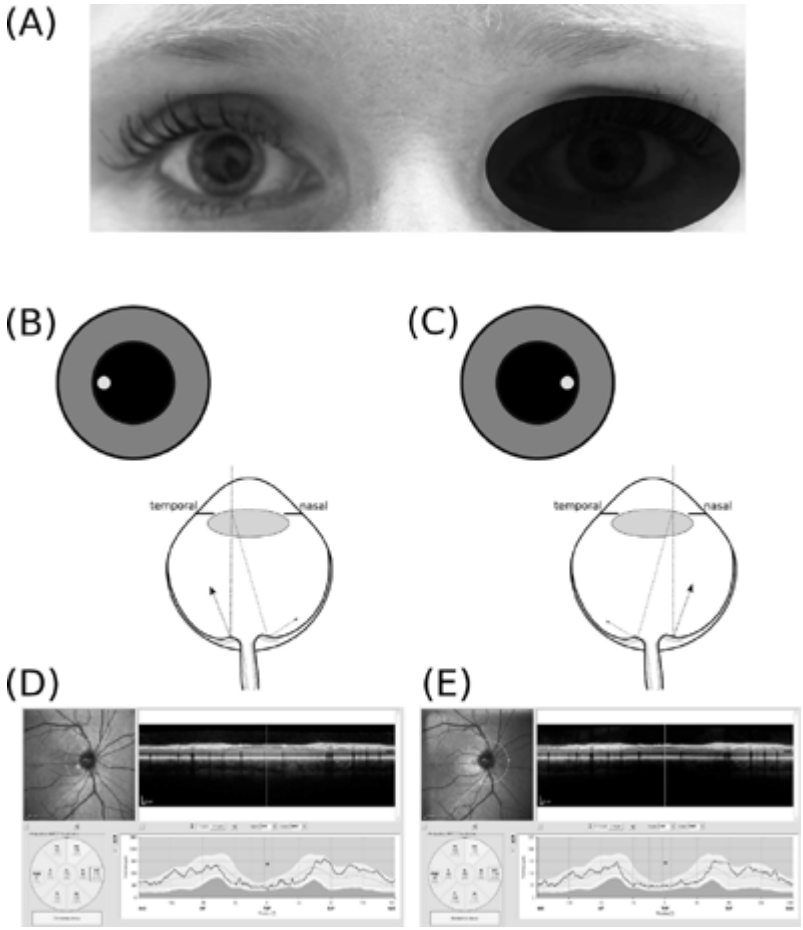

Figure 1. Off centre placement of the measurement beam. **(A)** The OCT measurement beam is focused on the dilated right eye of subject #1, **(B)** temporal off-axis placement of the measurement beam results in a shorter light path to the temporal part of the optic nerve head (dotted line) and a longer pathway from the nasal part of the optic nerve head (dotted-dashed line). The difference in path length results in a tilted appearance of the B-scan. **(C)** Nasal off-axis placement of the measurement beam results in a mirror pattern. The resulting averaged OCT image is of good quality (ART 25, signal strength 35 dB) for both **(D)** temporal off-axis placement and **(E)** nasal off-axis placement. The quantification of the RNFL thickness by the algorithm is however clearly different (Global average OD with temporal off-axis placement 106 µm and nasal off-axis placement 103 µm).

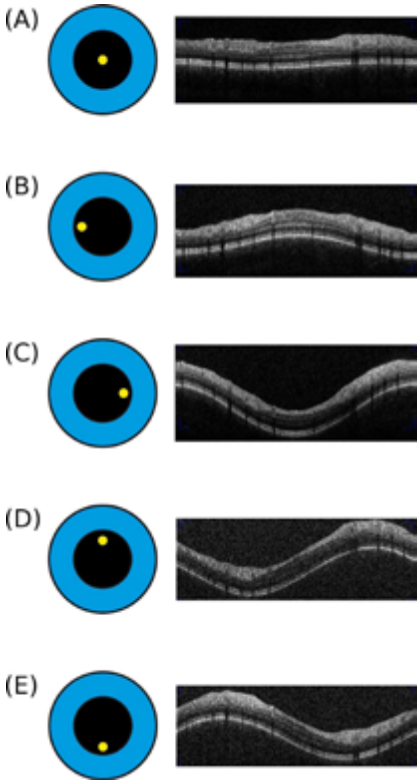

Figure 2. Off centre placement of the OCT measurement beam results in tilted images. Here we show the OCT live image obtained by the optic nerve head ring scan. **(A)** The reference scan with the measurement beam (yellow dot) being placed centrally in the pupil (black circle). This results in a correct, horizontal OCT live image. Note, the live image will not be visible to the reading centre (note the live image was taken as a screen shot during the imaging and appears in print in lower quality than in reality. Please see the video in the supplementary material for a live coverage image acquisition). **(B)** Temporal off-axis placement of the measurement beam results in a centrally convex live image. **(C)** Nasal off-axis placement results in a centrally concave OCT live image. **(D)** Superior off-axis placement results in a rising wave which is mirrored by **(E)** inferior off-axis placement (a falling wave). Please note that for didactic purposes the off-axis placement of the measurement beam is shown for an idealised situation with a central fixation target for a perfectly aligned right subject's eye from the OCT operators point of view.

The appearance of the tilted live OCT B-scan is highly reproducible on repeat assessments. A central OCT measurement beam placement always resulted in a horizontally aligned OCT retinal live image (Figure 2 A). Off-axis placement of the OCT measurement beam caused a reproducible and characteristic retinal pattern: (1) centrally convex if placed temporal (Figure 2 B), (2) centrally concave if placed nasal (Figure 2 C), (3) a rising wave if placed superior (Figure 2 D) and (4) a falling wave if placed inferior to the pupil centre (Figure 2 E). Of note, even a relative small degree off-

axis beam placement as used for the pilot study will cause a clearly visible wave OCT image waveform on the live screen (see also video S1).
Importantly, the live image will not be visible to a reading centre. In fact, the images shown in Figure 2 were taken with the computer's screen-shot function. A reading centre will receive a horizontally aligned average image. The average images corresponding to the live images from Figure 2 are shown in Figure 3. With central placement of the measurement beam the ONL reflectivity is homogeneous (bottom black arrow in Figure 3 A). The OCT signal strength was good and the automated segmentation algorithm correctly identifies the RNFL boundaries (red lines in Figure 3 A). Off-axis placement of the OCT measurement beam produces a reproducible change in light backscattering from the ONL. Figure 3 shows the effects on the ONL reflectivity for temporal, nasal, superior and inferior of off-axis placement. This inhomogeneity of the ONL reflectivity was also visible on all volume scans.

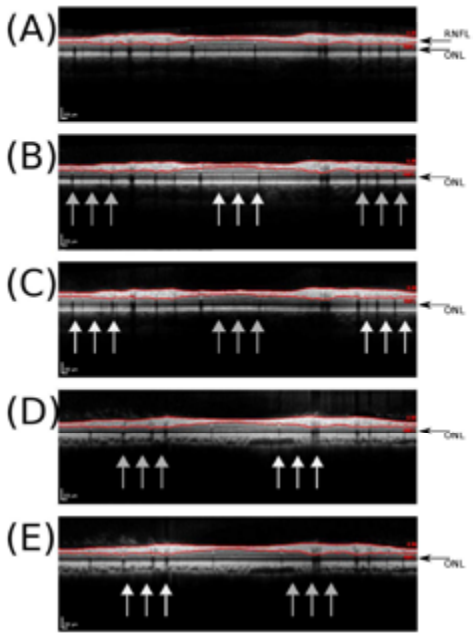

Figure 3. Inhomogeneous reflectivity of the outer part of the ONL indicates off centre placement of the OCT measurement beam. **(A)** The averaged summary scan obtained from the correctly, horizontally orientated live images of the reference scan shown in Figure 2A. This images shows a homogeneous reflectivity of the outer ONL (black arrow). The automated segmentation identifies the borders of the RNFL (red/grey lines). Note, this is the image which is send to the reading centre and used for automated calculation of the RNFL thickness shown in Table 1. **(B)** temporal off axis placement results in a inhomogeneous outer ONL reflectivity. The ONL reflectivity is increased for the centrally elevated part in Figure 2B (white arrows) and decreased in the periphery (grey arrows). **(C)** nasal off-axis placement **(D)** superior off axis placement **(E)** inferior off-axis placement.

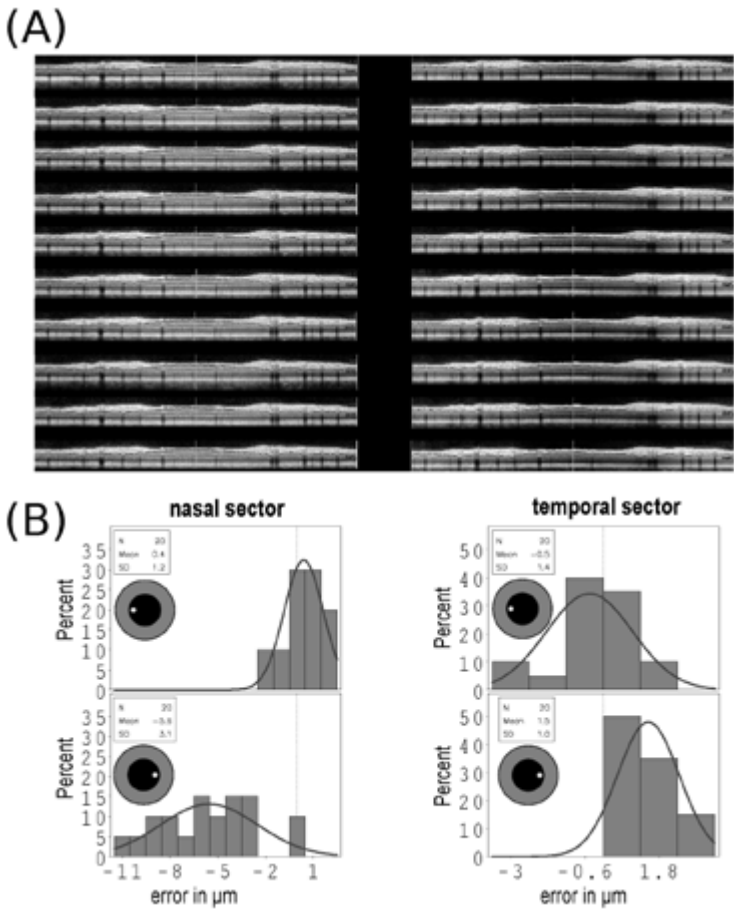

Figure 4. Scan quality and direction of changes in RNFL thickness. **(A)** All averaged ONH ring scan images are of high signal strength and quality (ART 25, signal >35 dB) taken for large temporal and nasal off-axis beam placement from subject #1 (OD) are shown (note the 10 additional scans with only small off-axis placement are of comparable quality). **(B)** The ring scan RNFL data was separately analyzed for the nasal and temporal sectors. The direction and size of the resulting measurement error compared to the reference scan (vertical dashed reference line) are shown as a histogram for the nasal and temporal sectors.
The inlay indicates direction of off-axis beam placement in each case. The overlaid Gaussian curve illustrates the mirror pattern of the resulting over-/underestimation of the RNFL thickness in this subject. The y-axis gives the percentage of scans for the range of measurement error in µm shown on the x-axis.

Automated, quantitative analysis of the RNFL thickness in the pilot study changed significantly with off-axis placement of the measurement beam. Table 1 shows the results of the scans performed in a undilated pupil. Importantly, the observed artefacts were not different when scans were made with a dilated pupil (data not shown). The largest artefacts (over 10 µm) were observed in the temporal superior (135±17.8 µm versus 148±5.4 µm) and nasal superior sectors (132±23.7 µm versus 143±2.5 µm). This

was followed by the PMB (48±0.8 µm versus 61±36.6 µm) and mid temporal sector (60±0.7 µm versus 72±36.4 µm). Measurement artefacts for the mid and inferior nasal, inferior temporal and global mean were less marked, but remained significant (Table 1). Importantly, signal strength was excellent (> 35 dB) for all scans and there was no algorithm failure accounting for erroneous RNFL thickness measurements (Figure 4A). Typically, for the nasal sector the RNFL thickness increased with temporal off-axis beam placement and decreased with nasal off-axis beam placement (Figure 4B). The opposite was observed for the temporal sector.

Table 1 Quantification of RNFL thickness.

	Beam placement					
	Central	**Right**	**Left**	**Top**	**Bottom**	**p-value**
Global mean [µm]	105±0.6	107±1.2	105±0.8	107±1.3	109±8.6	0.002
PMB [µm]	48±0.8	51±1.5	50±1.0	50±1.8	61±36.6	0.003
Sup. nasal [µm]	137±1.6	143±2.5	137±2.3	142±2.9	132±23.7	<0.0001
Nasal [µm]	98±1.3	95±4.1	97±1.0	100±1.9	98±1.1	0.002
Inf. nasal [µm]	124±1.3	122±1.5	123±1.8	121±1.4	122±1.6	0.03
Inf. temporal [µm]	126±1.0	126±1.9	125±1.8	124±1.5	127±1.4	0.01
Temporal [µm]	60±0.7	61±1.1	61±0.7	62±1.6	72±36.4	0.006
Sup. temporal [µm]	140±1.3	148±5.4	142±1.6	144±2.4	135±17.8	<0.0001

The pilot study shows that quantification of the RNFL thickness depends on placement of the measurement beam. The mean±standard deviation are shown. Group comparisons were done using the Kruskal-Wallis test. PMB= papillomacular bundle.

Ring scan main study

A total of 1,980 OCT ring scans were taken from 11 subjects (90 scans per subject per eye). Three scans from subject #8 were rejected because of an algorithm failure. The remaining 1,977 OCT ring scans were used for statistical analyses. The averaged scan quality was 27.4 dB with an ART of 69. The demographic data and average global RNFL thickness per subject and eye are summarised in Table 2. All subjects had normal visual fields on automated perimetry.

As in the pilot study, measurements done with central beam placement were taken as reference. The *averaged* measurement artefact caused by a small and large degree off-centre beam placement are shown in Table 3. Consistently, a larger off-centre beam placement caused a larger sized measurement error. In the pooled data analysis the size of the measurement artefact was *maximal* 17 µm for the global average RNFL thickness, 20 µm for the entire nasal sector, 31 µm for the superior nasal sector, 37 µm for the inferior nasal sector, 21 µm for the entire temporal sector, 42 µm for the inferior temporal sector, 23 µm for the superior temporal sector and 35 µm for the PMB.

Importantly, already minimal off-axis placement of the laser beam, with respect to the individual pupil size, gave rise to consistent, significant RNFL thickness measurement artefacts. The distribution of the size of the absolute error ($|x|$) for all measurements from all sectors of all subjects pooled (n=14,055) appears to be Gaussian (Figure 5).

Table 2 Subject characteristics.

Subject	Age [years]	Sex	Height [cm]	Weight [kg]	Pupil [mm]		Refraction [Dpt]		VF [MD]		RNFL [µm]	
					OD	OS	OD	OS	OD	OS	OD	OS
# 1	24	f	177	64	5.0	4.5	0	0	+0.82	+0.73	106	109
# 2	62	f	175	70	5.9	4.8	-1.75	-0.75	+0.12	-0.22	89	93
# 3	27	f	170	63	4.9	4.9	0	-1	-0.77	-1.11	103	106
# 4	27	f	167	91	4.1	3.8	-4	-4	-0.93	-1.01	100	103
# 5	51	m	178	68	3.8	3.9	-4.75	-1.5	+0.56	-0.42	85	86
# 6	49	m	182	90	3.7	3.6	+1	+1	-0.26	-0.73	98	94
# 7	51	f	163	61	5.0	5.5	0	0	+2.18	+1.14	92	92
# 8	31	f	181	74	4.7	4.3	0	0	+1.86	+1.39	96	105
# 9	27	f	176	78	4.5	3.7	-1.5	-1.5	-1.49	-1.08	104	110
# 10	29	f	169	58	4.6	4.8	-2.25	-3.5	-0.52	-0.32	94	93
# 11	24	m	186	75	5.2	4.8	0	0	+0.31	+1.05	98	98

Female = f, male =m, MD = mean field deviation, VF = visual field.

Table 3 The mean measurement artefacts caused by small and large off-centre beam placement compared to central beam placement are shown.

	Right	Left	Top	Bottom
Small off-centre beam placement				
Global mean [µm]	0.76 (±0.3)	0.95 (±0.8)	0.83 (±0.5)	0.84 (±0.5)
PMB [µm]	1.51 (±1.0)	1.52 (±0.8)	1.04 (0.9)	1.15 (±0.7)
Sup. nasal [µm]	1.57 (±0.8)	2.06 (±1.7)	1.84 (±1.4)	2.01 (±1.2)
Nasal [µm]	1.68 (±0.8)	2.16 (±2.7)	0.94 (±0.7)	1.99 (±1.0)
Inf. Nasal [µm]	1.83 (±1.2)	2.68 (±2.7)	1.32 (±0.8)	2.57 (±0.9)
Inf. Temporal [µm]	1.62 (±1.2)	2.44 (±2.4)	3.12 (±4.3)	2.20 (±1.1)
Temporal [µm]	0.85 (±0.7)	1.23 (±0.9)	0.82 (±0.6)	1.06 (±0.7)
Sup. temporal [µm]	1.51 (±0.6)	2.11 (±1.8)	1.54 (±0.8)	2.05 (±2.5)
Large off-centre beam placement				
Global mean [µm]	0.99 (±0.4)	0.86 (±0.8)	1.02 (±0.8)	1.07 (±0.7)
PMB [µm]	1.69 (±1.3)	1.75 (±1.0)	2.76 (±5.3)	1.74 (±0.9)
Sup. nasal [µm]	1.34 (±0.9)	2.30 (±1.5)	2.61 (±1.9)	2.59 (±2.3)
Nasal [µm]	2.65 (±1.6)	2.91 (±2.7)	1.49 (±1.4)	2.62 (±2.4)
Inf. nasal [µm]	2.36 (±1.2)	2.40 (±2.7)	2.88 (±3.2)	3.3 (±2.2)
Inf. temporal [µm]	2.20 (±1.4)	3.31 (±2.4)	3.23 (±3.6)	2.69 (±2.0)
Temporal [µm]	1.10 (±0.8)	1.42 (±0.8)	2.29 (±3.3)	1.68 (±1.0)
Sup. temporal [µm]	2.31 (±1.5)	2.70 (±2.0)	2.54 (±1.3)	2.32 (±2.0)

Values are reported as mean±standard deviation. PMB= papillomacular bundle.

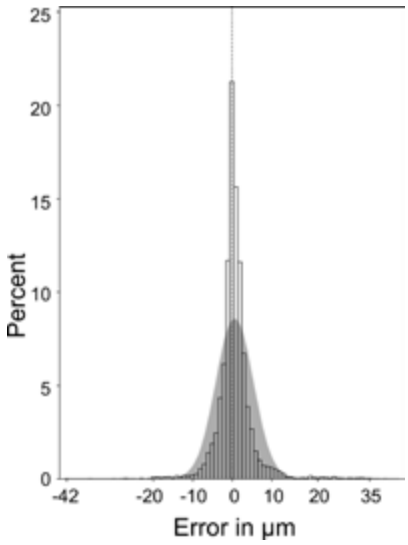

Figure 5. Measurement error in µm caused by off-axis beam placement. In about 78% of all measurements there is an error of ≥| 0 | µm, in 5% ≥| 9 | µm with a maximum error of | 42 | µm. An accurate measurement (0 µm error) is indicated by the dashed vertical reference line. The size of the measurement error demonstrates a Gaussian distribution to both sides of the vertical reference line (grey shaded curve). The y-axis gives the percentage of scans for the range of measurement error in µm shown on the x-axis.

Because of phenotype difference of the ONH the size and distribution of the measurement error was different between subjects. Therefore the statistical analyses were repeated for each subject individually (supplementary Tables 1 and 2). In each subject large off-axis placement of the laser beam caused a highly significant ($p<0.0001$) RNFL thickness measurement artefacts in almost all sectors.

DISCUSSION

This study demonstrates that off-axis placement of the OCT measurement beam causes a significant measurement artefact. The size of the error can be as large as 42 µm, but typically remains within ±9 µm (95%CI). The artefact is reproducible on an individual level in all healthy subjects investigated in this study. This error is readily recognised on the live image and technicians capturing the scans should be trained accordingly.
In the context of multicentre studies it is important to note that a central reading centre will not readily be able to recognize off-axis placement of the OCT measurement beam because an averaged summary scan (Figure 3) is sent instead of the live image captured with a screen-shot during the assessment (Figure 2). We therefore describe a new sign, the outer ONL reflectivity which allows for indirect, retrospective assessment of possible off-axis placement of the OCT measurement beam (Figure 2B-E).

We believe recognition of this artefact is relevant for multicentre studies using OCT. If left unrecognised the artefacts may compromise the value of retinal OCT as a primary outcome measure in treatment trials. The artefacts exceeds the estimated annual loss of the global average RNFL thickness in MS (1-2 µm).[4] There is a considerable degree of inter-individual variation of the ONH. For this reason the pooled group data of this study, although highly significant, is probably less informative than the detailed analyses of each individual subject.

An important practical question is what degree of off-axis laser measurement beam placement is required to cause a significant measurement artefact? In the pilot study we have shown that the moderate degree of displacement (about 2 mm in a 5 mm sized pupil) we have observed in day-to-day practice in our and other centres as well as during OCT training sessions at scientific meetings is sufficient to give rise to a significant measurement artefact. Not surprisingly a larger displacement which may only occasionally occur under difficult image acquisition conditions causes a much larger measurement artefact. The largest measurement error occur when performing the baseline scan at one extreme (for example to the top) and the follow-up scan at the other extreme (to the bottom). Of course if the second scan would be performed at the same degree off-centre placement as the first, only a systematic error would be introduced. The likelihood that an operator remembers the degree of off-centre placement in an individual patient over time is small. Therefore the practical advice for day-to-day practice is simply to try and get a horizontally aligned scan.

Could the error have been caused by an algorithm failure as suggested by Balasubramanian *et al*.?[6] We do not think so for several reasons. First, in the study by Balasubramanian *et al*. the images were taken out of focus (+2dpt). Second, ART was set to 2. And third, the RNFL thickness was not measured, but the entire retinal thickness.[6] The resulting algorithm failure was caused by a poor signal (<10 dB) and occurred at level of Bruch's membrane (see Figure 4 in reference 6). In contrast, the present study relied on OCT images with, according to the Balasubramanian *et al.* criteria, excellent signal quality (>20 dB) with a high ART. This strongly suggests that the measurement artefact introduced by off-axis beam placement was not caused by poor image quality as previously described.[6]

Importantly, already a minimal displacement of the measurement beam, which just about gave the impression of a waveform of the OCT live image caused significant measurement artefacts in all subjects in almost all sectors (see supplementary Table 1). We have attempted to find a mathematical expression describing the relationship between the magnitude of the measurement artefact and the amount of off-axis beam placement by measuring the resulting angle of the tilted OCT live image as performed by Lujan *et al* for line scans in the macular region.[7] Because of the large inter-individual

variation of the ONH between subjects it was not possible to express such a relationship for ring scans consistently with one mathematical expression. This is important, because in the occasional patient it may not be possible to obtain a perfect, horizontal aligned OCT ring scan due to anatomical reasons. In such a patient an inhomogeneous pattern of OPL/ONL may need to be accepted, but should be reproduced on follow-up scans.

How can the reproducible change in OPL/ONL reflectivity be explained? For the macular region the explanation is straight forward. The inner third of the OPL comprises photoreceptor synapses and the outer two thirds consist of obliquely orientated axonal extensions, called Henle fibres which are surrounded by the fibres of Müller.[8] In Macaque monkeys, Henle fibres are longest at the macula (300-350 µm) were photoreceptor's and ganglion cells are substantially displaced and shorter (≈ 12.5 µm) towards the ONH.[8] The distance between the macula and ONH is about 3.0 mm.[9] Typically, macular Henle fibres are not visible with central placement of the measurement beam.[10] Off-axis placement of the measurement beam results in angled backscattering. Nasal off centre placement causes the OCT measurement beam to be refracted temporally and vice versa. This mechanism is illustrated by the mirror pattern of the live images shown in Figure 2 B&C. The same optic principle applies to off-axis placement to the top and bottom, again revealing mirror pattern images (Figure 2 D&E). Therefore strong backscattering of the Henle fibres results with perpendicular OCT measurement beam placement. In contrast, oblique light backscattering from the Henle fibres results in a reduced outer OPL signal.[10] Although there are similarities between the macaque and human retina, comparable data from humans is to the best of our knowledge not available. It could be that the fibres of Müller and possibly also Müller cells which are present throughout the retina also contribute to the change in signal intensity. In this study the ring scan measured the retina at a radius of 1.2 cm from the ONH centre thus capturing the differently sized Henle fibres.[8] The degree of signal change of backscattered light from the ONL underlying the PMB (long Henle fibres) was more marked than for the other sectors (short Henle fibres) which is what one would expect from the data by Perry and Cowey.[8] We can only speculate that this signal change is due to Henle fibres and the fibres of Müller. An alternative explanation could be an oblique course of other retinal axons originating from the ONL as this layer approaches the human ONH. Acknowledging that we cannot provide a clear-cut anatomical explanation in the absence of histological studies it should be highlighted that this sign is highly reproducible. Future studies are needed to elucidate which degree of change in ONL/OPL reflectivity is relevant in clinical trial practise.

A limitation is that the segmentation software only calculated the RNFL thickness for the ring scan and we have therefore not presented any of the volume data. The change of angled light backscatter from ONL at level of the ONH and from the OPL at level of

the macula is however, so consistent that it readily allows for identification of volume scans taken with an off-axis measurement beam. Of note, Lujan *et al.*, using different OCT machines (Cirrus Zeiss and Bioptigen) have demonstrated changes in Henle fibre reflectivity to be associated with macular pathology.[7] Another shortcoming is that we have not tested if this artefact also occurs with other OCT machines. This would need to be tested prospectively. Likewise the sensitivity and specificity of this sign for practice in a reading centre environment will require prospective analysis. Finally, all measurements were taken in healthy eyes and we cannot extrapolate the size of the measurement artefact expected in patients with multiple sclerosis. We would caution against using this sign in ophthalmological diseases which may themselves cause inhomogeneity of the ONL such as central serous retinopathy, non-exudative age-related macular degeneration or drusen.[7]

Taken together, this study reports a new sign which allows to correctly identify off-axis placement of the OCT beam. Since off-axis placement of the OCT beam resulted in measurement artefacts over 8-times the estimated annual RNFL loss thought be related to neurodegeneration in MS, we believe this sign should be considered in the context of multicentre studies.

SUPPLEMENTARY MATERIAL

Supplementary Table 1 Small off-axis beam placement. A small off-axis placement of the measurement beam compared to central beam placement causes a significant measurement artefact in each eye of all subjects on an individual level.

Subject	eye	PMB	Sup-nas	Nas	Inf-nas	Inf-temp	Temp	Sup-temp	Global
# 1	OD	ns	***	***	***	***	**	***	†
# 1	OS	***	***	***	***	†	ns	†	***
# 2	OD	***	***	*	**	†	***	***	***
# 2	OS	***	†	***	***	**	***	ns	***
# 3	OD	†	***	***	***	***	*	***	***
# 3	OS	***	***	***	ns	***	***	**	***
# 4	OD	***	***	***	***	***	***	***	***
# 4	OS	***	***	***	ns	***	***	***	***
# 5	OD	***	***	**	†	**	***	***	**
# 5	OS	***	***	***	†	***	***	***	ns
# 6	OD	***	***	***	***	***	*	*	***
# 6	OS	***	***	***	***	***	ns	***	**
# 7	OD	***	***	***	***	**	***	**	***
# 7	OS	***	***	***	***	ns	**	†	***
# 8	OD	†	*	***	ns	***	***	†	*
# 8	OS	***	***	***	***	***	***	***	***
# 9	OD	***	***	***	***	***	***	ns	***
# 9	OS	***	***	***	***	***	***	***	***
# 10	OD	***	***	***	***	***	***	***	***
# 10	OS	***	***	***	***	***	**	***	**
# 11	OD	***	***	***	***	***	***	***	***
# 11	OS	***	***	ns	***	*	***	***	ns

The p-value (Kruskal-Wallis test) for each sector is shown as ns=not significant, p,0.0001=***, p,0.001=**, p,0.01=*, p,0.05=†.

Supplementary Table 2 Large off-axis beam placement. A large off-axis placement of the measurement beam compared to central beam placement causes a significant measurement artefact in each eye of all subjects on an individual level.

Subject	eye	PMB	Sup-nas	Nas	Inf-nas	Inf-temp	Temp	Sup-temp	Global
# 1	OD	***	***	***	***	***	***	***	***
# 1	OS	***	***	***	†	ns	*	†	†
# 2	OD	***	**	***	***	***	***	***	**
# 2	OS	***	***	***	***	***	***	***	***
# 3	OD	***	***	***	***	***	**	***	***
# 3	OS	***	**	***	**	***	***	**	**
# 4	OD	***	***	***	***	***	***	***	***
# 4	OS	***	***	***	***	***	***	***	***
# 5	OD	***	***	†	***	***	***	***	***
# 5	OS	***	***	***	***	**	***	***	**
# 6	OD	***	***	***	***	***	***	***	***
# 6	OS	***	***	***	***	***	***	***	***
# 7	OD	***	***	***	***	***	***	***	***
# 7	OS	***	***	***	***	***	***	***	***
# 8	OD	ns	**	***	**	**	***	***	***
# 8	OS	***	***	***	***	**	***	***	**
# 9	OD	***	***	***	***	***	***	**	***
# 9	OS	***	***	***	***	***	***	***	***
# 10	OD	***	***	***	***	***	***	***	***
# 10	OS	***	***	***	***	***	***	***	**
# 11	OD	***	***	***	***	***	***	***	***
# 11	OS	***	***	***	***	***	***	***	**

The p-value (Kruskal-Wallis test) for each sector is shown as ns=not significant, p,0.0001=***, p,0.001=**, p,0.01=*, p,0.05=†.

Supplementary Video 1

Live coverage of the effect of off axis measurement beam placement. This video shows the situation of off-centre beam placement, with the live OCT image in the acquisition window. This image shows the artefacts caused by temporal, nasal, inferior and superior off-centre placement of the measurement beam.

(Available at http://www.plosone.org/article/info%3Adoi%2F10.1371%2Fjournal.pone.0048222#s5)

REFERENCES

1. Wu H, de Boer JF, Chen TC. Reproducibility of retinal nerve fiber layer thickness measurements using spectral domain optical coherence tomography. *J Glaucoma* 2011;20:470-476.
2. Barkhof F, Calabresi PA, Miller DH, Reingold SC. Imaging outcomes for neuroprotection and repair in multiple sclerosis trials. *Nat Rev Neurol* 2009;5:256-266.
3. Petzold A, de Boer JF, Schippling S, et al. Optical coherence tomography in multiple sclerosis: a systematic review and meta-analysis. *Lancet Neurol* 2010;9:921-932.
4. Talman LS, Bisker ER, Sackel DJ, et al. Longitudinal study of vision and retinal nerve fiber layer thickness in multiple sclerosis. *Ann Neurol* 2010;67:749-760.
5. Domalpally A, Danis RP, Zhang B, Myers D, Kruse CN. Quality issues in interpretation of optical coherence tomograms in macular diseases. *Retina* 2009;29:775-781.
6. Balasubramanian M, Bowd C, Vizzeri G, Weinreb RN, Zangwill LM. Effect of image quality on tissue thickness measurements obtained with spectral domain-optical coherence tomography. *Opt Express* 2009;17:4019-4036.
7. Lujan BJ, Roorda A, Knighton RW, Carroll J. Revealing henle's fiber layer using spectral domain optical coherence tomography. *Invest Ophthalmol Vis Sci* 2011;52:1486-1492.
8. Perry VH and Cowey A. The lengths of the fibres of Henle in the retina of macaque monkeys: implications for vision. *Neuroscience* 1988;25:225-236.
9. Plant GT and Perry VH. The anatomical basis of the caecocentral scotoma. New observations and a review. *Brain* 1990;113:1441-1457.
10. Otani T, Yamaguchi Y, Kishi S. Improved visualization of henle fiber layer by changing the measurement beam angle on optical coherence tomography. *Retina* 2011;31:497-501.

Chapter 3.2

The OSCAR-IB consensus criteria for retinal OCT quality assessment

P Tewarie, LJ Balk, F Costello, A Green, R Martin, S Schippling, A Petzold

***PLoS One. 2012*;7:e34823**

ABSTRACT

Background Retinal optical coherence tomography (OCT) is an imaging biomarker for neurodegeneration in multiple sclerosis (MS). In order to become validated as an outcome measure in multicenter studies, reliable quality control (QC) criteria with high inter-rater agreement are required.

Methods/Principal Findings A prospective multicentre study on developing consensus QC criteria for retinal OCT in MS: (1) a literature review on OCT QC criteria; (2) application of these QC criteria to a training set of 101 retinal OCT scans from patients with MS; (3) kappa statistics for inter-rater agreement; (4) identification reasons for inter-rater disagreement; (5) development of new consensus QC criteria; (6) testing of the new QC criteria on the training set and (7) prospective validation on a new set of 159 OCT scans from patients with MS. The inter-rater agreement for acceptable scans among OCT readers (n = 3) was moderate (kappa 0.45) based on the non-validated QC criteria which were entirely based on the ophthalmological literature. A new set of QC criteria was developed based on recognition of: (O) obvious problems, (S) poor signal strength, (C) centration of scan, (A) algorithm failure, (R) retinal pathology other than MS related, (I) illumination and (B) beam placement. Adhering to these OSCAR-IB QC criteria increased the inter-rater agreement to kappa from moderate to substantial (0.61 training set and 0.61 prospective validation).

Conclusions This study presents the first validated consensus QC criteria for retinal OCT reading in MS. The high inter-rater agreement suggests the OSCAR-IB QC criteria to be considered in the context of multicentre studies and trials in MS.

INTRODUCTION

A consistent finding in patients with multiple sclerosis (MS) and MS related optic neuritis (MSON) is thinning of the retinal nerve fibre layer (RNFL), assessed by optical coherence tomography (OCT).[1,2] Loss of RNFL thickness is correlated with a number of clinical scales and brain imaging evidence for atrophy, suggesting a pathological link to neurodegeneration. This data is consistent with post-mortem evidence for neurodegeneration in about 80% of eyes from patients with multiple sclerosis.[3] Consequently, it has been proposed to investigate the value of OCT measures of retinal atrophy as a potential secondary outcome in neuroprotective treatment trials in MS.[4,5] As one pre-requisite for such a trial it will be necessary to validate the accuracy of RNFL thickness assessment in a multi-centre setting. An important step towards this goal is the assessment of OCT scans by well trained readers in a reading center. This assessment judges on the quality of an OCT scan whether or not it can be included into a study. A review of the ophthalmological literature shows that poor scan quality is frequently caused by boundary line errors, poor signal strength or de-centration of the ring scan at the optic nerve head (ONH).[6] There are, however, no consensus quality control criteria for RNFL assessment in patients with MS and MSON.

This study aimed to develop for the first time reliable and transparent consensus criteria for the quality assessment of retinal OCT scans in MS and MSON for application in the context of multi-centre studies.

METHODS

Retinal images were obtained using a Spectral Domain (SD)-OCT device (Heidelberg Spectralis, Software version 1.1.6.3) with the eye tracking function enabled. The OCT scans were recorded by qualified OCT operators at all centers: Amsterdam, Calgary, Hamburg and University of California San Francisco. In all patients a ring scan (diameter 12u or 2.4 cm) at the optic nerve head (ONH) was recorded. Given the purpose of this study, all scans, independent of either eye, were analysed together. All scans were anonymised and uploaded to an OCT reading center (Amsterdam). The OCT scans were then rated independently by three trained raters (PT, LB, AP) in Amsterdam. The first set of scans (101 eyes from 51 patients, Hamburg) was rated in random order, based on published criteria.[6] Scans failing on these criteria were rated as 'reject'. Scans were rejected following published recommendations on: decentration, poor scan quality, boundary line errors or algorithm failures.[6] Kappa statistics for multiple raters were calculated to assess the inter-rater agreement using the magree macro in SAS software

(V9.2).[7] The level of agreement was rated as slight (0-0.2), fair (0.2-0.4), moderate (0.4-0.6), substantial (0.6-0.8) or almost perfect (0.8-1).[8]
Next, the results were analysed to identify the main sources of disagreement. Based on this consensus a new set of criteria was summarised and tested on the training set of OCT scans from the Hamburg site in random order to check whether the inter-rater agreement could be improved. Finally, the consensus criteria were validated prospectively on a new set of 159 OCT scans from dedicated MS centres in Amsterdam, Calgary and UCSF. Again kappa statistics were used for data analyses.

Ethics Statement
All participants signed informed consents and in all centres this study was approved by the Medical Ethics Committee and the Commission for Scientific Research at the VU University Medical centre.

RESULTS

The inter-rater agreement based on published quality control criteria was moderate (kappa 0.45) for the 101 OCT scans from Hamburg. The main sources of disagreement were the overall scan quality (26%) and ring scan de-centration (22%). The revised consensus quality control criteria are summarised in Table 1.

Table 1 The OSCAR-IB quality control criteria for retinal OCT scans.

Item	criteria
O	Obvious problems not covered by items below. Please document for discussion + consensus agreement
S	Is the OCT signal sufficient? Signal strength > 15 (ring and volume scans) with appropriate averaging of multiple scans (ART activated).
C	Is the ring scan correctly centred? for circular discs: ONH must not cross more than two colours of the RAF logo (outer ring of RAF adjusted to outer ring of scan either by paper or electronically). In contrast to the ONH ring scan, post-hoc readjustment is possible for the macular volume scan.
A	Is there an algorithm failure? Red lines correctly identify the superior and inferior RNFL border (ring scan); Red lines correctly identify the retinal borders (volume scan)
R	Is there visible retinal pathology which may potentially impair the RNFL reading? See Table 2 (note these some of these conditions are also exclusion criteria for OCT studies in MS)
I	Is the fundus well illuminated? Retinal structures visible (ring and volume scans)
B	Is the measurement beam placed centrally? Homogeneous outer OPL reflectivity (ring and volume scans)

Each of the seven criteria is identifiable by the first letter, together giving the acronym 'OSCAR-IB' [(O)= obvious problems including violation of the protocol; (S) poor signal strength defined as ,15 dB; (C) wrong centration of scan; (A) algorithm failure; (R) retinal pathology other than MS related; (I) illumination; and (B) beam placement]. The fifth criterion describes the any form of retinal pathology (R) which may influence the OCT data. Because the list of diseases in this category is likely to grow further with increasing use of OCT we have summarised our current consensus in Table 2.

Table 2 Pathology of the retina to be considered by the OSCAR-IB criteria.

Summary	Diseases
Structural	Drusen, Cysts, Detachment, Large discs, Small crowed discs, Presence of myelinated axons, naevus, tumor, peri-papillary atrophy, optic disc oedema, more than 6 diopters of myopia or hyperopia.
Vascular	AION & PION, NA-AION & NA-PION, GCA, CRO, CRBO, AVM, Cotton-wool spots, CVA affecting the optic pathways
Immune	paraneoplastic, MAR, NMO, CAR, SLE, uveitis, birdshot retinochoroiditis
Infectious	viral, bacterial, fungus, HIV, Lyme, Secondary syphilis
Hereditary	Leber's, DOA, Albinism, Cone dystrophy, Retinitis pigmentosa
Iatrogen	Retina surgery, photocoalgulation, Solar retinopathy, Central serous chorioretinopathy, Purtscher's retinopathy, optic nerve sheet fenestration, Brain surgery affecting the optic pathways
Metabolic/toxic	diabetes, Vit A deficit, Alcohol-, tobacco- and malnutrition-induced amblyopia, Amiodarone, Chloroquine, Vigabatrin
Other	Glaucoma, Macular degeneration, Acute posterior multifocal placoid pigment epitheliopathy, Acute macular neuroretinopathy

Optic disc oedema in MS type optic neuritis (MSON) typically resolves within 1-2 months such that the first signs of RNFL loss following MSON can occasionally be observed after 2 months. For a literature review it is recommended to leave a 3 months time-frame before including RNFL data from these patients into analyses of RNFL loss.[16]

Using the seven new 'OSCAR-IB' criteria improved the inter-rater agreement from moderate to substantial (kappa 0.61) for reassessing the same set of OCT scans from Hamburg. The comparison between the first rating and the second rating based on the 'OSCAR-IB' criteria is shown in Table 3. Note that the highest rejection rate was based on the new criteria on placement of the measurement beam (B).

Table 3 Comparison of published criteria with the 'OSCAR-IB' criteria.

Criterium	Rater 1	Rater 2	Rater 3
Decentration	8/101 (8%)	3/101 (3%)	11/101 (11%)
Algorithm failure	0/101 (0%)	1/101 (1%)	5/101 (5%)
Image quality	13/101 (13%)	5/101 (5%)	8/101 (8%)
Total	19/101 (19%)	9/101 (9%)	17/101 (17%)
O	2/101 (2%)	6/101 (6%)	1/101 (1%)
S	5/101 (5%)	7/101 (7%)	4/101 (4%)
C	7/101 (7%)	5/101 (5%)	5/101 (5%)
A	2/101 (2%)	1/101 (1%)	3/101 (3%)
R	0/101 (0%)	0/101 (0%)	0/101 (0%)
I	4/101 (4%)	6/101 (6%)	10/101 (10%)
B	51/101 (51%)	35/101 (35%)	37/101 (37%)
Total	70/101 (70%)	60/101 (60%)	60/101 (60%)

The proportion of *rejected* OCT scans per reader for each of the published and new OSCAR-IB criteria is shown for the training set of 101 OCT scans from Hamburg.

The inter-rater agreement remained substantial (kappa 0.61) for external validation, rating an independent set of OCT scans (n= 159) applying the OSCAR-IB criteria.
The total number of rejected OCT scans from the pooled prospective validation set was high (42%-43%) in each of the readers (Table 3). The proportion of rejected OCT scans for each of the 'OSCAR-IB' criteria showed that the rejected scans frequently failed on more than one single criterion. For this reason there was some variation over the main criterion of rejection documented by the readers (Table 3). An almost perfect agreement was achieved in judging de-centration artifacts
(Table 3). As with the training set, the highest disagreement between readers was found for beam placement (B), with reader one preferring to label a scan as 'B' when readers two and three labeled them as 'I', 'S' or 'O'. Of note, in the two data sets there was a very low rate of scans showing retinal pathology other than MS related (n= 2). In one patient this was due to peripapillary atrophy and in the other due to serous retinopathy.

DISCUSSION

OCT is a new imaging biomarker allowing for rapid, noninvasive and highly precise quantification of axonal degeneration and neuronal loss in the retina of patients suffering from MS.[1-5] If successful, retinal OCT may become a key secondary outcome measure in MS treatment trials. Importantly there are to date no consensus quality control criteria to this purpose. This study identified pitfalls which can be reliably identified by trained OCT readers. These pitfalls may not necessarily be apparent to

all MS treating neurologists. The unexpected high rejection rate of 42% of retinal OCT scans from experienced centres participating in this study highlights the need for such quality control criteria.

The here presented novel, consensus quality control criteria, OSCAR-IB achieved a high inter-rater agreement (substantial, kappa 0.61). There are to the best of our knowledge no previously published data on inter-rater agreement in this context. Using experience from patients with macular degeneration or glaucoma[6] on our dataset of patients with MS was not convincing (kappa 0.45). The OSCAR-IB criteria allow rating of OCT images in a stringent and systematic approach. In this study the criteria were applied to ringscans of the optic nerve head, which provides an accurate and reproducible measure for RNFL loss in MS by many groups world-wide.[2]

The first of the OSCAR-IB criteria permits to rate and exclude scans on the basis of obvious failures which, if seen frequent, may be included more specifically in a future revision of these OCT quality control criteria (Figure 1).

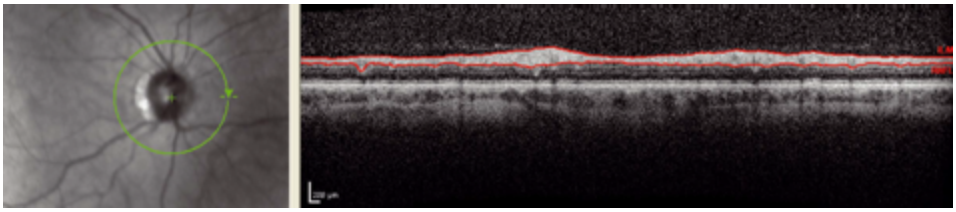

Figure 1. Obvious: The left image is blurred due to poor focusing. This results in increased noise and loss of transversal resolution in the OCT image on the right.

From our own anecdotal observations and the ophthalmological literature we anticipate that large floaters causing shadowing of the OCT image may be an obvious rejection criterium. Equally any damage to the optical pathway from corneal scars, severe keratitis sicca, lens opacities, vitreous haemorraghe to name but few are likely to preclude acquisition of a well illuminated and evenly focused retinal OCT image. In a number of scans rejection was due to more than one of the seven OSCAR-IB criteria. The reason for rejection requires further discussion. One obvious reason was violation of the protocol (no B-scan averaging (ART) enabled in eight scans), discovered by rater three. These eight scans were also very poorly illuminated, taken with off-center beam placement or had a poor signal strength (raters one and two). The influence of ART on image quality in addition to signal strength may need to be considered in a future revision of the criteria.

This is further illustrated by analysing the scan judgement based on the second criterion alone. We had arbitrarily defined that the signal strength had to be larger than 15 dB. There is published evidence that differences in signal strength are associated with

differences in average RNFL thickness.[9,10] Very recently Huang and colleagues showed a signal strength below 7 dB to be negatively correlated with RNFL thickness.[11] For the Heidelberg Spectralis there is however no systematic study investigating the combined influence of signal strength and number of averaged scans needed to achieve reliable performance of the automated algorithm for determination of RNFL thickness. Such studies are required for future refinement of this criterion. Probably the overall contrast between different retinal layers in the final image will become more relevant than one simple measure of signal strength. The rational for setting the limit arbitrarily to a threshold of 15 dB was that we learned from the training set data signal strength was sufficient to prevent algorithm failures due to noise (Figure 2). Based on this proposed cut off of 15 dB only 3-5% of scans were excluded per rater due to poor signal strength.

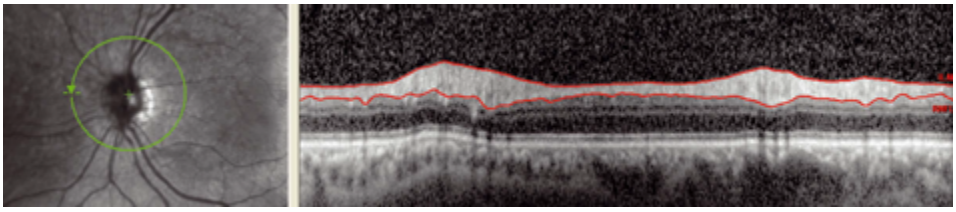

Figure 2. Signal: The signal strength for this image is 13 dB which is lower than the limit of 15 dB. This results in a more noisy OCT image with a lot of speckling.

The third of the OSCAR-IB criteria, ('C') addresses decentration artefacts. De-centration was found to be one of the main sources of disagreement in the first exploratory part of this study. Overall, 22 scans were rejected by at least one rater due to de-centration and a complete agreement of all three raters was only achieved for two scans. This poor inter-rater agreement is in accordance with the ophthalmological literature.[6] An important hurdle here was the large anatomical variation of the ONH between patients. Allowing for variation in size we argued that a small degree of de-centration of the ring scan around a small ONH would be acceptable because all retinal axons were sampled were they were already spread out in bundles. In contrast, a small degree of de-centration for a large ONH was considered to introduce a significant measurement bias if one part of the ring scan cut through the border of the disc where retinal axons merged and the other part more peripherally. To allow addressing this variation we used a circle with inner rings set at different diameters, a RAF logo (Figure 3).

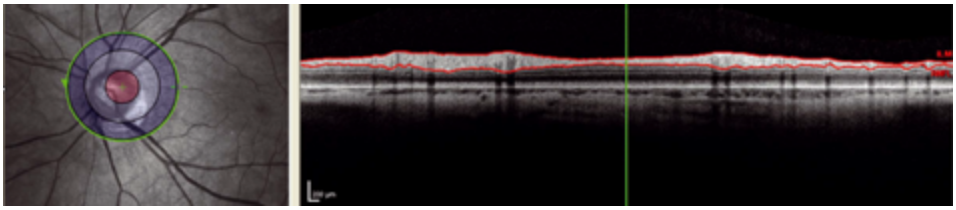

Figure 3. Decentration: The ring scan is not correctly centred as can be observed in the left image. The edge of the optic nerve head crosses more than two circles. Therefore the ringscan is rejected.

In cases, where the ONH crosses more than two colour bands of the RAF logo, a scan is rejected. Applying the third OSCAR-IB criterion substantially improved the overall agreement on judging de-centration artefacts. The number of OCT scans rejected on the basis of this criterion was about 5% and comparable between raters (Table 3). This finding is consistent with the ophthalmological literature where decentration artefacts by trained raters occurred in about 5% of the OCT scans sent out to a central reading center.[6] Hopefully, in the near future de-centration artefacts will be recognised by raster scan protocols that identify the center point.[6] Until then, utilization of the RAF logo seems reasonable.

The fourth criterium ('A') takes boundary line errors or algorithm failures into account. Although these are frequently occurring errors in ophthalmological diseases (15.3%),[6] they only occurred in about 6% in our study (Figure 4). The most likely explanation is that algorithm failures are more frequent in cases with a very thin RNFL, which is rarely the case in MS patients.

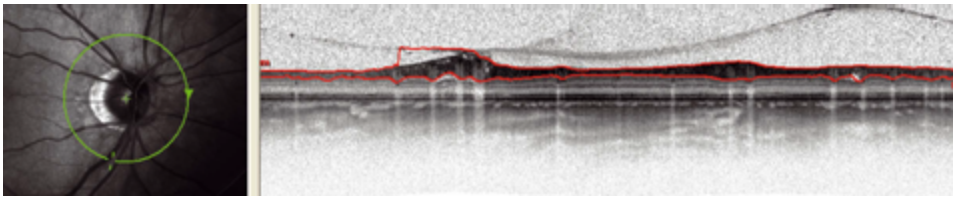

Figure 4. Algorithm failure: The red line in the OCT image right is not clearly at the border of the RNFL. The location corresponds to inferior of the ONH.

The fifth criterium ('R') is retinal pathology not caused by MS (see Table 2). Not only could other retinal pathology generally impair reading of the RNFL (Figure 5), but some diseases such as glaucoma cause RNFL thinning independently of MS and should thus be taken into account.[12]

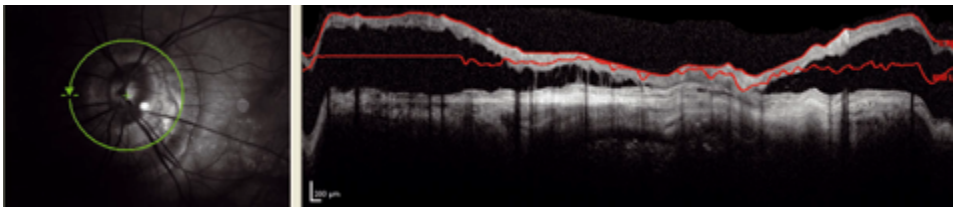

Figure 5. Retinal pathology: There is severe peri-papillary atrophy. It can be seen that this affects the RNFL enormously.

This list is likely to grow as OCT will be used for more diseases across all medical specialities. We propose to keep 'R' as a separate criterion in a future revision and regularly amend the list of diseases summarised in Table 2. Such future studies should also carefully revise whether or not severe myopia or hyperopia is a hard criterium for rejection or if these patients could be used as their own controls in longitudinal studies. One of the main sources of disagreement in the OCT training set was scan quality. In fact most scans from the training set were rejected due to poor illumination (Figure 6). Therefore illumination has been put forward as the sixth criterium ('I').

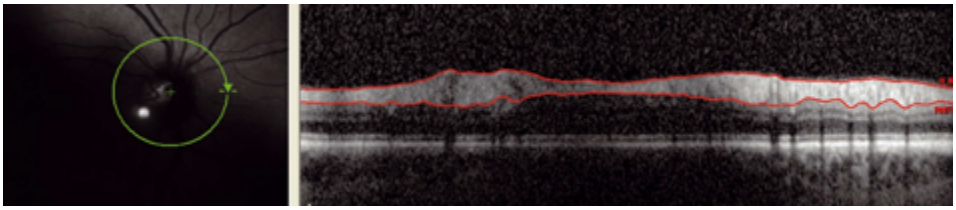

Figure 6. Illumination: The OCT scan here is badly illuminated. Also here this results in speckling and decrease of resolution.

The last criterium concerns beam placement ('B'). Recent literature has demonstrated that off-center beam placement causes an RNFL artifact in a range of up to 10 µm, which by far exceeds annual loss of 1-2 µm RNFL thought to be due to neurodegeneration in patients with MS.[13,14] This is a new finding which was not known to any of the participating centers at time of OCT scan acquisition. Not surprisingly a large number of scans were rejected based on this criterion alone. Re-applying this criterium to the training set resulted in a 60-70% rejection rate which seems excessive (Table 3). A more realistic but still high (16-28%) rejection rate for the 'B' criterium was seen in the validation set (Table 4).

Whilst taking an OCT scan it is easy to place the laser beam off-center. Off-center beam placement causes the live image to tilt. The tilting depends on the direction of beam misplacement.[14] Especially in multi-center studies this criterion is of utmost importance

since in contrast to live images tilting during scan acquisition is not necessarily visible on averaged summary scans transferred to a central reading center. However, these artefacts can be detected even in averaged summary scans by looking at the outer nuclear layer (ONL) to the ONL reflectivity (Figure 7).[14]

Table 4 Proportion of *rejected* OCT scans per reader, broken up to each of the seven 'OSCAR-IB' criteria based on the prospective validation set of 159 OCT scans from Amsterdam, San Francisco and Calgary.

Criterium	Rater 1	Rater 2	Rater 3
O	0/159 (0%)	4/159 (3%)	8/159 (5%)
S	8/159 (5%)	7/159 (4%)	5/159 (3%)
C	11/159 (7%)	11/159 (7%)	11/159 (7%)
A	10/159 (6%)	10/159 (6%)	12/159 (8%)
R	2/159 (1%)	1/159 (1%)	1/159 (1%)
I	19/159 (12%)	18/149 (1%)	34/159 (21%)
B	45/159 (28%)	29/159 (18%)	25/159 (16%)
Total	67/159 (42%)	68/159 (43%)	67/159 (42%)

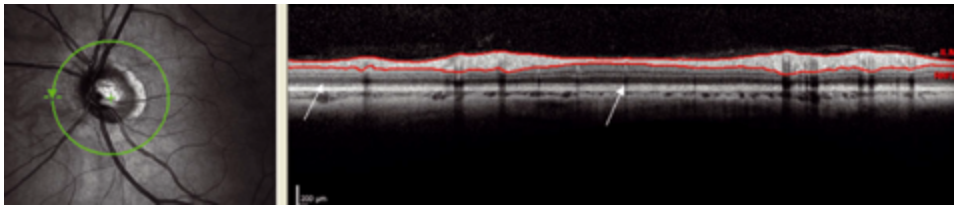

Figure 7. Beam placement: the laser beam is not placed centrally. This can be seen at the outer nuclear layer (ONL). The two arrows point to two regions of the ONL. The left arrow points to a light gray region whereas the other points to a darker gray region. If there is too much difference in colour of the ONL itself a scan is rejected.

The rigorous application of the 'B' criterium was considered necessary because of the large error (up to 42 µm) introduced into measurement of the RNFL thickness. The resulting high rejection rate of almost a third of all scans may come as a disappointment, but hopefully will contribute to improving future retinal OCT studies in MS where an annual RNFL thinning of 2 µm is anticipated.[15]

There are some limitations about our study. A possible drawback of the 'OSCAR-IB' criteria could be that rating in such a way could be too strict, leading to a high rejection rate of OCT scans. In addition, the proposed criteria were applied to ring scans only, but are expected to be also applicable to volume- and other scans as well. Further studies have to be carried out to verify this. In fact, given the increasing evidence for damage to the macula in patients with multiple sclerosis such studies are warranted. From the ophthalmological literature one would expect an increased rejection rate based on algorithm failure either due to a very thin RNFL or other structural problems such as for

example an epiretinal membrane.[6] Whether such scans would also need to be rejected or require hand-correction of the automated algorithm we are unable to tell from the present study. Another weakness of our study is that the criteria were not validated for retinal OCT images obtained from machines produced by other manufacturers. One would expect similar artefacts and image acquisition problems in OCT machines from other manufacturers, but is difficult to indicate to what extent. For algorithm failures and signal strength one could expect a difference in rejection rate between machines since these artefacts are entirely machine and type of algorithm dependent. On the other hand the rejection rate associated with other criteria are partially influenced by human subjects or raters, thus less machine dependent. Further studies are required to investigate this.

We believe that one of the requirements of MS OCT criteria is that their application should remain simple and practical in daily routine. In the future new findings and new parameters should of course be taken into consideration if these lead to a higher detection rate of artefacts. To conclude, the OSCAR-IB criteria are a first step towards a consensus on quality assessments of retinal OCT measurements in MS. We propose these criteria to be considered for future OCT studies in MS research and to be regularly revised as our experience with this new technology grows.

REFERENCES

1. Frohman E, Costello F, Zivadinov R, et al. Optical coherence tomography in multiple sclerosis. *Lancet Neurol* 2006;5:853-863.
2. Petzold A, de Boer J, Schippling S, et al. Optical coherence tomography in multiple sclerosis: a systematic review and meta-analysis. *Lancet Neurol* 2010;9:921-932.
3. Green AJ, McQuaid S, Hauser SL, Allen IV, Lyness R. Ocular pathology in multiple sclerosis: retinal atrophy and inflammation irrespective of disease duration. *Brain* 2010;133:1591-1601.
4. Jindahra P, Hedges TH, Mendoza-Santiesteban CE, Plant GT. Optical coherence tomography of the retina: applications in neurology. *Curr Opin Neurol* 2010;23:16-23.
5. Barkhof F, Calabresi PA, Miller DH, Reingold SC. Imaging outcomes for neuroprotection and repair in multiple sclerosis trials. *Nat Rev Neurol* 2009;5:256-266.
6. Domalpally A, Danis RP, Zhang B, Myers D, Kruse CN.Quality issues in interpretation of optical coherence tomograms in macular diseases. *Retina* 2009;29:775-781.
7. Fleiss JL. Statistical Methods for Rates and Proportions. 3th edition. New York: John Wiley & Sons. 2003 pp 618-622.
8. Landis JR, Koch GG. The measurement of observer agreement for categorical data. *Biometrics* 1977;33:159-174.
9. Vizzeri G, Bowd C, Medeiros FA, Weinreb RN, Zangwill LM. Effect of Signal Strength and Improper Alignment on the Variability of Stratus Optical Coherence Tomography Retinal Nerve Fiber Layer Thickness Measurements. *Am J Ophthalmol* 2009;148:249-255.
10. Yim Lui Cheung C, Kai Shun Leung C, Lin D, Pang CP, Shun Chiu Lam D. Relationship between Retinal Nerve Fiber Layer Measurement and Signal Strength in Optical Coherence Tomography. *Ophthalmology* 2008;115:1347-1351.
11. Huang J, Liu X, Wu Z, Sadda S. Image quality affects macular and retinal nerve fiber layer thickness measurements on fourier-domain optical coherence tomography. *Ophthalmic Surg Lasers Imaging* 2011;42:216-21.
12. Kanamori A, Nakamura M, Escano MFT, et al. Evaluation of the glaucomatous damage on retinal nerve fiber layer thickness measured by optical coherence tomography. *Am J Ophthalmol* 2003;135: 513-520.
13. Otani T, Yamaguchi Y, Kishi S. Improved visualization of henle fiber layer by changing the measurement beam angle on optical coherence tomography. *Retina* 2011;31: 497-501.
14. Balk L, de Vries-Knoppert WAEJ, Petzold A. A simple sign for recognizing off-center OCT measurement beam placement in the context of multicentre studies. *PLoS One. 2012;7:e48222.*
15. Talman LS, Bisker ER, Long DA, et al. Longitudinal study of vision and retinal nerve fiber layer thickness in multiple sclerosis. *Ann Neurol* 2010;67:749-760.
16. Costello F. Evaluating the Use of Optical Coherence Tomography in Optic Neuritis. *Multiple sclerosis Int* 2011:148394.

Chapter 3.3

Quality control for retinal OCT in Multiple Sclerosis: Validation of the OSCAR-IB criteria

S Schippling*,LJ Balk*, F Costello*, P Albrecht, L Balcer, P Calabresi, JL Frederiksen, E Frohman, AJ Green, A Klistorner, O Outteryck, F Paul, GT Plant, G Traber, P Vermersch, P Villoslada, S Wolf, A Petzold

* These authors contributed equally to the manuscript

Mult Scler. **2014 Jun 16. [Epub ahead of print]**

ABSTRACT

Background Retinal optical coherence tomography (OCT) permits quantification of retinal layer atrophy relevant to assessment of neurodegeneration in multiple sclerosis (MS). Measurement artefacts may limit the use of OCT to MS research.

Objective An expert task force convened with the aim to provide guidance on the use of validated quality control (QC) criteria for the use of OCT in MS research and clinical trials.

Methods A prospective multi-centre (n=13) study. Peripapillary ring scan QC rating of a OCT training set (n=50) was followed by a test set (n=50). Inter-rater agreement was calculated using kappa statistics. Results were discussed at a round table after the assessment had taken place.

Results The inter-rater QC agreement was substantial (kappa=0.7). Disagreement was found highest for judging signal strength (kappa=0.40). Future steps to resolve these issues were discussed.

Conclusion Substantial agreement for QC assessment was achieved with aid of the OSCAR-IB criteria. The task force has developed a website for free online training and QC certification. The criteria may prove useful for future research and trials in MS using OCT as a secondary outcome measure in a multi-centre setting.

INTRODUCTION

Retinal optical coherence tomography (OCT) is increasingly used in multiple sclerosis (MS) research as a tool to quantify changes of retinal layer thickness.[1] Following MS-associated optic neuritis (MSON) there may be severe atrophy of the peripapillary retinal nerve fibre layer (pRNFL). Importantly, a small degree of pRNFL atrophy can also be observed in patients with MS who never experienced a clinical episode of MSON.[1] In addition to these cross-sectional data, longitudinal data from time-domain OCT suggests that the annual loss of pRNFL in MS accounts for as little as 1-2 µm compared to about 0.1 µm among healthy individuals.[2] This degree of pRNFL atrophy is within the measurement range of recently introduced spectral-domain OCT devices from a number of manufactures. Therefore longitudinal spectral-domain OCT assessments of the retina in patients with MS may emerge as a surrogate for neurodegeneration, even in the absence of MSON.

In this context it is important to recognize that the magnitude of localised measurement artefacts introduced by a poor OCT scanning technique can be significant, measuring up to 40 µm when caused by off-centre placement of the measurement beam,[3] over 3.4 µm when due to displacement of the peripapillary ring-scan (outside an ellipse of 200 µm (horizontal shift) and 600 µm (vertical shift)),[4] and up to 10 µm when arising from poor signal quality alone.[5] Therefore, OCT scans containing such measurement artefacts should be excluded from clinical studies or trials as they may obscure the detection and interpretation of the much smaller degree of retinal layer atrophy expected from longitudinal studies.[2]

In addition to these quantitative considerations there are qualitative reasons to reject peripapillary OCT scans which may contain inherent inaccuracies. These comprise boundary line errors or algorithm failures and de-centration of the ring scan.[6] Poor illumination and obvious protocol violations are other reasons for OCT scans to be deemed poor in quality. In a previous study we developed a set of quality control (QC) criteria which address all of these issues.[7] In a multicentre validation approach we found a substantial inter-rater agreement (kappa 0.61) for the seven criteria that we named the OSCAR-IB QC criteria.[7]

The present study aimed to test the practicability and reliability of the OSCAR-IB criteria in a world-wide multi-centre setting. To this end we created a training (n = 50) and a test set (n = 50) of retinal OCTs from healthy subjects and patients with MS. Trained OCT readers from 13 centres participated. The group of participating experts from MS clinics, ophthalmology, and statistics convened in Lyon, France, to discuss the data and make recommendations for future OCT QC reading in MS research.

METHODS

Retinal images were obtained using a spectral domain (SD)-OCT device (Heidelberg Spectralis, software version 1.1.6.3) with the eye tracking function (EBF) enabled. All OCT scans were recorded from MS patients and healthy subjects who gave written informed consent for participation at the MS Centre in Amsterdam. In all subjects a peripapillary ring scan (diameter 12°) around the optic nerve head (ONH) was recorded. All scans were anonymised, randomised, and split into a training (n = 50) and test (n = 50) set.

The training set was rated individually by two trained OCT readers (LB, AP) with an inter-rater kappa of 1.0. A slide presentation was prepared which first showed the scans and then the dichotomised QC results: accept or reject. In case of rejection the reason for rejection was detailed. This could be one single out of the seven OSCAR-IB criteria,[7] or, more frequently, a combination of several criteria (e.g. a poor signal strength can also lead to an algorithm failure). The training set was sent to each of the participating OCT readers.

Next, another slide presentation was prepared, containing the test set. This time only the OCT scan was shown without giving any more information on QC rating. For this new technology, expert centres were defined as those who have published in the field (see references in Petzold et al.[1]) and were either of ophthalmological or neurological background. First and corresponding authors of these papers were approached either by email or personal contact. In addition, contact was made with established OCT reading centres. The raters from those 13 centres who had agreed to participate were asked to indicate if a scan was accepted or rejected in a spreadsheet document. In case of rejection the raters were also asked to fill in which one(s) of the OSCAR-IB criteria was (were) missed. This information was then sent back to the MS Centre in Amsterdam for statistical evaluation.

Data analysis

Kappa statistics for multiple raters were calculated to assess the inter-centre agreement using the Magree macro in SAS software (V9.3).[8] The level of agreement was rated as slight (0-0.2), fair (0.2-0.4), moderate (0.4-0.6), substantial (0.6-0.8) or almost perfect (0·8-1).[9]

Results were presented at a joint meeting of the participating centers at the 2012 ECTRIMS meeting in Lyon, France. Sources of disagreement were identified and discussed.

RESULTS

A total of 13 centres participated in the study (Table 1). Most centres (n = 9) provided data for a single rater. Data from multiple raters were provided by four centres (Table 1). Equipped with the OSCAR-IB criteria (Table 2), all raters participated in a training set (n = 50) prior to performing their own rating (n = 50) subject to statistical analysis (Figure 1). Two raters had to be excluded because the order of scans rated became irretrievably mixed up. The inter-rater level of agreement for the overall accept-reject classification was substantial (kappa 0.7, $p < 0.0001$). The average rejection rate was 55% of scans (range 48-74%; see Table 1).

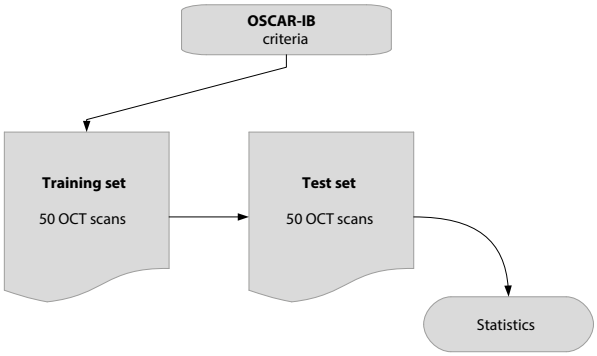

Figure 1. Study design

Table 1 Participating centres in alphabetical order, specifying the respective clinical specialty, number of raters and overall QC acceptation rate.

Centre	Specialty	Number of raters	QC accept (%)
Amsterdam	Neurology	3	52
Baltimore	Neurology	1	39
Berlin	Neurology	1	38
Bern	Ophthalmology	4	52
Calgary	Neurology	1	38
Copenhagen	Neurology	1	44
Dusseldorf	Neurology	1	52
Lille	Neurology	1	50
London	Neurology	1	52
Philadelphia	Ophthalmology	1	48
Sydney	Ophthalmology	1	26
Dallas	Neurology	2	39
Zurich	Neurology, Ophthalmology	2	50

Raters had the right to accept-reject based on one or more of the OSCAR-IB criteria. In order to evaluate the relative utility of individual features individual inter-centre kappa's were calculated. The individual kappa values were lower compared to the overall accept-reject kappa (Table 3). The data demonstrates that a scan poorly centred at the optic disc was a clear reject for most (highest kappa 0.579). A comparable level of agreement was found for the R- (kappa 0.543), I- (kappa 0.565) and B-criteria (kappa 0.549). Disagreement between raters was largest for the S- (kappa 0.404), O- (kappa 0.434), and A-criteria (kappa 0.482).

Table 2 The OSCAR-IB quality control criteria for retinal OCT scans.

Item	criteria
O	Obvious problems not covered by items below. Please document for discussion + consensus agreement
S	Is the OCT signal sufficient? Signal strength > 15 (ring and volume scans) with appropriate averaging of multiple scans (ART activated)
C	Is the ring scan correctly centred? for circular discs: ONH must not cross more than two colours of the RAF logo (outer ring of RAF adjusted to outer ring of scan either by paper or electronically). In contrast to the ONH ring scan, post-hoc readjustment is possible for the macular volume scan.
A	Is there an algorithm failure? Red lines correctly identify the superior and inferior RNFL border (ring scan); Red lines correctly identify the retinal borders (volume scan)
R	Is there visible retinal pathology which may potentially impair the RNFL reading? See Table 2 in Tewarie et al.[7] (Note: some of these conditions are also exclusion criteria for OCT studies in MS)
I	Is the fundus well illuminated? Retinal structures visible (ring and volume scans)
B	Is the measurement beam placed centrally? Homogeneous ONL reflectivity (ring and volume scans)

Table 3 Inter-centre kappa's for each of the individual OSCAR-IB QC criteria. Note that individual kappa's are lower compared to the overall kappa of 0.7 because raters had the right to reject a scan based on one OSCAR-IB criterion alone, also several may apply simultaneously.

QC criterion	Kappa
O	0.434
S	0.404
C	0.579
A	0.482
R	0.543
I	0.565
B	0.549

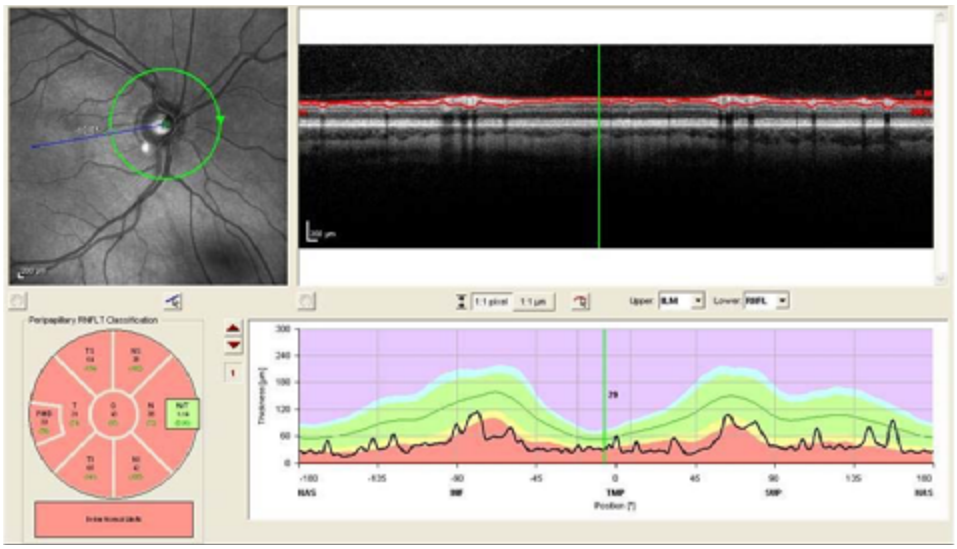

Figure 2. Example of an OCT scan rejected by some raters for the I-criterion. Shadow seen on the bottom right of the fundus image is cast by a floater.

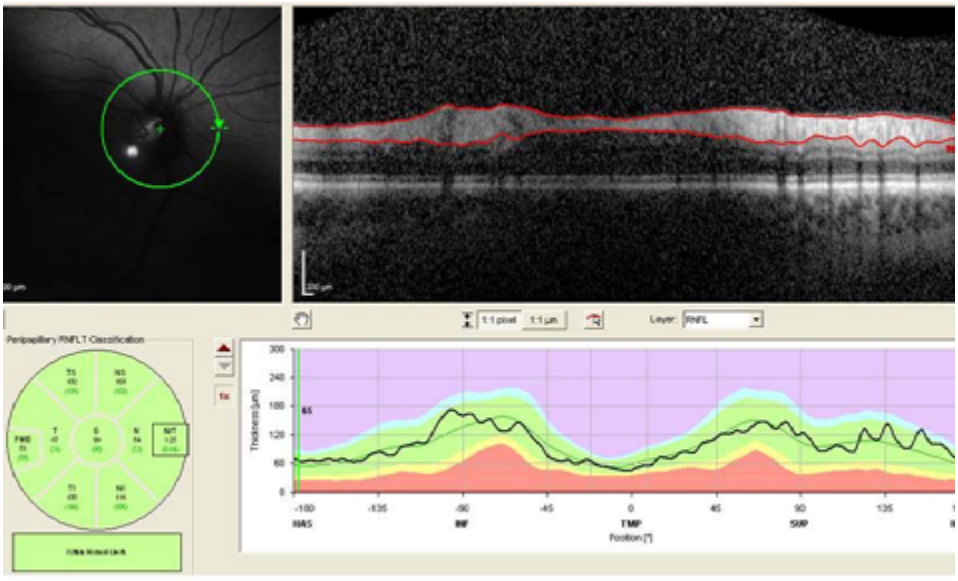

Figure 3. Example of a scan to be rejected due to truly poor illumination (I-criterion).

The consensus discussion at the round table meeting included scans like the one exemplified in Figure 2. This scan of a patient with MSON showing severe thinning of the pRNFL was rejected by a number of readers for the I-criterion. The shadow seen

on the bottom right of the infrared fundus image was cast by a floater. However, the illumination of the scan is acceptable, the contrast of the pRNFL in the OCT B-scan is good and there is no algorithm failure. Such an image should be accepted because the quantitative data is reliable. In contrast, Figure 3 shows a scan with truly poor illumination that should be rejected based on the I-criterion.

Another point of discussion was related to the B-criterion that was not intuitively clear to each reader. The two scans in the supplementary Figure 1 illustrate the problem of an off-centred beam-placement in different directions for a baseline and follow-up scan in the same subject. It can be readily seen that in the first scan the signal intensity is lowest in the ONL/OPL inferonasally, highest at the opposite part of the ring scan (located clockwise to sectors 7 o'clock and 1 o'clock). The localised measurement error is illustrated by the red/green shaded areas in the summary image. Such a scan should thus be rejected.

DISCUSSION

OCT is a promising new imaging technique that allows rapid and reliable quantification of retinal structures.[1,2] To date, pRNFL thickness has been the OCT measurement most commonly used in tracking longitudinal changes in optic neuritis (ON) and MS patients. A recent meta-analysis of time domain OCT studies (14 studies (2063 eyes)) demonstrated that RNFL values are reduced between 5 to 40 µm in MSON eyes.[1] Based upon the wealth of information derived from the OCT studies to date, pRNFL thickness changes may open a real window of opportunity for patient friendly assessment of neuro-axonal degeneration in ON and MS.[1,2,10,11]

As with each new technique entering the clinical arena, quality control becomes an issue. In absence of any consensus guidelines on QC rating of retinal OCT scans we recently developed and validated a set of seven criteria (OSCAR-IB) addressing major sources of artefacts causing inaccurate measurements. The intent was to guarantee high quality image acquisition and interpretation for multicentre OCT studies in which reading was to be done at a central site. The aim of the current study was to build on this experience and extend the validation of the OSCAR-IB criteria to a multi-reading centre setting. Twenty independent raters from thirteen international OCT expert centres participated in the trial. Results were discussed during a round table meeting in Lyon in order to provide further guidance for the use of the OSCAR-IB criteria in clinical trial settings.

In a set of test scans consisting of 50 optic nerve head ring scans (12°), the OSCAR-IB criteria proved to work better than in the pilot study with a substantial level of

agreement reaching an inter-centre kappa of 0.7 with an average rejection rate of 55% of scans (range 48-74%). This seeming high rejection rate is due to the fact that the dataset was put together with the intention to have a balanced number of good versus poor scans. It needs to be highlighted that none of the readers was aware that the intended rejection rate was 48%. In line with our previous experience, OCT scans were rejected for several reasons.

For the first of the OSCAR-IB criteria, 'Obvious' (O), scans were rejected for highly apparent issues including

severe lens opacities or vitreous haemorrhage. Likewise, rejection also occurred based on a protocol violation such as deliberately not averaging several B-scans by turning off the ART mode. As the rejection rate based on this criterion was overall low our expert panel expressed no new concerns regarding the use of this criterion.

For the second trial criterion, 'Signal strength' (S), we arbitrarily defined a cut off of 15 dB in the pilot study,[7] based on our experience and published evidence suggesting that poor signal strength decreases the signal-to-noise ratio of RNFL measures.[12-14] However, scans with poor signal strength (defined as <15 dB) but relatively good contrast between layers allowing for proper image post-processing and segmentation do exist. This might also be reflected by the fact that the S-criterion had the lowest inter-rater agreement in our study (inter-centre kappa 0.404). In the absence of any FDA approved retinal layer segmentation algorithm and corresponding normal control databases it is currently not possible to systematically test the relative contribution of signal strength and number of averaged A-scans to the final B-scan image quality. The contrast level between the retinal layer interfaces is likely to become a major criterion to judge the quality of OCT scans in ON and MS patients. In the future, this warrants further systematic studies. We opted to leave the cut off of 15 dB unchanged until such data is being provided.

The third criterion, a correctly 'Centred' ring scan (C) remains an important issue.[4] More recent scanning

algorithms from the Heidelberg Spectralis device are centring the ring scans after defining the borders of the Bruch´s membrane opening (new Nsite protocol; e.g. used in the PASSOS trial; NCT01705236). Preliminary experience with new protocols suggests that a perfectly centred ring-scan may not be required. The C-criterion is therefore not fully applicable to scans obtained using the Nsite protocol. However, as a change of position (vertical or horizontal) at follow-up scans may introduce relevant measurement artifacts,[4] it is crucial to set the baseline scans as reference and use the device's follow-up setting to assure consistency of scan placement during longitudinal investigations.

Admittedly, 'Algorithm' failures (A) remain a problem. In selected cases it may be possible to correct such errors by image post-processing techniques such as manual correction. However, this procedure is time-consuming when analysing large collectives. A decision may be made on individual scans. Whilst this criterion should be handled rather strictly on the baseline scan in order to ensure optimal settings for longitudinal studies, we accept that a minor, manually correctable algorithm failure on a valuable follow-up scan should not necessarily lead to immediate rejection.

As a fifth criterion, 'Retinal pathology' (R) unrelated to MS can independently influence RNFL measures and should thus be taken into account. Previously, we listed a number of pathologies that should be considered

when it comes to OCT scan interpretation (see supplementary Table 1).[7] Such a list will naturally grow with further experience generated by the use of OCT in different disease models as with the improvement of the technology per se. Of note, a number of recent OCT studies have provided evidence that retinal pathology other than RNFL thinning exists in MS,[10,11,15,16] including microcystic macular oedema (MMO) predominantly affecting the inner nuclear layer (INL) of the retina. In the studies to date, MMO (and INL thickening) appear to be associated with higher degrees of MS-related disability.[11,17-19] Hence, we do not recommend rejecting OCT scans showing evidence of MMO because this may be a clinically relevant finding in the disease and the impact of MMO on RNFL quantification is low.

Poor 'Illumination' of scans (I) raised some discussion between experts. Scans displaying shadow casts on the retina by large vitreous floaters were rejected by some raters based on the I-criterion whereas these scans were accepted by others. Although floaters were identified as potential cause of shadowing, they were not listed as a general exclusion criterion in the original OSCAR-IB manuscript. In most cases the contrast of retinal layers underneath the shadow cast was expected to remain of sufficient quality to enable accurate retinal layer segmentation by automated algorithms.

In contrast, poor illumination by a sub-optimal placement of the laser beam causes partial illumination of the retina with just about acceptable B-scan quality in some areas and very dark B-scans from poorly illuminated areas. Typically, the poorly illuminated areas are located at the border of the infrared image. Clearly, in poorly illuminated areas the signal may drop to such low levels that no image post-processing can be performed. In summary, causes for shadows such as floaters, cataracts, long eye lashes, etc. should not be considered a general reason for exclusion by the I-criterion in cases where A- and B-scan quality is good.

The relevance of the 'B' (beam placement) criterion was not intuitively obvious to all raters. It is important to keep the OCT scan in the live window horizontally orientated whenever possible. Problems arise when a scan is tilted in one direction at baseline and to the opposite direction at follow-up, because, as a consequence, measurement errors

in the range 9-40 um can be introduced.[3] Scans with sub-optimal beam placement as described, should be rejected. In some cases the anatomy of the retina or refraction anomalies such as astigmatism may make it difficult to achieve a perfectly horizontally aligned OCT. In this context, the QC rating of the follow up scan will ensure that the same direction of tilting is repeated, thus ensuring consistency. The principle of the B-criterion is that the direction of tilt causes a characteristic, reproducible, robust signal pattern in the outer plexiform- (OPL) and outer nuclear layers (ONL). This sign allows tracing back possible errors due to off-centre beam placement. Notably, a post-hoc analysis of the present data excluding all cases that were rejected based on the B-criterion resulted in a comparable kappa as the original analysis.

A limitation of the OSCAR-IB criteria is that they are entirely based on the pRNFL measures from the Spectralis device (Heidelberg Engineering). There is a need to test the criteria also on other machines on the market. As segmentation algorithms will certainly be used in multi-centre OCT studies in MS in the near future as soon as the necessary post-processing software becomes more broadly available, we cannot be sure about limitations to such measures' quality that in turn impact on the inter-rater agreement of segmentation analyses. While data on inter-rater and agreement between different segmentation algorithms has been provided,[20] sources of disagreement due to poor quality have not yet been identified. As for peripapillary ring scans, a sharp and good contrast between layers is likely to be the core pre-requisite for the segmentation of macular volume scans as well. This is covered by the O-, S-, R-, I-, and B-criteria of the OSCAR-IB criteria. For a reading centre working with a large number of sites and photographers the criteria may be rather strict. In our experience the initial rejection rate may be as high as 43%.[7] It is therefore recommended that OCT technicians are specifically trained to comply with the OSCAR-IB criteria, and pass a certification procedure before starting to include patients into clinical trials. In order to evaluate the influence of the QC criteria for the 'real' world one would need to test their impact by power calculations, ideally from on-going studies. Probably some pragmatism will be needed to permit for reasonable sample size estimates in a 'real' world multi-centre setting.

In summary, the OSCAR-IB QC has shown substantial inter-rater agreement in hands of experienced OCT raters in this multi-centre validation study. Experts participating in the meeting agreed that making the training set more broadly available would be helpful in order to guarantee rigorous QC in future clinical OCT trials in MS and other diseases. Rigorous QC will be particularly important for longitudinal clinical studies were only a small degree of retinal layer atrophy can be expected. The training and test set of this manuscript can be accessed for free on www.oscar-ib.org. Likewise, revisions to the criteria might become necessary as the use of OCT technology grows and scanning protocols continue to evolve.

SUPPLEMENTARY MATERIAL

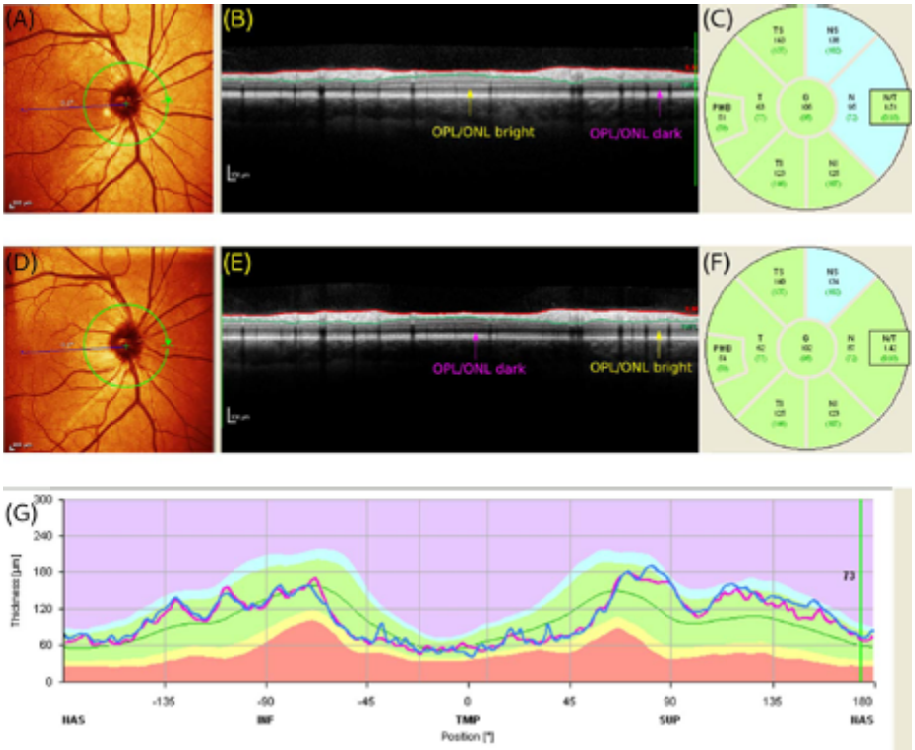

Supplementary Figure 1. Two scans originating from the same subject (top scan: baseline; bottom scan: follow-up) illustrating the problem of off-centre beam-placement. Mind that the signal intensity in the top scan is lowest in the ONL/OPL below the PMB and highest at the opposite part of the ring scan.

Supplementary Table 1 Pathology of the retina or optic nerve to be considered by the OSCAR-IB criteria.

Summary	Diseases
Structural	Drusen, cysts[a], retinal detachment, large discs, small crowed discs, presence of myelinated axons, naevus, tumour, peri-papillary atrophy, optic disc oedema, more than 6 diopters of myopia or hyperopia.
Vascular	Anterior ischaemic optic neuropathy (AION) & posterior ischaemic optic neuropathy (PION), giant cell arteritis (GCA), central retinal artery occlusion (CRAO), central retinal vein occlusion (CRVO), branch retinal artery/vein occlusion (BRAO, BRVO), arteriovenous malformations (AVM), cotton-wool spots, cerebrovascular accident (CVA) affecting the optic pathways.
Immune	Paraneoplastic, melanoma associated (MAR) and carcinoma associated retinopathy (CAR), neuromyelitis optica (NMO), systemic lupus erythematosus (SLE), uveitis retinochoroiditis
Infectious	Viral, bacterial, fungus, HIV, Lyme, neurosyphilis
Hereditary	Leber's hereditary optic neuropathy, dominant hereditary optic atrophy (DOA), albinism, cone dystrophy, retinitis pigmentosa.
Iatrogen	Vitreoretinal surgery, photocoagulation, optic nerve sheath fenestration, brain surgery affecting the optic pathways.
Metabolic/toxic	Diabetes, vitamin B12 and vitamin A deficiency, alcohol-, tobacco- and malnutrition-induced optic neuropathy, ethambutol, amiodarone, vigabatrin, chloroquine and other drugs known to cause an optic neuropathy.
Other	Glaucoma, macular degeneration, central serous chorioretinopathy, birdshot retinochoroidopathy and other white dot syndromes, Purtscher's retinopathy.

[a] Since the original publication of the OSCAR-IB criteria a new OCT sign in MS was described by the UCSF group: microcystic macular oedema (MMO). In about 1-5% of patients with MS, MMO is seen and should not be considered as an exclusion criterion.

REFERENCES

1 Petzold A, de Boer JF, Schippling S, et al. Optical coherence tomography in multiple sclerosis: a systematic review and meta-analysis. *Lancet Neurol* 2010;9:921-932.

2 Talman L S, Bisker ER, Sackel DJ, et al. Longitudinal study of vision and retinal nerve fiber layer thickness in multiple sclerosis. *Ann Neurol* 2010;67:749-760.

3 Balk LJ, de Vries-Knoppert WAEJ, Petzold A. A Simple Sign for Recognizing Off-Axis OCT Measurement Beam Placement in the Context of Multicentre Studies. *PLoS One* 2012;7:e48222.

4 Gabriele M L, Ishikawa H, Wollstein G, et al. Optical coherence tomography scan circle location and mean retinal nerve fiber layer measurement variability. *Invest Ophthalmol Vis Sci* 2008;49:2315-2321.

5 Balasubramanian M, Bowd C, Vizzeri G, Weinreb RN, Zangwill LM. Effect of image quality on tissue thickness measurements obtained with spectral domain-optical coherence tomography. *Opt Express* 2009;17:4019-4036.

6 Domalpally A, Danis RP, Zhang B, Myers D, Kruse CN. Quality issues in interpretation of optical coherence tomograms in macular diseases. *Retina* 2009;29:775-781.

7 Tewarie P, Balk LJ, Costello F, et al. The OSCAR-IB Consensus Criteria for Retinal OCT Quality Assessment. *PLoS One* 2012;7:e34823.

8 Fleiss J. Measuring nominal scale agreement among many raters. Psych Bull 1971;76:378-382.

9 Landis J and Koch G. The measurement of observer agreement for categorical data. *Biometrics* 1977;33:159-174.

10 Saidha S, Syc SB, Ibrahim MA, et al. Primary retinal pathology in multiple sclerosis as detected by optical coherence tomography. *Brain* 2011;134:518-533.

11 Brandt AU, Oberwahrenbrock T, Ringelstein M, et al. Primary retinal pathology in multiple sclerosis as detected by optical coherence tomography. *Brain* 2011;134:e193.

12 Vizzeri G, Bowd C, Medeiros FA, Weinreb RN, Zangwill LM. Effect of Signal Strength and Improper Alignment on the Variability of Stratus Optical Coherence Tomography Retinal Nerve Fiber Layer Thickness Measurements. *Am J Ophthalmol* 2009;148:245-255.

13 Yim Lui Cheung C, Kai Shun Leung C, Lin D, Pang CP, Shun Chiu Lam D. Relationship between Retinal Nerve Fiber Layer Measurement and Signal Strength in Optical Coherence Tomography. *Ophthalmol* 2008;115:1347-1351.

14 Huang J, Liu X, Wu Z, Sadda S. Image quality affects macular and retinal nerve fiber layer thickness measurements on fourier-domain optical coherence tomography. *Ophthalmic Surg Lasers Imaging* 2011;42:216-21.

15 Gelfand JM, Nolan R, Schwartz D M, Graves J, Green AJ. Microcystic macular oedema in multiple sclerosis is associated with disease severity. *Brain* 2012;135:1786-93.

16 Saidha, S Sotirchos ES, Ibrahim MA, et al. Microcystic macular oedema, thickness of the inner nuclear layer of the retina, and disease characteristics in multiple sclerosis: a retrospective study. *Lancet Neurol* 2012;11:963-72.

17 Balk LJ, Killestein J, Polman C H, Uitdehaag BM, Petzold A. Microcystic macular oedema confirmed, but not specific for multiple sclerosis. *Brain* 2012;135:e226.

18 Sotirchos ES, Saidha S, Byraiah G, et al. In vivo identification of morphologic retinal abnormalities in neuromyelitis optica. *Neurology* 2013;80:1406-1414.

19 Wolff B, Basdekidou C, Vasseur V, Mauget-Faÿsse M, Sahel JA, Vignal C. Retinal inner nuclear layer microcystic changes in optic nerve atrophy: a novel spectral-domain OCT finding. *Retina* 2013;33:2133-8.

20 Seigo MA, Sotirchos ES, Newsome S, et al. In vivo assessment of retinal neuronal layers in multiple sclerosis with manual and automated optical coherence tomography segmentation techniques. *J Neurol* 2012;259:2119-30.

Chapter 4

Optical coherence tomography in MS

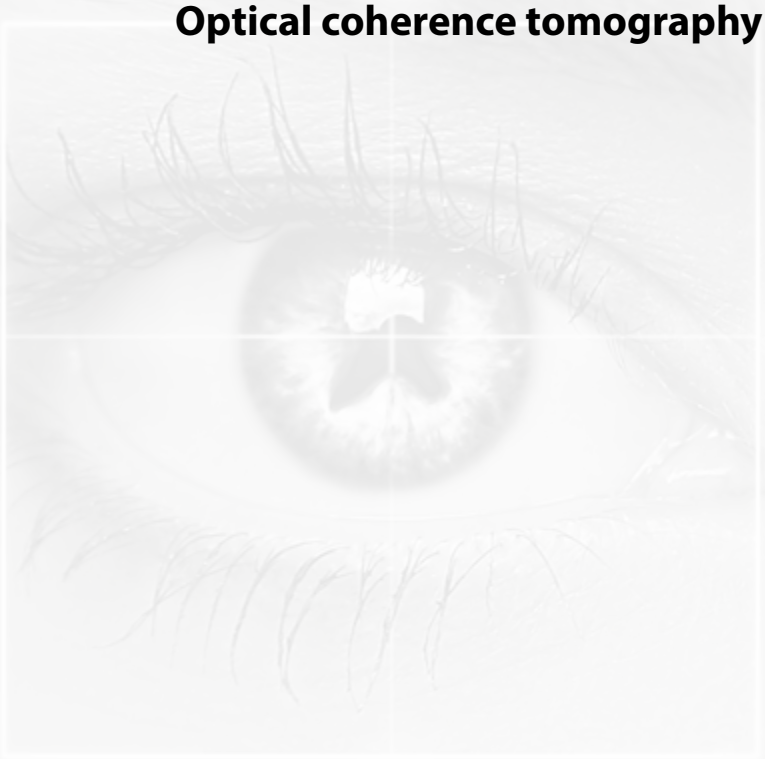

Chapter 4.1

Disease course heterogeneity and OCT in Multiple Sclerosis

LJ Balk, P Tewarie, J Killestein, CH Polman, BMJ Uitdehaag, A Petzold

Mult Scler. **2014;20:1198-1206**

ABSTRACT

Background The heterogeneity of the disease course in multiple sclerosis (MS) remains a challenge for patient management and clinical trials.

Objective To investigate the relationship between disease course heterogeneity and retinal layer thicknesses in MS.

Methods 230 MS patients and 63 healthy control subjects were included. Spectral-domain OCT scanning of the peripapillary and macular regions was performed, followed by automated 8-layer segmentation. Generalised estimation equations were used for comparisons. Receiver operating characteristic (ROC) curves were calculated for distinguishing a benign from a typical disease course.

Results Primary progressive patients showed relative preservation of inner retinal layers, compared to relapsing onset MS types. Only in MS eyes without optic neuritis, patients with typical MS showed more thinning of the inner retinal layers, compared to patients with a benign disease course, even after an average disease course of 20 years.

Conclusion The thicknesses, particularly of the innermost retinal layers (RNFL, GCC), were significantly related to the heterogeneous disease course in MS. The relative preservation of these layers in primary progressive and benign MS suggests rather limited susceptibility of the retina to neurodegeneration which may be relevant for future neurodegenerative treatment trials employing OCT as a secondary outcome measure in primary progressive MS.

INTRODUCTION

The disease course in multiple sclerosis (MS) is highly heterogeneous. A large proportion (about 80-85%) of patients experiences a relapsing remitting (RR) onset of the disease. In time, around 65% of RR patients will enter the secondary progressive (SP) phase in which clinical relapses become less pronounced and slowly change into a gradual worsening of the disease. In around 15-20% of patients, the disease has a progressive onset (PP).[1,2] Compared with relapse-onset MS, patients with PPMS are older at onset, show a larger degree of spinal cord atrophy and a higher proportion are men.[3]

The disease course is benign in around 10% to 20% of patients. Although this is dependent on the definition used to define benign MS (BMS), most studies refer to benign MS as having limited disability (EDSS ≤ 3.0) after 10 or 15 years of MS disease.[4,5] Although patients with BMS have relatively preserved motor functions, leading to lesser walking disabilities, they do have similar whole brain atrophy compared with SPMS and also similar or even greater T2 MRI lesion burden compared to those with RRMS.[6]

The highly heterogeneous disease course in MS may be explained by diverse pathological processes, such as the amounts of de- and remyelination, but also the degree of axonal and neuronal damage.[1,7,8] Neuroaxonal loss has been demonstrated within inflammatory lesions,[8] but also in white and grey matter and the spinal cord[9,10] and is being held responsible for disease progression and irreversible disability.[11] To date, it is however not entirely clear what mechanism induces neuroaxonal degeneration and how this is different between the MS subtypes. Previous MRI studies which directly compared different MS subtypes have shown that the estimates of brain atrophy rates varied greatly between different MS subtypes.[12-15]

Brain atrophy findings, based on MRI, may however reflect something different than axonal loss, since atrophy quantified by MRI can partially be caused by loss of non-neuronal cells.[16,17] Importantly, a relatively new method to quantify neuroaxonal degeneration in vivo, is optical coherence tomography (OCT), which is not influenced by the aforementioned methodological bias. This technique, first described in 1991 by Huang et al.,[18] has the advantage of imaging the only part of the human CNS where non-myelinated axons are visible, the retina. Newer OCT segmentation algorithms made it possible to quantify multiple individual retinal layers, offering new possibilities for investigating both neuronal and axonal loss, allowing for investigating the cascade of neuroaxonal degeneration in MS.[19]

Some previous studies have compared the peripapillary RNFL thickness between the different MS disease types, but results have been inconclusive. No differences in RNFL thickness between PPMS and relapsing onset MS were reported in several studies,[20-22]

while others described significantly lower RNFL thickness in progressive disease stages, compared to RRMS or CIS patients.[23-25] More recent studies with data available on the individual retinal layers, reported the most severe atrophy of the RNFL and ganglion cell+inner plexiform layer (GCIP) in SPMS, followed by RRMS and PPMS,[26-27] although this observation was not confirmed by Albrecht et al., who reported that all MS subtypes had significant thinning of the RNFL and the ganglion cell layer (GCL) and inner plexiform layer (IPL).[28] The inconsistency of these results may be caused by the small sample sizes, especially of the progressive subgroups.
Therefore, the aim of this study was to investigate the patterns of retinal axonal and neuronal degeneration in different MS subtypes, including primary progressive and benign MS, in a large cohort of patients with longstanding MS.

METHODS

Study design and patient population

MS subjects and controls were recruited from the VU University medical centre Amsterdam. This study was approved by the medical ethical committee (protocol number 2010/336) and the scientific research committee (protocol number CWO/10-25D) of the of the VU University Medical Centre in Amsterdam, the Netherlands. Written informed consent was obtained from all included subjects.
Patients were eligible for inclusion if they were aged 18-80 years and had a diagnosis of either RRMS or SPMS or PPMS at the time of their assessment (defined by Lublin-Reingold criteria).[29] Patients who were pregnant, received a course of steroids or had a relapse within the preceding month, had HIV or other immunodeficiency syndrome, reported history of substance abuse (drug or alcohol) in the past five years or had specific MRI findings that could interfere with evaluation, were excluded from the study. Healthy control subjects were included if they were aged 40-60 years at the time informed consent was signed and if they had no history of any neurological or psychiatric disease, were not pregnant and had no familial relation (1st or 2nd degree) to an MS patient.

OCT imaging

Retinal imaging was performed with sd-OCT (Spectralis®, Heidelberg Engineering Inc, Heidelberg, Germany. Software version 1.7.1.0), using dual beam simultaneous imaging, with the eye tracking function enabled for optimal measurement accuracy.
Peripapillary data was obtained using a 12° ring scan. In order to obtain data on the macular area, a macular volume scan (20 x 20 degrees field, 25 B-scans) was performed.

All OCT scans were performed by four trained and certified technicians. Scans were excluded from the analyses if they violated international consensus quality control criteria (OSCAR-IB).[30]

Image post-processing was performed for both scans, using new segmentation software (Heidelberg Engineering Inc, Heidelberg, Germany). The software enabled reliable segmentation four distinct layers in the peripapillary area; the RNFL, INL, outer nuclear layer (ONL) and the outer plexiform layer (OPL) (Figure 1A). For all layers, a thickness map was provided of which the layer specific global mean values were used in this study. At the macular region, the software allowed for segmentation of three retinal layers; the retinal nerve fibre layer (RNFL), the ganglion cell complex (GCC=ganglion cell layer+inner plexiform layer) and the inner nuclear layer (INL). Furthermore, the outer retinal layers (ORLs) were calculated for the macular region by subtracting the RNFL, GCC and INL from the complete retinal thickness (Figure 1B). For all layers, the software generated a thickness map on a 1, 3 and 6 mm grid, as defined by the Early Treatment Diabetic Retinopathy Study (ETDRS).

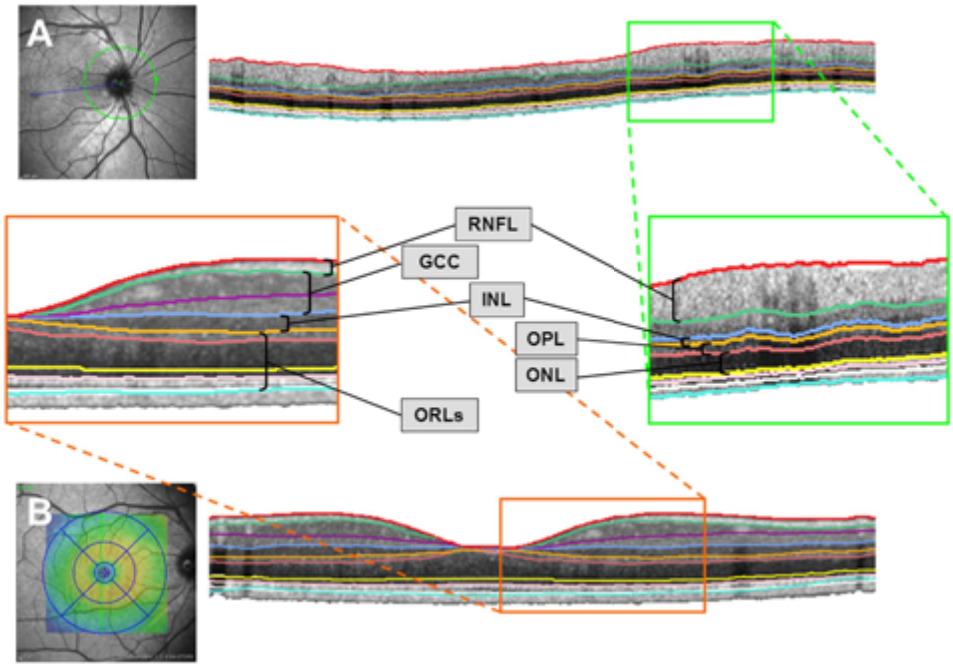

Figure 1. Segmentation protocol for the retinal OCT scan used in this study. Segmented layers of the peripapillary ring scan (A, upper image) and macular volume scan (B, bottom image). RNFL: retinal nerve fibre layer; GCC: ganglion cell complex (=ganglion cell layer+inner plexiform layer); INL: inner nuclear layer; OPL: outer plexiform layer; ONL: outer nuclear layer; ORLs: outer retinal layers, equal to [retina - (RNFL + GCC + INL)]

Of the nine sectors provided by this grid, only the mean of the four inner sectors composing the perimacular rim were used in this study. This was done because segmentation of the individual layers in the outer sectors was shown to be of poorer reproducibility, compared to the four inner ETDRS sectors.[31] All scans and all layers computed by this segmentation process, were verified by two independent OCT technicians. In case of obvious algorithm failure on a small area (due to a vessel or a small artefact), the deviating line was corrected manually. Scans were excluded if the algorithm failure covered a large part or the complete OCT B-scan area.

Clinical assessments

Medical history with respect to visual symptoms, was obtained in all patients and controls. The expanded disability status scale (EDSS) was determined by a certified examiner to assess level of disability. Benign MS (BMS) was defined as an EDSS score of 3.0 or less, after a disease duration of at least 15 years (from onset). In the analyses with BMS, patients with a non-benign MS course, i.e. an EDSS score of 3.5 or higher after a disease duration of at least 15 years from onset, were considered patients with 'typical MS'. Importantly, patients with a disease duration of less than 15 years from onset, were not included in the BMS analyses. The MS functional composite (MSFC) was assessed in all patients and includes three tests that evaluate ambulation (timed foot walk test), arm dexterity (9-hole peg test) and cognition (paced auditory serial addition test, PASAT).

Statistical analyses

Differences in retinal layer thickness between eyes with a RR, SP and PP disease course were analysed with generalised estimation equations (GEE). This method was used because the analyses were performed on eye-level instead of subject-level. In the GEE analyses (adjusting for intra-subject inter-eye correction, using an exchangeable correlation structure), age was included as a covariate to adjust for confounding. In order to avoid contamination of the study groups by pooling eyes with a history of ON (MSON eyes, showing a severe degree of RNFL loss) with eyes without a history of ON (MSNON eyes, showing a small degree RNFL loss),[32] these analyses were all performed separately for MSON, MSNON and healthy control (HC) eyes. Subsequently, retinal layer thickness was compared between BMS, typical MS and healthy control eyes, again using GEE analyses, adjusted for age.

In order to determine the discriminative value of both OCT and clinical markers for a benign disease course, receiver operating characteristic (ROC) curves were calculated, based on logistic regression models, only including MSNON eyes. The logistic regression models contained either solely OCT data (both the peripapillary ring scan and macular volume scan), solely MSFC data (absolute data of the three test combined) or a combination of OCT and MSFC data.

Statistical analyses were performed using SPSS version 20.0, with a significance level of 0.05. Additionally, significance levels after a Bonferroni correction (to adjust for multiple testing) are provided.

RESULTS

A total of 230 MS patients (140 RRMS, 61 SPMS, 29 PPMS) with longstanding MS and 63 healthy controls were included in this study. The MS patients had a mean disease duration of 20.4 (±7.0) years. Over 34% (N=59) of all patients with a disease duration of at least 15 years (N=173), had a benign disease course.
Moreover, PPMS patients were older (63.8±7.5) than RRMS and SPMS patients (50.7±9.6 and 57.9±7.4 respectively), but showed a shorter disease duration than SPMS patients due to the relatively high age at onset of PPMS patients (42.4±8.9 years). Subject characteristics are shown in Table 1.

Table 1 Subject characteristics by disease course. Values are reported as mean±sd, unless stated otherwise

	Disease course				
	RR N=140	**SP N=61**	**PP N=29**	**BMS* N=59**	**HC N=63**
Sex (% male)	26.4%	36.1%	48.3%	22.0%	34.9%
Age (years)	50.7 (±9.6)	57.9 (±7.4)	63.8 (±7.5)	51.3 (±8.8)	50.5 (±7.2)
Age at onset (years)	31.6 (±9.3)	34.9 (±7.7)	42.4 (±8.9)	30.3 (±8.2)	n/a
Disease duration (years)	19.1 (±6.2)	23.0 (±8.0)	21.4 (±6.8)	21.1 (±4.5)	n/a
Range	[8.8-37.6]	[9.7-45.9]	[10.3-35.3]	(15.1-37.6]	
EDSS (median [range])	3.0 [1.0-8.0]	6.0 [3.0-8.0]	6.0 [3.0-8.0]	3.0 [1.5-3.0]	n/a
History of ON (N [%])					
Unilateral	42 (30%)	20 (33%)	1 (3%)	22 (37.3%)	
Bilateral	24 (17%)	13 (21%)	2 (7%)	11 (18.6%)	n/a
Unknown	15 (11%)	6 (10%)	0 (0%)	4 (6.8%)	

RR=relapsing remitting, SP=secondary progressive, PP=primary progressive, BMS=benign MS, HC=healthy control, ON=optic neuritis, n/a=not applicable
* EDSS ≤ 3.0, after ≥15 years disease duration (from onset). The BMS group represents a selection of patients who were also included as RR, SP and PP.

Retinal layer atrophy and disease type

In the eyes of MS patients without a history of ON (MSNON), the PPMS eyes showed highest values for all retinal layers, both at the peripapillary and macular region (Table 2). The SPMS patients showed the most atrophy for all layers except the ORLs, compared to RRMS and PPMS eyes.
For the MSON eyes, there were no significant differences observed between RRMS and SPMS patients for any retinal layer. Since the amount of PP patients who experienced

ON was very small (5 eyes), no statistically meaningful comparison could be made with this patient group.

Table 2 Patients with a primary progressive disease course experienced less atrophy of the individually segmented retinal layers, compared to patients with a relapsing remitting or secondary progressive disease course

	RR	SP	PP	p-value* RR vs SP	p-value* SP vs PP	p-value* RR vs PP
MSNON eyes N=279	N=161	N=65	N=53			
Volume scan						
RNFL	26.0 ± 2.6	25.4 ± 2.7	27.1 ± 2.6	0.286	0.016	0.095
GCC	85.5 ± 13.1	79.1 ± 13.1	87.0 ± 10.9	0.020	0.013	0.536
INL	41.4 ± 2.7	41.2 ± 2.9	42.2 ± 3.8	0.473	0.191	0.075
ORLs	167.1 ± 9.1	169.6 ± 8.5	171.1 ± 8.3	0.095	0.739	0.069
Ring						
RNFL	86.5 ± 10.6	81.6 ± 8.8	89.0 ± 7.2	0.074	0.003	0.162
INL	16.8 ± 1.3	16.2 ± 1.2	16.8 ± 0.9	0.057	0.009	0.241
OPL	28.1 ± 1.6	27.7 ± 1.4	28.3 ± 1.4	0.463	0.074	0.190
ONL	59.4 ± 3.9	58.9 ± 3.3	60.4 ± 3.8	0.941	0.028	0.024
MSON eyes N=144	N=91	N=48	N=5‡			
Volume scan						
RNFL	23.8 ± 3.0	24.1 ± 2.6		0.694	-	-
GCC	70.8 ± 16.2	68.3 ± 18.9		0.470	-	-
INL	42.5 ± 2.9	41.9 ± 3.4		0.741		
ORLs	170.8 ± 8.4	172.1 ± 9.8		0.800		
Ring						
RNFL	76.5 ± 12.6	76.4 ± 10.2		0.812	-	-
INL	16.1 ± 1.5	15.6 ± 1.6		0.519	-	-
OPL	28.0 ± 1.5	27.5 ± 1.9		0.604	-	-
ONL	60.4 ± 3.5	58.8 ± 4.6		0.575	-	-

* GEE with correction for age and intra-subject inter-eye correlation. Significance level after Bonferroni correction: (N=8) $p<0.006$

‡ Group too small to make any statistical meaningful comparisons

Inner retinal layer atrophy is most severe in typical MS, followed by benign MS and healthy controls

In MSNON eyes, retinal layer atrophy was most severe in typical MS eyes, followed by BMS and then HC eyes for only the inner retinal layers (RNFL, GCC, see Figure 2). Specifically, the macular GCC and the peripapillary RNFL and INL showed significantly more thinning ($p<0.05$) in typical MS, compared to BMS. No such difference was observed for the macular INL and ORLs and the peripapillary OPL and ONL (supplementary Table 1 and Figure 2).

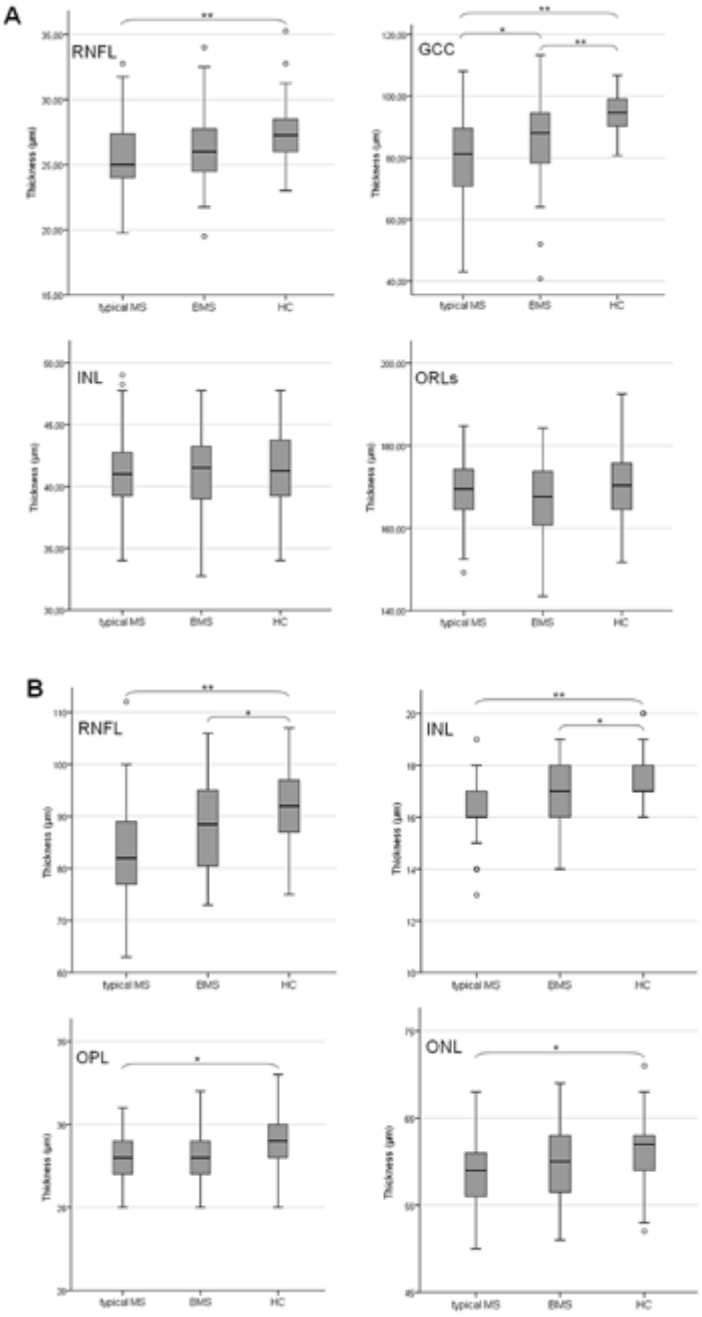

Figure 2. Retinal layer thickness of MSNON eyes in benign and typical MS. A benign MS disease course is associated with significant atrophy of the dominant inner retinal layers of (**A**) the macular region and (**B**) peripapillary region.
* p<0.01, **p<0.001

Although eyes of BMS patients showed less atrophy than typical MS for all layers except the ORLs, they still revealed more atrophy than HC eyes. This difference between BMS and HC was significant ($p<0.05$) for all layers, except the macular INL and ORLs. In the MSON eyes, no significant differences in retinal layer thickness were observed between typical MS and BMS eyes, due to the severe retinal layer thinning in both groups (data not shown).

Sensitivity and specificity for distinguishing a benign from a typical disease course

In order to determine the discriminative value of both OCT and clinical markers for a benign MS disease course, three ROC curves were calculated with only MSNON eyes included. The three models include OCT data, MSFC data and a combination of the two, respectively. In figure 3, the ROC curves for the three models are presented. Distinguishing a benign disease course with solely OCT data, resulted in an AUC of 0.73. A combination of the three components of the MSFC showed a better discriminative value, with an AUC of 0.90. The combination of both OCT and MSFC data however, increased the AUC to 0.94.

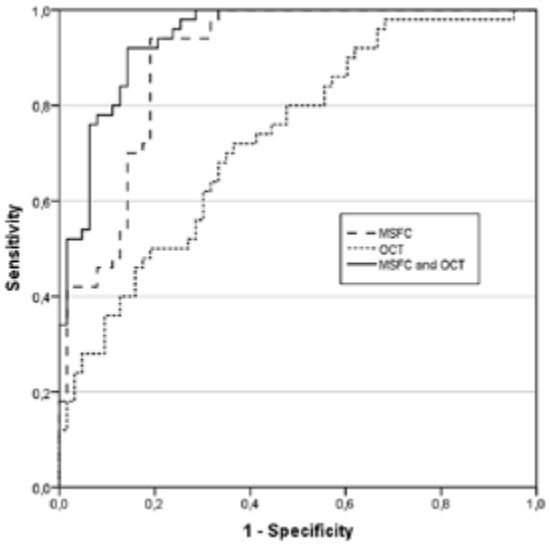

Figure 3. ROC curves for OCT data (dotted line, AUC 0.73) MSFC data (dashed line, AUC 0.90), and a combination of MSFC and OCT data (black line, AUC 0.93).

DISCUSSION

Firstly, this study showed that retinal layer atrophy was least severe in PPMS, compared to relapsing onset MS. Retinal layer atrophy, and especially atrophy of the innermost layers (RNFL and GCC) was most pronounced in SPMS patients. Secondly, this study demonstrated that BMS patients have significant thinning of the inner retinal layers (RNFL, GCC and INL) compared to controls, however less severe than in typical MS patients. Finally, retinal layer thickness should not be used solely to discriminate between a benign and a typical disease course, but may be of added value when combined with clinical measures.

Atrophy of the retinal layers is probably a reflection of 1) damage to the afferent visual pathways, 2) retinal pathology and 3) to a certain extent global cerebral damage.[32] The relative sparing of retinal layers in PPMS patients is in accordance with several other studies,[21,26,27] and may be explained by the fact that the afferent visual pathways are less often affected in PPMS. In addition, early MRI studies have shown that PPMS patients showed smaller lesion loads, lower frequency of gadolinium-enhancing lesions, but also more extensive spinal cord atrophy compared to patients with relapsing-onset MS.[33-35] The relative sparing of the retinal layers in PPMS is therefore presumably also explained by the limited reflection of spinal cord damage in the retinal layers.

The severe retinal layer thinning in SPMS patients compared to RRMS patients on the other hand, is thought to be a result of the progressive phase of the SPMS patients. Being in the secondary progressive phase of the disease, is strongly associated with a larger degree of degeneration of axons and neurons, which in turn leads to more global cerebral damage and subsequently to more severe retinal layer thinning.[12] The observed difference between SPMS and RRMS remained significant after adjustments for disease duration, suggesting that not disease duration, but the presence or duration of the progressive phase is responsible for the larger amount of retinal damage.

When the disease types were compared in MSON eyes, no differences were observed. This lack of difference is probably due to the large impact of the experienced episode of ON on the retinal layers. The damage caused by the episode of ON will supersede the more subtle effects of the disease subtype. The present data therefore suggests that the sub-clinical atrophy of the retinal layers in the MSNON eyes may be a better reflection of global CNS damage than the retinal layers in severely damaged MSON eyes.

Furthermore, some retinal layers showed clear differences between BMS and typical MS. Especially the macular GCC (a combination of the GCL, consisting of mainly neurons and the IPL, consisting of synaptic contacts of neurons) and the peripapillary RNFL (consisting of mainly unmyelinated axons) showed a consistent trend, in which these layers were thinnest in typical MS, followed by BMS and then HC eyes. Consistent with

the disease type comparisons, the outermost layers, such as the OPL, ONL and ORLs, did not show any differences between a benign or typical disease course, suggesting that the macular GCC and the peripapillary RNFL are the most sensitive measures reflecting global cerebral neuroaxonal degeneration.

In order to investigate whether OCT measures could be used to distinguish between a typical and a benign disease course, ROC curves were calculated. Clearly, the clinical measures (components of the MSFC) were much better in distinguishing BMS from typical MS than solely OCT measures (AUC 0.90 and 0.73 respectively). This was expected, because the definition of BMS is exclusively based on a well established clinical measure (EDSS score). A strongly related clinical measure (MSFC) is then expected to better distinguish BMS from typical MS than any other measure. When clinical and OCT measures were combined however, OCT measures did increase the AUC from 0.90 to 0.94. Therefore, OCT measures should not be used solely to identify a benign disease course, but it could add valuable information when combined with standardised clinical measures.

To the best of our knowledge, this study is first to examine individual retinal layer atrophy in different disease types in such a large cohort with longstanding MS, including a relatively large proportion of progressive patients. The findings of the present study extend on the data by Albrecht et al., who investigated retinal macular layer thickness in a younger cohort of MS patients and healthy controls. They reported that even in MSNON, all MS subgroups had significant thinning of the peripapillary RNFL, the macular retinal thickness and the retinal ganglion cell- and inner plexiform layer. Only in PPMS patients, the INL was reduced, which they attributed to primary retinal pathology.[28] Also consistent with the findings of the present study, was the GCC thinning in SP compared to RR and PP, reported by Saidha et al., although the progressive subgroups were relatively small.[27] Earlier studies investigating retinal layer atrophy in different disease types were restricted to the peripapillary RNFL. Results of these studies remained inconclusive,[20-25,27] which is possibly due to the relatively small sample sizes, particularly of the progressive subgroups, measurement noise due to lack of OCT quality control criteria and the different statistical approaches that were used.

The main limitation of the present study was that, although long-term, the data is only cross-sectional and data cannot be extrapolated for prognostication. Secondly, records of ON were mainly based on a combination of clinically confirmed episodes and a patient reported history on earlier events during the disease. As a result, a proportion of less severe episodes of ON may have gone unnoticed, in particular in the relapsing onset groups, where ON is more common than in PPMS. Lastly, medical history (with respect to other visual symptoms) was assessed by patient reported history. There has been no standardised consensus assessment of either the afferent or efferent visual

system and it might be possible that some of the transient visual symptoms may have been due to Uhthoff's phenomenon or impaired eye movements. This may have led to an overestimation of the presence of optic neuritis. Likewise, subtle changes in visual function only affecting the peripheral visual field may have been overlooked causing an underestimation of optic neuritis episodes. These are important limitations of the present and also other studies in this field.

In summary, thinning of the inner retinal layers (RNFL, GCC and INL) is significantly influenced by the heterogeneous disease course in MS, with the most severe atrophy observed in SPMS patients. Primary progressive and benign MS patients showed evident thinning of these inner retinal layers compared to controls, although less severe than following a RR or SP disease course. Future neuroprotective treatment trials may need to take the disease course heterogeneity into account before employing sd-OCT as a secondary outcome measure, as it may only be of limited value for PPMS.

SUPPLEMENTARY MATERIAL

Supplementary Table 1 Comparison of individually segmented retinal layer atrophy between BMS, typical MS and healthy controls.

	Typical MS	BMS	HC	p-value* Typical MS vs BMS	p-value* BMS vs HC	p-value* Typical MS vs HC
MSNON eyes	N=61	N=85	N=126			
Perimacular area						
RNFL	25.6 ± 2.6	26.2 ± 2.8	27.3 ± 2.1	0.073	0.013	<0.001
GCC	80.2 ± 12.3	86.5 ± 13.0	94.2 ± 6.0	0.004	<0.001	<0.001
INL	41.3 ± 3.0	42.8 ± 2.6	41.4 ± 2.9	0.282	0.676	0.310
ORLs	169.2 ± 7.3	167.0 ± 9.2	170.2 ± 8.9	0.499	0.094	0.149
Peripapillary area						
RNFL	83.8 ± 9.2	88.3 ± 9.2	91.7 ± 6.9	0.011	0.003	<0.001
INL	16.4 ± 1.1	16.9 ± 1.22	17.4 ± 1.0	0.045	0.005	<0.001
OPL	27.8 ± 1.5	28.1 ± 1.6	28.8 ± 1.5	0.596	0.021	.001
ONL	58.8 ± 3.4	59.5 ± 4.1	61.2 ± 3.6	0.302	0.039	<0.001
MSON eyes	N=64	N=41	-			
Perimacular area						
RNFL	24.2 ± 2.8	23.9 ± 3.2		0.890		
GCC	68.6 ± 17.1	72.2 ± 16.9		0.195		
INL	42.3 ± 3.2	41.1 ± 3.0		0.668		
ORLs	170.8 ± 9.2	172.5 ± 8.6		0.634		
Peripapillary area						
RNFL	74.6 ± 9.9	77.1 ± 13.2		0.200		
INL	15.7 ± 1.3	16.1 ± 1.8		0.497		
OPL	27.7 ± 1.6	27.9 ± 1.8		0.981		
ONL	59.6 ± 4.2	60.3 ± 3.5		0.778		

* GEE with correction for age and intra-subject inter-eye correlation. Significance level with Bonferroni correction: (N=8) p<0.006.

REFERENCES

1. Compston A, Coles A. Multiple sclerosis. *Lancet* 2008;372:1502-17.
2. Thompson AJ, Montalban X, Barkhof F, et al. Diagnostic criteria for primary progressive multiple sclerosis: a position paper. *Ann Neurol* 2000;47:831-5.
3. Thompson A. Overview of primary progressive multiple sclerosis (PPMS): similarities and differences from other forms of MS, diagnostic criteria, pros and cons of progressive diagnosis. *Mult Scler* 2004;10 Suppl 1:S2-S7.
4. Correale J, Ysrraelit MC, Fiol MP. Benign multiple sclerosis: does it exist? *Curr Neurol Neurosci Rep* 2012;12:601-9.
5. Ramsaransing GS, De Keyser J. Benign course in multiple sclerosis: a review. *Acta Neurol Scand* 2006;113:359-69.
6. Rovaris M, Barkhof F, Calabrese M, et al. MRI features of benign multiple sclerosis: toward a new definition of this disease phenotype. *Neurology* 2009;72:1693-701.
7. Patrikios P, Stadelmann C, Kutzelnigg A, et al. Remyelination is extensive in a subset of multiple sclerosis patients. *Brain* 2006;129:3165-72.
8. Trapp BD, Peterson J, Ransohoff RM, et al. Axonal transection in the lesions of multiple sclerosis. *N Engl J Med* 1998;338:278-85.
9. Geurts JJ, Calabrese M, Fisher E, et al. Measurement and clinical effect of grey matter pathology in multiple sclerosis. *Lancet Neurol* 2012;11:1082-92.
10. Evangelou N, DeLuca GC, Owens T, et al. Pathological study of spinal cord atrophy in multiple sclerosis suggests limited role of local lesions. *Brain* 2005;128:29-34.
11. Miller DH. Biomarkers and surrogate outcomes in neurodegenerative disease: lessons from multiple sclerosis. *NeuroRx* 2004;1:284-94.
12. Fisher E, Lee JC, Nakamura K, et al. Gray matter atrophy in multiple sclerosis: a longitudinal study. *Ann Neurol* 2008;64:255-65.
13. Rovaris M, Rocca MA, Filippi M. Magnetic resonance-based techniques for the study and management of multiple sclerosis. *Br Med Bull* 2003;65:133-44.
14. Kalkers NF, Ameziane N, Bot JC, et al. Longitudinal brain volume measurement in multiple sclerosis: rate of brain atrophy is independent of the disease subtype. *Arch Neurol* 2002;59:1572-6.
15. De Stefano N, Giorgio A, Battaglini M, et al. Assessing brain atrophy rates in a large population of untreated multiple sclerosis subtypes. *Neurology* 2010;74:1868-76.
16. Khoury S, Bakshi R. Cerebral pseudoatrophy or real atrophy after therapy in multiple sclerosis. *Ann Neurol* 2010;68:778-9.
17. Barkhof F, Calabresi PA, Miller DH, et al. Imaging outcomes for neuroprotection and repair in multiple sclerosis trials. *Nat Rev Neurol* 2009;5:256-66.
18. Huang D, Swanson EA, Lin CP, et al. Optical coherence tomography. *Science* 1991;254:1178-81.
19. Balk LJ, Twisk JWR, Steenwijk MD, et al. A dam for axonal degeneration in multiple sclerosis. *Mult Scler* 2013;19:74-558.
20. Siepman TAM, Bettink-Remeijer MW, Hintzen RQ. Retinal nerve fiber layer thickness in subgroups of multiple sclerosis, measured by optical coherence tomography and scanning laser polarimetry. *J Neurol* 2010;257:1654-60.
21. Henderson APD, Trip SA, Schlottmann PG, et al. An investigation of the retinal nerve fibre layer in progressive multiple sclerosis using optical coherence tomography. *Brain* 2008;131:277-87.
22. Gelfand JM, Goodin DS, Boscardin WJ, et al. Retinal axonal loss begins early in the course of multiple sclerosis and is similar between progressive phenotypes. *PLoS One* 2012;7:e36847.

23. Oberwahrenbrock T, Schippling S, Ringelstein M, et al. Retinal damage in multiple sclerosis disease subtypes measured by high-resolution optical coherence tomography. *Mult Scler Int* 2012;2012:530305.

24. Pulicken M, Gordon-Lipkin E, Balcer LJ, et al. Optical coherence tomography and disease subtype in multiple sclerosis. *Neurology* 2007;69:2085-92.

25. Costello F, Hodge W, Pan YI, et al. Differences in retinal nerve fiber layer atrophy between multiple sclerosis subtypes. *J Neurol Sci* 2009;281:74-9.

26. Ratchford JN, Saidha S, Sotirchos ES, et al. Active MS is associated with accelerated retinal ganglion cell/inner plexiform layer thinning. *Neurology* 2013;80:47-54.

27. Saidha S, Syc SB, Durbin MK, et al. Visual dysfunction in multiple sclerosis correlates better with optical coherence tomography derived estimates of macular ganglion cell layer thickness than peripapillary retinal nerve fiber layer thickness. *Mult Scler* 2011;17:1449-63.

28. Albrecht P, Ringelstein M, Muller AK, et al. Degeneration of retinal layers in multiple sclerosis subtypes quantified by optical coherence tomography. *Mult Scler* 2012;18:1422-9.

29. Lublin FD, Reingold SC. Defining the clinical course of multiple sclerosis: results of an international survey. National Multiple Sclerosis Society (USA) Advisory Committee on Clinical Trials of New Agents in Multiple Sclerosis. *Neurology* 1996;46:907-11.

30. Tewarie P, Balk L, Costello F, et al. The OSCAR-IB consensus criteria for retinal OCT quality assessment. *PLoS One* 2012;7:e34823.

31. Oberwahrenbrock T, Traber G, Gabilondo I, et al. Multicenter inter-rater reliability of retinal layer segmentation using spectral-domain OCT. ECTRIMS Meeting, Kopenhagen, Denmark, 2–5 October 2013, poster 480.

32. Petzold A, de Boer JF, Schippling S, et al. Optical coherence tomography in multiple sclerosis: a systematic review and meta-analysis. *Lancet Neurol* 2010;9:921-32.

33. Thompson AJ, Kermode AG, MacManus DG, et al. Patterns of disease activity in multiple sclerosis: clinical and magnetic resonance imaging study. *BMJ* 1990;300:631-4.

34. Thompson AJ, Kermode AG, Wicks D, et al. Major differences in the dynamics of primary and secondary progressive multiple sclerosis. *Ann Neurol* 1991;29:53-62.

35. Miller DH, Leary SM. Primary-progressive multiple sclerosis. *Lancet Neurol* 2007;6:903-12.

Chapter 4.2

A dam for retrograde axonal degeneration in multiple sclerosis?

LJ Balk, JWR Twisk, MD Steenwijk, M Daams, P Tewarie,
J Killestein, BMJ Uitdehaag, CH Polman, A Petzold

J Neurol Neurosurg Psychiatry. **2014;85:782-9**

ABSTRACT

Objective Trans-synaptic axonal degeneration is a mechanism by which neurodegeneration can spread from a sick to a healthy neuron in the central nervous system. This study investigated to what extent trans-synaptic axonal degeneration takes place within the visual pathway in multiple sclerosis (MS).

Methods A single-centre study, including patients with long-standing MS and healthy controls. Structural imaging of the brain (MRI) and retina (spectral-domain optical coherence tomography) were used to quantify the extent of atrophy of individual retinal layers and the primary and secondary visual cortex. Generalised estimation equations and multivariable regression analyses were used for comparisons.

Results Following rigorous quality control (OSCAR-IB), data from 549 eyes of 293 subjects (230 MS, 63 healthy controls) were included. Compared with control data, there was a significant amount of atrophy of the inner retinal layers in MS following optic neuritis (ON) and also in absence of ON. For both scenarios, atrophy stopped at the level of the inner nuclear layer. In contrast, there was significant localised atrophy of the primary and secondary visual cortex in MS following ON, but not in MS in absence of ON.

Interpretation These data suggest that retrograde (trans-synaptic) axonal degeneration stops at the inner nuclear layer, a neuronal network capable of plasticity. In contrast, there seems to be no neuroplasticity of the primary visual cortex, rendering the structure vulnerable to anterograde (trans-synaptic) degeneration.

INTRODUCTION

In the last two decades, great progression in monitoring and treating the inflammatory pathology of multiple sclerosis (MS) has occurred.[1-3] Despite these advances, a large proportion of patients suffering from MS continue to progress, due to axonal and neuronal degeneration.[4] To date, it is however not known what mechanism drives neurodegeneration, but early neuroplasticity was suggested to be of prognostic relevance already at disease onset.[5] If correct, neuroplasticity should protect against axonal loss, the main reason for sustained disability, over the long term.

The hypothesis is that axonal loss and neurodegeneration are related and can be quantified by atrophy measurements. Anterograde axonal degeneration has been known for some time,[6] but only with the recent description of *in vivo* trans-synaptic axonal degeneration a bidirectional pathophysiological mechanism was available to explain progression of neurodegeneration in the human central nervous system (CNS).[7,8] This discovery was made possible by use of retinal optical coherence tomography (OCT). Retinal OCT has matured into a highly sensitive and accurate tool for quantifying minute (1-2 µm) amounts of atrophy, which permits to separate individual retinal layers.[9] This opens avenues for investigating the structural cascade of anterograde and retrograde (trans-synaptic) axonal degeneration in MS. Clearly, post-mortem data demonstrated atrophy of retinal layers after long-standing disease.[10] In absence of direct damage to the retina it is likely that retinal layer atrophy was caused by retrograde trans-synaptic axonal degeneration following more central damage to the optic pathways. There is yet no comparable in vivo data from patients with longstanding MS, but a meta-analysis of the literature on patients with a shorter disease duration suggests that atrophy of the retinal nerve fibre layer (RNFL) may be caused by retrograde axonal degeneration following optic neuritis (MSON), and trans-synaptic retrograde axonal degeneration in absence of ON (MSNON).[11] Besides retinal atrophy, caused by retrograde (trans-synaptic) degeneration there is also evidence for anterograde trans-synaptic degeneration in the visual system.[12-14] Anterograde degeneration along the visual pathway takes place in the lateral geniculate nucleus and visual cortex following ON or diffuse white matter axonal pathology.[14] These data are consistent with optic tract diffusion abnormalities and reduced magnetisation transfer ratio in the occipital cortices following ON.[15-17]

Taken together, there seems to be evidence for retrograde and anterograde (trans-synaptic) axonal degeneration in MS. If left unrestricted, this process may be allowed to spread through the visual pathway and, given the many connections between the visual system and the rest of the brain, potentially the entire human CNS like a 'domino effect' (denoting a chain of trans-synaptic events). While there is evidence for the former,[14-17]

the latter was never observed. Therefore, the aim of this study was to confirm trans-synaptic axonal degeneration and to investigate if there was a physiological barrier to this process within the visual system of patients with long-standing MS.

METHODS

Study design and patient population

Patients and controls were enrolled from the VU University Medical Centre Amsterdam, between March 2011 and August 2012 for this cross-sectional study. This study was approved by the medical ethical committee (protocol number 2010/336) and the scientific research committee (protocol number CWO/10-25D) of the VU University Medical Centre in Amsterdam, the Netherlands. Written informed consent was obtained from all included subjects.

Patients were eligible for inclusion if they completed a written informed consent, were aged 18-80 years and had a diagnosis of either relapsing remitting (RR), secondary progressive (SP) or primary progressive (PP) MS at the time of their assessment (defined by Lublin-Reingold criteria).[18] Patients were excluded if they fulfilled any of the following criteria: pregnancy; received a course of steroids or had a relapse within the preceding month; HIV or other immunodeficiency syndrome; history of substance abuse (drug or alcohol) in the past 5 years and specific MRI findings that could interfere with evaluation.

Healthy control (HC) subjects were included if they were willing to sign an informed consent form, aged 40-60 years at the time informed consent was signed and if they had no history of any neurological or psychiatric disease. Exclusion criteria for HC subjects were pregnancy and if they were related (1st or 2nd degree) to a patient with MS.

OCT imaging

OCT images were acquired with a SD-OCT (Spectralis, Heidelberg Engineering, Heidelberg, Germany, software version 1.7.1.0), using dual beam simultaneous imaging, with the eye tracking function enabled for optimal measurement accuracy.[19]

In order to obtain data on the peripapillary region, a 12° ringscan (corresponding to an approximately 3.4-mm-diameter circle in a normal eye) was used. The ring scan was centred manually on the papilla after activating the eye tracking function in each subject. Likewise, the macular volume scan (20 x 20° field, 25 B-scans) was manually centred over the macula after activation of the eye tracking function. Both scan areas are depicted in Figure 1A (peripapillary) and B (macula).

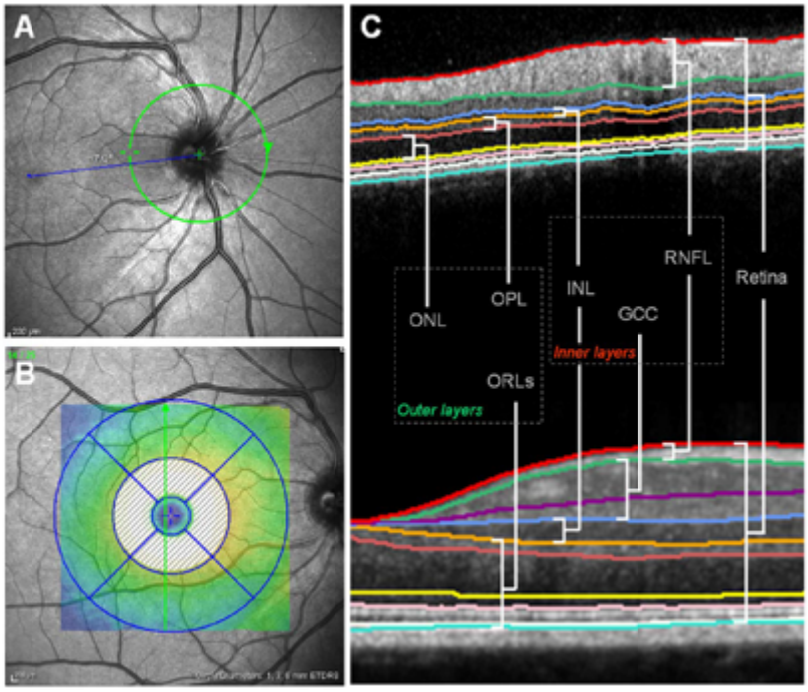

Figure 1. Scan and segmentation protocol for the retinal OCT used in this study. **(A)** Peripapillary ring scan of the right eye. **(B)** Macular volume scan (20 x 20 degrees field, 25 vertical B-scans) of the right eye. The coloured map represents a thickness map with a 1, 3 and 6 mm EDTRS grid of which only the perimacular rim (grey shaded area) was used in this study. **(C)** Segmented layers of the peripapillary ring scan (top image) and macular volume scan (bottom image) as used from data in (A) and (B) (see method section). ONL: outer nuclear layer, OPL: outer plexiform layer, ORLs: outer retinal layers (=retina-(GCC+INL+RNFL)), INL: inner nuclear layer, GCC: ganglion cell complex (=ganglion cell layer+inner plexiform layer), RNFL: retinal nerve fibre layer.

All OCT scans were performed by four trained and certified technicians. Scans were excluded from the analyses if they violated international consensus quality control criteria (OSCAR-IB).[20]

Image post-processing was performed as follows. The peripapillary ring scan and the macular volume scan were analysed with the aid of new segmentation software (Heidelberg Engineering, Heidelberg, Germany). The software allows for reliable segmentation of three retinal layers at the macular region; the retinal nerve fibre layer (RNFL), the ganglion cell complex (GCC=ganglion cell layer(GCL)+inner plexiform layer(IPL)) and the inner nuclear layer (INL). Furthermore, the outer retinal layers (ORLs) were calculated for the macular region by subtracting the RNFL, GCC and INL from the complete retinal thickness (shown in Figure 1C, bottom image). For every layer, the OCT software generated a thickness map on a 1 mm, 3 mm and 6 mm grid, as defined by the Early Treatment Diabetic Retinopathy Study (ETDRS). Of the nine areas provided by

this grid, only the mean of the four inner regions composing the perimacular rim were used in this study (grey shaded area in Figure 1B). This was done because segmentation of the individual layers in the outer regions was shown to be of poorer reproducibility, compared to the four inner ETDRS sectors.[21] The foveolar thickness is dominated by the ORLs, which precluded any reliable quantification of inner retinal layers from this area. In the peripapillary region, the software enabled segmentation of four distinct layers; the RNFL, INL, outer nuclear layer (ONL) and the outer plexiform layer (OPL) (shown in Figure 1C, upper image). For all layers, a thickness map was provided of which the layer specific global mean values were used for statistical analysis.
After the segmentation process, all scans and all layers were verified by two independent OCT technicians. In case of obvious algorithm failure on a small area (due to a vessel or a small artefact), the deviating line was corrected manually. Scans were excluded if the algorithm failure covered the complete OCT B-scan area. The retinal layer segmentation software used in this study has shown to be reliable, with intraclass correlation coefficients (ICCs) above 0.94 for all layers, except the IPL (ICC 0.70), which was an important source of disagreement. This issue was solved by combining the GCL and IPL to form the GCC (ICC of 0.99).[21]

Clinical assessments
The Expanded Disability Status Scale (EDSS) was determined by a certified examiner to assess level of disability. Visual acuity (VA) testing was performed monocularly in all patients, using the Snellen acuity chart (5m distance, using decimal notation). Medical history with respect to visual symptoms was obtained in all patients and controls.

MRI data acquisition and analysis
Magnetic resonance imaging (MRI) was performed on a 3T whole body scanner (GE Signa HDxt, Milwaukee, Wisconsin, USA) using an eight-channel phased array head coil. The protocol included a three-dimensional T1-weighted fast spoiled gradient echo sequence (FSPGR; repetition time 7.8 ms, echo time 3 ms, flip angle 12°, 240 x 240 mm^2 field of view, 176 sagittal slices of 1 mm thickness, 0.94 x 0.94 mm^2 in-plane resolution) for cortical thickness measurements, and a three-dimensional fluid attenuated inversion recovery image (FLAIR; repetition time 8000 ms, echo time 125 ms, inversion time 2350 ms, 250 x 250 mm^2 field of view, 132 sagittal slices of 1.2 mm thickness, 0.98 x 0.98 mm^2 inplane resolution) for lesion detection.
White matter lesion segmentation was automatically performed using the FLAIR and FSPGR images.[22] Cortical thickness measurements were performed using the FreeSurfer pipeline (version 5.1) as previously described.[23,24] Before applying FreeSurfer, the binary lesion mask was used to minimise the impact of white matter lesions on the cortical

thickness measurements by applying a lesion filling algorithm.[25] After running the FreeSurfer pipeline, the primary visual cortex (V1) and secondary visual cortex (V2) were segmented in each subject by surface based registration of an atlas.[26] The resulting cortical parcellations were then used to compute the average thickness of V1 and V2. In order to assess localised atrophy of V1/V2, normalised V1/V2 thicknesses were calculated by dividing the V1/V2 cortical thickness by complete cortical thickness.

Statistical analyses

Demographic data was compared between patients and controls using independent sample T tests, χ^2 tests and linear regression analyses. For all segmented retinal layers the relative thickness (individually normalised to complete retinal thickness) was calculated in order to investigate the layer-specific contribution to the complete retina. This was done for the perimacular rim and the peripapillary area.

Differences in retinal layer thickness between eyes with a history of ON (MSON), without a history of ON (MSNON) and HC eyes, were analysed with generalised estimation equations (GEE). This method was used because the analyses were performed on eye level instead of subject level. In the GEE analysis (adjusting for intra-subject inter-eye correlation, using an exchangeable correlation structure), age was used as a covariate to adjust for confounding.

In order to assess the relationship between cortical thickness of V1 and V2, (absolute and normalised to total mean cortical thickness) and retinal layer thickness, linear multiple regression analyses (with adjustments for age and sex) were used. In order to avoid contamination of the study groups by pooling of MSON eyes (showing a severe degree of RNFL loss) with MSNON eyes (showing a small degree RNFL loss),[11] these analyses included only patients in whom both eyes had the same history of ON (both eyes MSON or both eyes MSNON). In these analyses, the mean of both eyes was used.

Statistical analyses were performed using SPSS version 20.0, with a statistical significance level of 0.05. A Bonferroni correction was applied to adjust for multiple testing.

RESULTS

A total of 230 patients with MS (140 RRMS, 61 SPMS, 29 PPMS) and 63 HCs were included (Table 1). Patients had a mean disease duration of 20.4 (±7.0) years (median: 20.2 years, IQR: 9.4, total range 8.8-45.9). Patients were older (median: 54.1 years, IQR: 14.4, total range: 30.7-81.1) compared to control subjects (median: 50.8 years, IQR: 8.6, total range: 27.5-62.9, p=0.001). An episode of unilateral MSON was experienced by 27%, while an episode of bilateral (simultaneous or sequential) MSON by 19%. Only

one patient showed signs of unilateral microcystic macular oedema. Exclusion of data from this patient did not change the level of significance for any of the following calculations. The visual acuity (VA) was worse for MSON (0.74±0.25) compared with MSNON eyes (0.86±0.19, p<0.001). Although visual cortical thicknesses of both V1 and V2 were less in patients compared with controls (p=0.005 and p<0.001, respectively), no localised atrophy of V1 or V2 was observed in patients, as the normalised visual cortical thicknesses did not differ between patients and controls (p=0.634, p=0.102, respectively).

OCT scans were performed in 549 eyes (423 in MS, 126 in HC). The remaining eyes were not scanned, essentially due to problems with visual fixation using either an internal or external target. The exclusion of the acquired scans after quality control (OSCAR-IB) and layer segmentation is depicted in a flowchart (Figure 2).

Table 1 Subject characteristics. Values are reported as mean±sd or total numbers (N) and percentages (%).

	Patients N=230	**Controls** N=63	**p-value**
Age (years)	54.3 (±10.0)	50.5 (±7.2)	0.001[a]
Sex (% male)	31.7%	34.9%	0.633[b]
MS type (N [%])			
RR	140 (60.9%)	n/a	
SP	61 (26.5%)		
PP	29 (12.6%)		
Disease duration (years)	20.4 (±7.0)	n/a	
Range	[8.8 – 45.9]		
EDSS (median [range])	4.0 [1-8]	n/a	
History of ON (N [%])			
Unilateral	62 (27%)	n/a	
Bilateral	44 (19%)		
Mean cortical thickness	2.47 (0.10)	2.56 (0.09)	<0.001
Visual cortical thickness			
V1	3.55 (±0.24)	3.66 (±0.22)	0.005[c]
V2	4.09 (±0.24)	4.28 (±0.22)	<0.001[c]
Normalised visual cortical thickness*			
V1	1.44 (±0.08)	1.43 (±0.08)	0.634[c]
V2	1.66 (±0.06)	1.68 (±0.05)	0.102[c]

ON = optic neuritis, n/a=not applicable, * normalised to mean cortical thickness
a. Independent samples T-test
b. Chi-square test
c. Linear regression analysis with adjustment for age

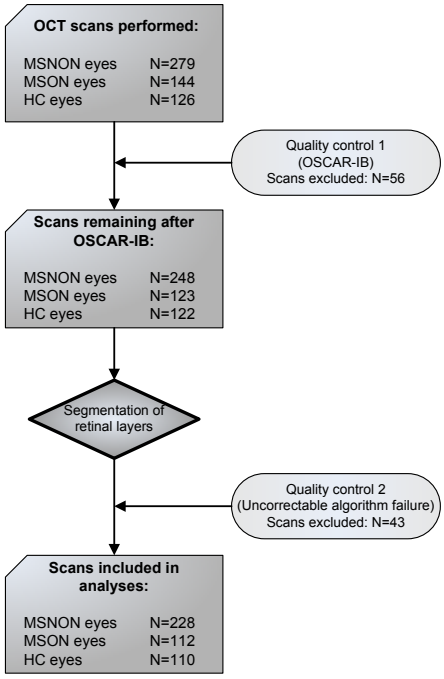

Figure 2. Flowchart of exclusion of peripapillary OCT scans following quality control (OSCAR-IB) and segmentation of retinal layers. Of all scans included, 10% (N=56) of scans did not fulfil the OSCAR-IB criteria and were therefore excluded. After the segmentation of individual layers, another 9% (N=43) of scans was excluded due to uncorrectable algorithm failure.

Optic neuritis causes severe retrograde degeneration of inner retinal layers

Table 2 (upper part) shows the relative thickness of all retinal layers for MSON, MSNON and HC eyes. In the macular area, there was a significant amount of atrophy of the inner, but not the outer layers in MSON and MSNON eyes, compared with HC (Table 2). Specifically, the macular RNFL and GCC showed the largest relative thickness in HC eyes (8.2% and 28.3%, respectively), compared with MSON and MSNON eyes (Table 2). In contrast, the INL and ORLs of the macular area showed the largest relative thickness in MSON eyes (13.9% and 56.0% respectively), compared with MSNON or HC eyes ($p<0.001$ for all comparisons).

Importantly, the analysis of the relative thickness values from the peripapillary region clearly demonstrated that the INL did not differ significantly between groups while the thickness of the innermost layer (RNFL) was significantly reduced in MSON and MSNON eyes compared with HC eyes. In contrast, the outermost layers (counting from the INL) were significantly thicker in MSON eyes compared with MSNON or HC eyes ($p<0.001$ in all comparisons). Figure 3 shows the direct comparison between MSNON and HC eyes for all retinal layers. For transparency, the corresponding absolute thickness data of all retinal layers are also shown in Table 2 (bottom part).

Table 2 Clinical and OCT data of included eyes. Eyes were stratified into those with (MSON) and without ON (MSNON) and healthy control eyes (HC). The OCT data is presented as absolute (µm, mean +/- sd) *and* relative data (normalised as percentage of the individual retinal thickness). The significant highest values per retinal layer are shown in bold.

	MSON eyes N=144	**MSNON eyes** N=279	**HC eyes** N=126	**p-value** MSON vs MSNON†	**p-value** MSNON vs HC†	**p-value** MSON vs HC†
Vision (N [%])						
0-0.65	50 (37%)	41 (16%)	-			
≥0.8	85 (63%)	217 (84%)				
RELATIVE VALUES						
Perimacular area						
Retina	100%	100%	100%			
RNFL	7.8%	8.1%	**8.2%**	<0.001*	0.197	<0.001*
GCC	22.8%	26.2%	**28.3%**	<0.001*	<0.001*	<0.001*
INL	**13.9%**	13.0%	12.4%	<0.001*	<0.001*	<0.001*
ORLs	**56.0%**	52.8%	51.0%	<0.001*	<0.001*	<0.001*
Peripapillary area						
Retina	100%	100%	100%			
RNFL	26.4%	28.4%	**29.3%**	<0.001*	<0.001*	<0.001*
INL	5.5%	5.5%	5.6%	0.120	0.150	0.013
OPL	**9.6%**	9.3%	9.2%	<0.001*	0.007	<0.001*
ONL	**20.7%**	19.8%	19.6%	<0.001*	0.071	<0.001*
ABSOLUTE VALUES						
Perimacular area						
Retina	306.6 (18.5)	320.1 (17.7)	**332.6 (12.9)**	<0.001*	<0.001*	<0.001*
RNFL	24.0 (2.9)	26.1 (2.7)	**27.3 (2.1)**	<0.001*	<0.001*	<0.001*
GCC	70.5 (17.3)	84.2 (13.1)	**94.2 (6.0)**	<0.001*	<0.001*	<0.001*
INL	42.3 (3.0)	41.5 (3.0)	41.4 (2.9)	<0.001*	0.518	0.014
ORLs	170.9 (8.9)	168.3 (8.9)	170.2 (8.9)	0.006	0.158	0.927
Peripapillary area						
Retina	289.3 (19.0)	301.0 (17.0)	**312.2 (13.4)**	<0.001*	<0.001*	<0.001*
RNFL	76.4 (11.6)	85.5 (10.1)	**91.7 (6.8)**	<0.001*	<0.001*	<0.001*
INL	15.9 (1.5)	16.6 (1.2)	**17.5 (1.1)**	<0.001*	<0.001*	<0.001*
OPL	27.8 (1.6)	28.0 (1.5)	**28.8 (1.5)**	0.001*	0.002*	<0.001*
ONL	59.8 (3.8)	59.4 (3.7)	61.3 (3.6)	0.507	0.005	0.003*

MSON=MS eyes with optic neuritis. MSNON=MS eyes without optic neuritis. HC=healthy control eyes
* p-value significant with Bonferroni correction: (N=16) 0.05/16=0.003.
† GEE analyses with adjustment for age and intra-subject inter-eye correlation.

Anterograde trans-synaptic axonal degeneration causes atrophy of the primary visual cortex

Axons from the temporal visual field cross at the chiasm, demanding stratification of patients into two subgroups which are either bilateral normal (MSNON, n=107) or bilateral MSON (n=39). The average data of the right and left sides were used.

The mean thicknesses of the complete cortex, V1 and V2 (absolute and normalised) were all significantly thinner in patients with MS compared with HC subjects,

irrespective of the presence of MSON. The thickness of the complete cortex did not differ between patients with MSON and patients with MSNON (2.45 vs 2.47, p=0.425). In contrast, the thicknesses of V1 and V2 (absolute and normalised) were consistently thinner in patients with MSON compared with patients with MSNON. These differences were significant for all comparisons, except for absolute V2 thickness, where statistical significance was narrowly missed (Table 3, p=0.053).

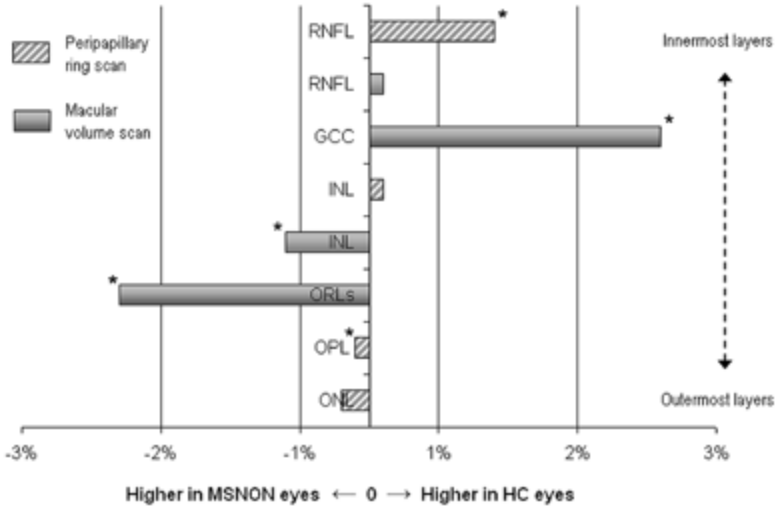

Figure 3. Comparison of the relative layer thicknesses between MSNON and HC eyes. Data is shown for the peripapillary ring scan (hatched bars) and macular volume scan (shaded bars). The innermost layers (RNFL, GCC) are presented at the top of the graph. The outermost layers (ONL, OPL, ORLs) are presented at the bottom. Clearly, in MSNON eyes there is a significant loss of especially the peripapillary RNFL and macular GCC, compared to healthy control eyes. The opposite was observed for the more outer retinal layers, but only the macular INL and the ORLs were significantly thicker in MSNON eyes compared to HC eyes.
* p≤0.003 (Bonferroni correction: 0.05/16=0.003)

Table 3 MSON patients show more thinning of the visual cortex than MSNON patients. Data is presented as mm (mean +/- sd).

	MSON N=39	**MSNON N=107**	**HC N=63**	**p-value* MSON vs MSNON**
Cortical thickness	2.45 (±0.10)	2.47 (±0.10)	2.56 (±0.09)	0.425
V1 thickness	3.46 (±0.22)	3.58 (±0.25)	3.66 (±0.22)	0.011
V2 thickness	4.03 (±0.23)	4.13 (±0.23)	4.28 (±0.22)	0.053
V1 norm	1.41 (±0.06)	1.45 (±0.08)	1.43 (±0.08)	0.008
V2 norm	1.65 (±0.05)	1.67 (±0.05)	1.68 (±0.05)	0.015

*linear regression with adjustment for disease duration

Retinal layer atrophy is not related to thickness of the visual cortex

There was no significant association observed between retinal layer thicknesses and V1 thickness, either in patients with MSON, patients with MSNON, or HCs, after Bonferroni correction for multiple comparisons. Results of the regression analyses, with adjustments for disease duration or age, are shown in Table 4.

Likewise, there were no significant associations between retinal layer thicknesses with V2 thickness (data not shown). Moreover, results did not change when normalised V1/V2 thicknesses were used (data not shown).

Table 4 Individual retinal layer atrophy is not related to the thickness of the visual cortex (V1) in patients with bilateral MSON, with no evidence of MSON at all (bilateral MSNON) and HC.

	MS ON	N=39		**MS NON**	N=107		**HC**	N=63	
	ß	(95%CI)	p-value	ß	(95%CI)	p-value	ß	(95%CI)	p-value
V1 thickness									
Macula									
RNFL	0.06	-4.7 – 4.8	0.979	1.4	-1.1 – 3.9	0.281	0.9	-1.3 – 3.1	0.397
GCC	31.6	1.0 – 62.2	0.044	8.2	-3.1 – 19.5	0.153	3.7	-3.6 – 11.0	0.316
INL	1.4	-6.1 – 8.9	0.697	-1.4	-4.2 – 1.4	0.328	-1.3	-5.0 – 2.7	0.457
ORLs	12.2	-0.8 – 25.3	0.065	7.1	-2.9 – 17.1	0.161	9.8	-0.15 – 19.7	0.054
Papilla									
RNFL	14.7	-9.0 – 38.4	0.210	4.2	-5.4 – 13.8	0.389	2.0	-7.1 – 11.1	0.663
INL	3.2	-0.4 – 6.7	0.077	0.5	-0.6 – 1.6	0.362	-0.4	-1.8 – 1.1	0.614
OPL	2.2	-1.9 – 6.2	0.271	0.3	-1.0 – 1.6	0.651	0.07	-2.0 – 2.1	0.944
ONL	8.2	0.1 – 16.2	0.047	1.3	-2.0 – 4.5	0.441	0.3	-4.8 – 5.4	0.909

Linear regression analyses with adjustments for disease duration (MS patients) and age (control subjects). Significance level with Bonferroni correction: (N=24) 0.05/24=0.002.

DISCUSSION

This study identified a possible physiological barrier to axonal degeneration within the visual system (Figure 4). Retrograde (trans-synaptic) axonal degeneration is directed towards and is possibly being blocked in the retina. Anterograde (trans-synaptic) axonal degeneration is directed towards the V1 where it causes localised atrophy. The present data suggests that retrograde (trans-synaptic) axonal degeneration is halted at an anatomical structure capable of neuroplasticity, the INL of the retina. The INL represents a neuronal network of bipolar, amacrinal and horizontal cells, which appears to act as a dam to retrograde (trans-synaptic) axonal degeneration resulting from axonal loss during an episode of MSON or diffuse axonal pathology (Figure 4). In contrast with the extensive damage observed in the inner retinal layers, almost no atrophy could be shown beyond the INL after an average disease duration of 20 years.

Therefore this study also closes a gap of the literature, biased towards cross-sectional studies of the early disease course. Importantly, plasticity of the V1 is blocked early in life.[27] This may be the reason why anterograde (trans-synaptic) degeneration leads to atrophy of V1 and V2. A finding which is consistent with other studies.[15-17]

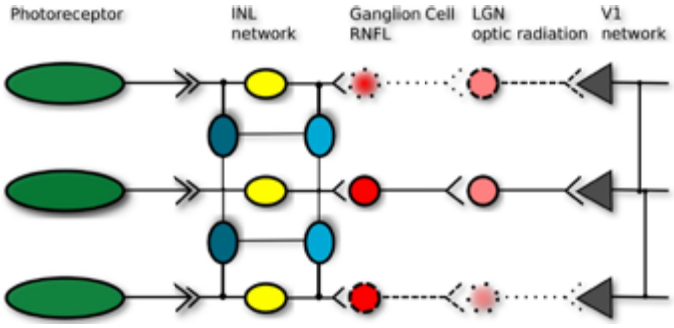

Figure 4. A model which explains how plasticity within the INL network may act as a physiological barrier against anterograde trans-synaptic degeneration (top row, towards V1) and retrograde trans-synaptic axonal degeneration (bottom row, towards retina). The normal (healthy) situation is shown in the middle. An analogue signal originating from the photoreceptors (green) is translated into a digital signal by the INL network (bipolar cells in yellow, amacrine cells in dark blue, horizontal cells in light blue). The necessary multiple axonal connections within a large synaptic tree (for simplicity not shown in the image) keeps the neurons of the INL functionally alive even in cases of MSON. The situation of MSON is shown to the top of the graph. Axonal trans-section (dotted line, top) results in anterograde trans-synaptic degeneration (dashed line, top). In contrast, in V1 there seems to be no neuroplasticity and localised atrophy ensues. Likewise, diffuse axonal damage within the optic radiations (dotted line, bottom) results in retrograde trans-synaptic degeneration (dashed line, bottom) with loss of the hard-wired RNFL and ganglion cells, but stops at the INL where the corresponding bipolar cells are protected by the INL network.

The observed differences in RNFL thickness between MSON and MSNON eyes are also consistent with the literature.[11] The thinning of the RNFL was more severe in MSON eyes (retrograde axonal degeneration) compared with MSNON eyes (trans-synaptic retrograde axonal degeneration). This consistent observation can be explained by the fact that the optic nerve is a vulnerable structure because of the anatomically high density of the closely packed, hard-wired, axons. Thus, an episode of ON will immediately damage a large amount of axons, eventually resulting in axonal degeneration. Ganglion cell loss and RNFL thinning will be relatively less severe following diffuse axonal pathology in the white matter of the MS brain (MSNON) because axons are spread out over a large area in Meyer's loop.[28,29]

Although large differences between MSON and MSNON eyes were observed, it can be concluded that after two decades of MS, MSON and MSNON, eyes revealed substantial atrophy (especially of the inner layers of the retina), compared with healthy eyes. The present data suggest that neuroplasticity may be a mechanism by which retrograde (trans-synaptic) axonal degeneration can be halted.

The damage observed in the inner retinal layers is caused by retrograde (trans-synaptic) axonal degeneration and it appears that this mechanism mainly affects physiologically hard-wired neuroaxonal connections such as the dominant projections from the first order neurons (retinal ganglion cells), to the second order neurons (within the lateral geniculate nucleus) and finally third order neurons, located within layer four of V1.

Retinal bipolar cells in the INL differ from the hard-wired 1st, 2nd and 3rd order neurons because of their extensive synaptic tree.[30] Amacrinal and horizontal cells feed into this synaptic tree which has an extraordinary capacity for plasticity.[31] Plasticity of the INL is also exploited for retinal implants.[32,33] Likewise, neuroplasticity is the recognised mechanism for cortical filling-in of circumscribed scotoma (V1) following retinal lesions.[34,35] The likely anatomical substrate for neuroplasticity following scotoma are horizontal within-cortical connections because the hard-wired connections from the lateral geniculate nucleus to V1 remain unaltered.[36]

In the present study, clear differences in visual cortical thickness were observed between MSON, MSNON and HC. Nonetheless, no association was observed between retinal layer thickness and visual cortical thickness in MSON, MSNON or HC. These findings are consistent with a study published while this paper was under revision, reporting clear atrophy of the visual cortex in patients with severe MSON, and to a lesser extent in patients with mild MSON, compared with patients with MSNON.[37] Furthermore, Gabilondo et al reported a significant association between RNFL thickness and visual cortex volume in the complete patient group, but this effect disappeared when patients with MSNON and patients with MSON were analysed separately. The lack of association between retinal layer thickness and visual cortical thickness may be potentially explained by presence of silent lesions in the optic radiations in patients with MSON and possible subclinical episodes of ON.To the best of our knowledge, this study is the first study to examine retinal layer atrophy in patients with longstanding MS. This is relevant because axonal degeneration in the CNS can be an extremely slow process.[38,39] Therefore, the short disease duration of previous studies does not permit the drawing of any definite conclusions in the long term.[40-44] Therefore our data predicts that longitudinal studies are likely to find a plateau effect for inner retinal layer atrophy with preservation of the outermost layers.

In human retinal post-mortem samples, extensive retinal atrophy has been demonstrated after about 20 years of disease duration.[10] This matches the time lag of the present study, which therefore closes the gap between *in vivo* and *post-mortem* data on retinal atrophy.

The main limitation of this study is that it relies on indirect data only, as a direct investigation of retinal structures and visual pathways by histology will not be possible in the acute phase, with the exception of some extraordinary rare autopsy reports.

Although long-term, the data remains cross-sectional, though we predict a plateau effect for retrograde axonal degeneration. Another shortcoming is that testing of visual function was restricted to high contrast VA. As Balcer et al. pointed out,[45,46] this is a rather poor measure for visual function in MS. Next, controls were younger than patients. This was taken into account by using the individually normalised (relative) data and age-adjusted statistical tests. Finally, records of MSON were based on a mix of clinically confirmed episodes and a patient history on earlier events during the disease. Although this approach is consistent with other studies in the field, it may have introduced a bias towards more severe episodes of MSON.

In summary, this study describes neuroplasticity of the INL as a possible physiological barrier, to retrograde (trans-synaptic) axonal degeneration.

REFERENCES

1. Ramli N, Rahmat K, Azmi K, et al. The past, present and future of imaging in multiple sclerosis. *J Clin Neurosci* 2010;17:422-7.
2. Barkhof F, Calabresi PA, Miller DH, et al. Imaging outcomes for neuroprotection and repair in multiple sclerosis trials. *Nat Rev Neurol* 2009;5:256-66.
3. Killestein J, Rudick RA, Polman CH. Oral treatment for multiple sclerosis. *Lancet Neurol* 2011;10:1026-34.
4. Compston A, Coles A. Multiple sclerosis. *Lancet* 2008;372:1502-17.
5. Jenkins TM, Toosy AT, Ciccarelli O, et al. Neuroplasticity predicts outcome of optic neuritis independent of tissue damage. *Ann Neurol* 2010;67:99-113.
6. Waller A. Experiments on the Section of the Glossopharyngeal and Hypoglossal Nerves of the Frog, and Observations of the Alterations Produced Thereby in the Structure of Their Primitive Fibres. *Phil Trans R Soc* 1850;140:423-9.
7. Jindahra P, Petrie A, Plant GT. The time course of retrograde trans-synaptic degeneration following occipital lobe damage in humans. *Brain* 2012;135:534-41.
8. Jindahra P, Petrie A, Plant GT. Retrograde trans-synaptic retinal ganglion cell loss identified by optical coherence tomography. *Brain* 2009;132:628-34.
9. Wu H, de Boer JF, Chen TC. Reproducibility of retinal nerve fiber layer thickness measurements using spectral domain optical coherence tomography. *J Glaucoma* 2011;20:470-6.
10. Green AJ, McQuaid S, Hauser SL, et al. Ocular pathology in multiple sclerosis: retinal atrophy and inflammation irrespective of disease duration. *Brain* 2010;133:1591-601.
11. Petzold A, de Boer JF, Schippling S, et al. Optical coherence tomography in multiple sclerosis: a systematic review and meta-analysis. *Lancet Neurol* 2010;9:921-32.
12. Boucard CC, Hernowo AT, Maguire RP, et al. Changes in cortical grey matter density associated with long-standing retinal visual field defects. *Brain* 2009;132:1898-906.
13. Yucel Y, Gupta N. Glaucoma of the brain: a disease model for the study of transsynaptic neural degeneration. *Prog Brain Res* 2008;173:465-78.
14. You Y, Gupta VK, Graham SL, et al. Anterograde degeneration along the visual pathway after optic nerve injury. *PLoS One* 2012;7:e52061.
15. Audoin B, Fernando KT, Swanton JK, et al. Selective magnetization transfer ratio decrease in the visual cortex following optic neuritis. *Brain* 2006;129:1031-9.
16. Dasenbrock HH, Smith SA, Ozturk A, et al. Diffusion tensor imaging of the optic tracts in multiple sclerosis: association with retinal thinning and visual disability. *J Neuroimaging* 2011;21:e41-e49.
17. Reich DS, Smith SA, Gordon-Lipkin EM, et al. Damage to the optic radiation in multiple sclerosis is associated with retinal injury and visual disability. *Arch Neurol* 2009;66:998-1006.
18. Lublin FD, Reingold SC. Defining the clinical course of multiple sclerosis: results of an international survey. National Multiple Sclerosis Society (USA) Advisory Committee on Clinical Trials of New Agents in Multiple Sclerosis. *Neurology* 1996;46:907-11.
19. Balk LJ, Petzold A. Influence of the eye-tracking-based follow-up function in retinal nerve fiber layer thickness using fourier-domain optical coherence tomography. *Invest Ophthalmol Vis Sci* 2013;54:3045.
20. Tewarie P, Balk L, Costello F, et al. The OSCAR-IB consensus criteria for retinal OCT quality assessment. *PLoS One* 2012;7:e34823.
21. Traber G, Oberwahrenbrock T, Gabilondo I, et al. Multicenter Inter-rater Reliability of Retinal Layer Segmentation Using Spectral-domain OCT. Nanos Meeting Oxford, April 2013.
22. Steenwijk M, Pouwels PJW, Daams M et al. Accurate white matter lesion segmentation by k nearest neighbor classification with tissue type priors (kNN-TTPs). *Neuroimage Clin* 2013;3:462–469
23. Dale AM, Fischl B, Sereno MI. Cortical surface-based analysis. I. Segmentation and surface reconstruction. *Neuroimage* 1999;9:179-94.
24. Fischl B, Sereno MI, Dale AM. Cortical surface-based analysis. II: Inflation, flattening, and a surface-based coordinate system. *Neuroimage* 1999;9:195-207.
25. Chard DT, Jackson JS, Miller DH, et al. Reducing the impact of white matter lesions on automated measures of brain gray and white matter volumes. *J Magn Reson Imaging* 2010;32:223-8.

26. Fischl B, Rajendran N, Busa E, et al. Cortical folding patterns and predicting cytoarchitecture. *Cereb Cortex* 2008;18:1973-80.

27. Ferster D. Neuroscience. Blocking plasticity in the visual cortex. *Science* 2004;303:1619-21.

28. Krolak-Salmon P, Guenot M, Tiliket C, et al. Anatomy of optic nerve radiations as assessed by static perimetry and MRI after tailored temporal lobectomy. *Br J Ophthalmol* 2000;84:884-9.

29. Jeelani NUO, Jindahra P, Tamber MS, et al. 'Hemispherical asymmetry in the Meyer's Loop': a prospective study of visual-field deficits in 105 cases undergoing anterior temporal lobe resection for epilepsy. *J Neurol Neurosurg Psychiatry* 2010;81:985-91.

30. Masland RH. The neuronal organization of the retina. *Neuron* 2012;76:266-80.

31. Liets LC, Eliasieh K, van der List DA, et al. Dendrites of rod bipolar cells sprout in normal aging retina. *Proc Natl Acad Sci U S A* 2006;103:12156-60.

32. Stingl K, Bartz-Schmidt KU, Besch D et al. Artificial vision with wirelessly powered subretinal electronic implant alpha-IMS. *Proc Biol Sci* 2013;280:20130077.

33. Zrenner E. Will retinal implants restore vision? *Science* 2002;295:1022-1025.

34. Kaas JH, Krubitzer LA, Chino YM et al. Reorganization of retinotopic cortical maps in adult mammals after lesions of the retina. *Science* 1990;248:229-231.

35. Gilbert CD, Wiesel TN. Receptive field dynamics in adult primary visual cortex. *Nature* 1992;356:150-152.

36. Engel SA, Rumelhart DE, Wandell BA et al. fMRI of human visual cortex. *Nature* 1994; 369:525.

37. Gabilondo I, Martínez-Lapiscina EH, Martínez-Heras E, et al. Trans-synaptic axonal degeneration in the visual pathway in multiple sclerosis. *Ann Neurol* 2014;75:98-107.

38. Stoll G, Trapp BD, Griffin JW. Macrophage function during Wallerian degeneration of rat optic nerve: clearance of degenerating myelin and Ia expression. *J Neurosci* 1989;9:2327-35.

39. Stoll G, Griffin JW, Li CY, et al. Wallerian degeneration in the peripheral nervous system: participation of both Schwann cells and macrophages in myelin degradation. *J Neurocytol* 1989;18:671-83.

40. Saidha S, Syc SB, Ibrahim MA, et al. Primary retinal pathology in multiple sclerosis as detected by optical coherence tomography. *Brain* 2011;134:518-33.

41. Syc SB, Saidha S, Newsome SD, et al. Optical coherence tomography segmentation reveals ganglion cell layer pathology after optic neuritis. *Brain* 2012;135:521-33.

42. Albrecht P, Ringelstein M, Muller AK, et al. Degeneration of retinal layers in multiple sclerosis subtypes quantified by optical coherence tomography. *Mult Scler* 2012;18:1422-9.

43. Sriram P, Graham SL, Wang C, et al. Transsynaptic retinal degeneration in optic neuropathies: optical coherence tomography study. *Invest Ophthalmol Vis Sci* 2012;53:1271-5.

44. Tatrai E, Simo M, Iljicsov A, et al. In vivo evaluation of retinal neurodegeneration in patients with multiple sclerosis. *PLoS One* 2012;7:e30922.

45. Balcer LJ, Baier ML, Cohen JA, et al. Contrast letter acuity as a visual component for the Multiple Sclerosis Functional Composite. *Neurology* 2003;61:1367-73.

46. Balcer LJ, Galetta SL, Polman CH, et al. Low-contrast acuity measures visual improvement in phase 3 trial of natalizumab in relapsing MS. *J Neurol Sci* 2012;318:119-24.

Chapter 4.3

Bidirectional trans-synaptic axonal degeneration in the visual pathway in multiple sclerosis

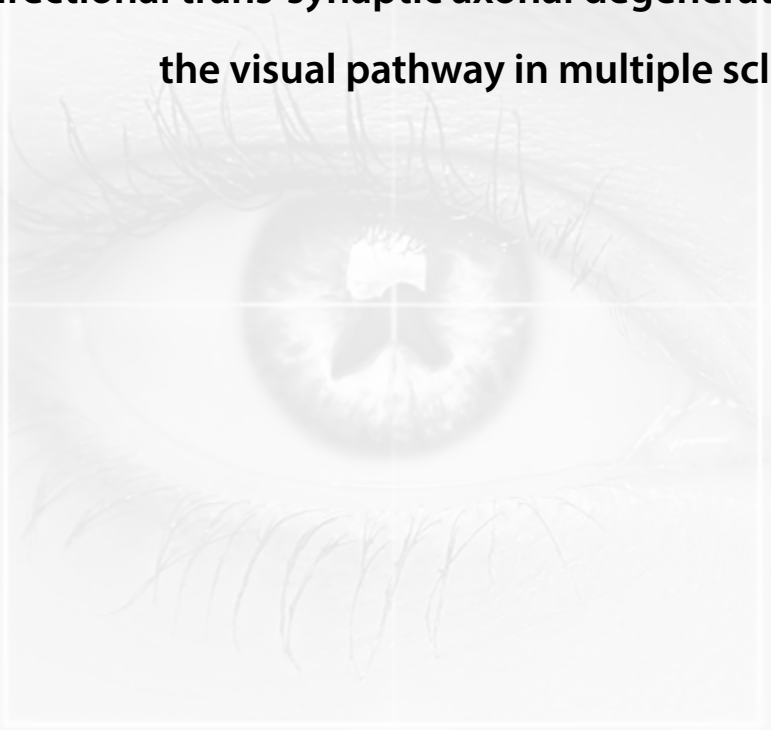

LJ Balk, MD Steenwijk, P Tewarie, M Daams, J Killestein, F Barkhof, H Vrenken, M Wattjes, CH Polman, BMJ Uitdehaag, A Petzold

***J Neurol Neurosurg Psychiatry*. 2014 Jun 27. [Epub ahead of print]**

ABSTRACT

Objective To investigate the coexistence of anterograde and retrograde trans-synaptic axonal degeneration, and to explore the relationship between selective visual pathway damage and global brain involvement in longstanding multiple sclerosis (MS).

Methods In this single-centre, cross-sectional study, patients with longstanding MS (N=222) and healthy controls (HC, N=62) were included. We analysed thickness of retinal layers (optical coherence tomography), damage within optic radiations (OR) (lesion volume and fractional anisotropy and mean diffusivity by diffusion tensor imaging) and atrophy of the visual cortex and that of grey and white matter of the whole-brain (structural MRI). Linear regression analyses were used to assess associations between the different components and for comparing patients with and without optic neuritis and HC.

Results In patients with MS, an episode of optic neuritis (MSON) was significantly associated with decreased integrity of the ORs and thinning of the peripapillary retinal nerve fibre layer (pRNFL) and macular ganglion cell complex (GCC). Lesion volume in the OR was negatively associated with pRNFL and GCC thickness in patients without optic neuritis (MSNON). The pRNFL and GCC showed associations with integrity of the OR, thickness of the primary visual cortex (only in patients with MSON), and also with global white and grey matter atrophy. In HCs, no such relationships were demonstrated.

Conclusion This study provides evidence for presence of bidirectional (both anterograde and retrograde) trans–synaptic axonal degeneration in the visual pathway of patients with MS. Additionally, thinning of the retinal pRNFL and GCC are related to global white and grey matter atrophy in addition to pathology of the visual pathway.

INTRODUCTION

Neuroaxonal degeneration largely contributes to irreversible disability in multiple sclerosis (MS).[1–4] It is, however, still not known what mechanism drives neuroaxonal degeneration. To investigate the dynamics of neuroaxonal degeneration, the visual pathway is a particularly suitable model, as it is a hard-wired, single pathway model (Figure 1). Previously, we and others have demonstrated that an episode of optic neuritis in patients with MS (MSON) is related to thinning of the inner layers of the retina, most likely as a result of retrograde (towards the retina) axonal degeneration.[5–7] Importantly, significant thinning of the innermost retinal layers was also observed in patients without any history of optic neuritis (MSNON), which was suggested to be a result of retrograde trans-synaptic degeneration. More recent studies have suggested that this mechanism is responsible for the spreading of neuroaxonal degeneration in patients with MS and stroke.[8–11] In addition to the previously described evidence for retrograde trans-synaptic degeneration (related to thinning of the inner retinal layers),[7] there is also evidence for anterograde (directed towards the visual cortex) trans-synaptic degeneration (related to damage of the optic radiations (ORs) and primary visual cortex) in the visual system of patients with MS.[10-12] Therefore, the unifying term 'bidirectional (trans-synaptic) axonal degeneration' was proposed,[4] to better describe what originally was reported as 'insidious atrophy'.[13] The relation between retrograde and anterograde trans-synaptic degeneration in the visual pathway of patients with MS (as a result of either lesions is the optic nerve or elsewhere in the visual pathway), and its relationship with whole-brain atrophy, is however not entirely clear.

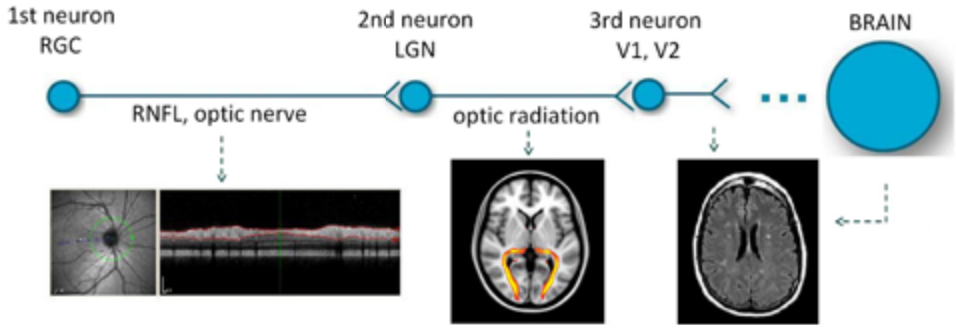

Figure 1. Anatomical depiction of the visual pathway with imaging techniques used. The retinal ganglion cell (RGC), visualised with spectral domain optical coherence tomography (SD-OCT), projects to the lateral nucleus (LGN) in the midbrain. The axon of the 2nd order neuron in the LGN projects through the optic radiations (OR), assessed using diffusion tensor imaging, to the primary visual cortex. Next, this hard-wired, single pathway integrates other parts of the brain via the higher visual cortex. The visual cortex and global brain measures are assessed using structural MRI.

Therefore, the aim of this study was to investigate for the presence of bidirectional (comprising anterograde and retrograde) trans-synaptic degeneration in the visual system of patients with MS, and to explore how damage of the visual system is associated with damage in the rest of the brain.

METHODS

This study was approved by the medical ethical committee (protocol number 2010/336) and the scientific research committee (protocol number CWO/10-25D) of the VU University Medical Center in Amsterdam, The Netherlands. Written informed consent was obtained from all included subjects.

Study design and patient population

Patients with MS and healthy controls (HC) were enrolled from the VU University medical centre Amsterdam. This cohort has been previously described.[7,14] From eight of the original 230 patients with MS and one of the 63 HCs described earlier, MRI diffusion tensor imaging (DTI) data was not available. Therefore, the present paper reports the remaining 222 patients and 62 HCs. All included patients adhered to the following inclusion criteria: aged between 18 years and 80 years, a diagnosis of either relapsing remitting MS (RRMS), secondary progressive MS (SPMS) or PPMS at the time of their assessment (defined by Lublin-Reingold criteria).[15] Patients were excluded if they fulfilled any of the following criteria: pregnancy; received a course of steroids or had a relapse within 6 weeks prior to inclusion; HIV or other immunodeficiency syndrome; history of substance abuse (drug or alcohol) and non-MS radiological findings that could interfere with evaluation.

Healthy control subjects were eligible for inclusion if they were aged between 18 years and 80 years at the time informed consent was signed, and if they had no history of any neurological, ophthalmological or psychiatric disease. Exclusion criteria for healthy control subjects were similar to those for MS patients, with the addition of 1st-degree or 2nd-degree familial relation to an MS patient.

SD-OCT

Retinal imaging was performed with spectral domain optical coherence tomography (SD-OCT, Spectralis, Heidelberg Engineering, Heidelberg, Germany), with the eye tracking function enabled for optimal measurement accuracy.[16] A detailed description of the scan protocol has been described elsewhere.[7] In brief, peripapillary data were obtained using a 12° ring scan and macular data with a macular volume scan (20×20°

field, 25 B-scans, see supplementary Figure 1). Scans were excluded from the analyses if they violated, validated international consensus quality control criteria (OSCAR-IB).[17,18] In order to assess retinal pathology potentially resulting in exclusion of OCT scans, the personal and medical history of visual
symptoms was obtained from all patients and controls and judged in view of the clinical examination. The assessment of history of symptomatic MSON was based on established, phenotypic diagnostic criteria.[19] An exclusion criterion was an episode of MSON in the past 6 months. Image postprocessing was performed for both scans, using commercial segmentation software (Heidelberg Engineering, Heidelberg, Germany). Although the software enabled reliable segmentation of multiple layers in the peripapillary and macular area,[20] the mean peripapillary retinal nerve fibre layer (pRNFL) and the macular ganglion cell complex (GCC) (perimacular rim) have shown to be most sensitive to changes in the central nervous system (CNS),[5–7] and are, therefore, used in this study (see supplementary Figure 1).

Magnetic resonance imaging

Structural MRI was performed on a 3 T whole-body scanner (GE Signa HDxt, Milwaukee, Wisconsin, USA), using a three-dimensional T1-weighted fast spoiled gradient echo sequence (FSPGR) for volumetics, a three-dimensional fluid-attenuated inversion recovery image (FLAIR) for lesion detection, and DTI for integrity measurements and tractography (see supplementary material for more details).

Brain and lesion volumes

Normalised grey and white matter volumes (NGMV and NWMV respectively) and lesion volumes were quantified automatically using kNN-TTP,[21] and SIENAX (part of the FMRIB Software Library (FSL) 5.0.4, http://www.fmrib.ox.ac.uk/fsl). Lesion filling was applied to minimise the effect of lesions on atrophy measurements.[22] FreeSurfer 5.1 was used to quantify the average thicknesses of V1, V2, and V5 (see supplementary material for more details).

DTI data processing and segmentation of the optic radiations

The DTI images were corrected for head movement and eddy current distortions using FMRIB's Diffusion Toolbox (FDT; also part of FSL). Subsequently, the diffusion tensor was fitted, from which the fractional anisotropy (FA), mean diffusivity (MD) were calculated. The diffusion images were then used to segment the ORs and derive tract-specific pathology measures. As tractography in the presence of MS pathology might lead to unreliable results, this was done by means of an atlas based on the healthy controls. Probabilistic tractography was performed between the thalamus and V1 in each

hemisphere to obtain the ORs in each healthy control. The tractography results were thresholded, non-linearly registered to a standard space and averaged to obtain an atlas. The atlas was subsequently propagated to each subject to obtain a subject specific OR-segmentation (see supplementary material for more details).
For each subject and tract separately, the weighted average FA and MD values inside the tract, as well as the lesion volume in the tract, were computed using the atlas probability values as a weighting factor. Weighting was performed to emphasise integrity values in the centre of the tract. Also, the weighted lesion
volume inside each tract was computed as described above. Note that the weighted lesion volume is a relative, instead of an absolute value, and cannot be compared with absolute whole-brain lesion volumes.

Statistical analyses
In order to compare demographic data between patients and healthy controls, independent sample t-test and χ^2 tests were performed. Next, linear regression analyses with adjustments for age were used to test for differences in the individual structures of the visual pathway between patients with MS and HCs.
With the aim of investigating the effect of an episode of optic neuritis (MSON) on anterograde (towards ORs) and retrograde (towards retina) degeneration, integrity of the OR and retinal layer thickness were compared between patients with patients with MSON, MSNON and HCs. The analyses with MD and FA were adjusted for lesion load in the OR. Importantly, for the analyses including pRNFL and GCC thickness, the mean data of both eyes was used. Therefore, these analyses only included patients in whom both eyes had the same history of ON (bilateral MSON or bilateral MSNON). This was done to avoid contamination of the study groups by pooling of MSON eyes (showing a severe degree of pRNFL loss) with MSNON eyes (showing a small degree pRNFL loss).[8]
Furthermore, it is important to note that an episode of MSON acted as an effect modifier in the multiple regression analyses investigating the associations between retinal layer thickness and other structures of the visual pathway and global brain. Therefore, all these analyses were stratified by MSON, MSNON and HCs.
The effect of lesion volume in the OR on retinal layer thickness (retrograde trans-synaptic degeneration) was investigated using linear regression analyses with adjustments for age.
Next, the associations between retinal layer thickness and integrity of the OR (as measured by weighted FA and MD), NGMV and NWMV were investigated using linear regression analyses with adjustments for age.
In order to increase comparability and ease interpretation of the multiple regression analyses, all values from regression analyses are reported as standardised ß. Statistical analyses were performed using SPSS V.22.0, with a statistical significance level of 0.05.

RESULTS

A total of 222 MS patients (137 RRMS, 57 SPMS, 28 PPMS) and 62 healthy control subjects (HCs) were included in this study. Patients with MS were slightly older than HCs ($p<0.05$) and had a mean disease duration of 20.3 (±7.0) years (range 8.8–45.9). One hundred and two patients (45.9%) had ever experienced an episode of MSON, and 38 (17.1%) had experienced bilateral MSON. The remaining 103 patients (46.4%) had never experienced an episode of MSON. Only one patient (with previous MSON) showed signs of unilateral microcystic macular oedema (MMO). Exclusion of data from this patient did not change the level of significance for any of the following analyses. An overview of the clinical and demographic data is shown in Table 1.

Table 1 Subject characteristics

	Patients	Controls	p-value
N	222	62	
Age (years)	54.1 (±10.0)	50.5 (±7.3)	.002[a]
Sex (% male)	32.0%	35.5%	.603[b]
MS type (N [%]) RR SP PP	 137 (61.7%) 57(25.7%) 28 (12.6%)	 n/a	
Disease duration (years)	20.3 (±7.0)	n/a	
EDSS (median [range])	4.0 [1-8]	n/a	
History of MSON (N [%]) Bilateral MSON Bilateral MSNON	102 (45.9%) 38 (17.1%) 103 (46.4%)	n/a	

a. independent sample t-test
b. χ^2 test
EDSS, expanded disability status scale; MS, multiple sclerosis; MSNON, MS without optic neuritis; MSON, MS optic neuritis; PP, primary progressive; RR, relapsing remitting; SP, secondary progressive.

Visual pathway damage in MS

The differences between patients with MS and HCs for all subsequent components of the visual system are shown in Table 2. All structural measures were significantly decreased in patients with MS, compared with HC ($p<0.005$ for all comparisons). Additionally, NWMV and NGMV showed significant reductions in patients with MS, compared with HC ($p<0.001$ for both comparisons). For comparisons of all components between MSON and MSNON patients, see supplementary Table 1.

Table 2 Quantification of the components of the visual pathway.

	Patients	Controls	p-value[a]
N	222	62	
Eye			
pRNFL (µm)	83.2±11.1	91.8±6.7	<0.001
GCC (µm)	82.8±14.8	94.2±6.0	<0.001
Optic radiations			
FA	0.41±0.04	0.46±0.02	<0.001
MD (10^{-3} mm^2/s)	0.95±0.10	0.84±0.03	<0.001
Brain - visual cortex			
V1 (mm)	1.77±0.12	1.83±0.11	0.005
V2 (mm)	2.05±0.12	2.14±0.11	<0.001
V5 (mm)	2.35±0.14	2.46±0.12	<0.001
Brain - global			
NWMV (ml)	662.8±45.5	698.4±34.1	<0.001
NGMV (ml)	755.4±59.6	795.8±51.9	<0.001

Quantitative structural measures are shown for the eye (OCT), optic radiations (DTI) and visual cortex (structural MRI). In addition to this single pathway data, global atrophy measures of white and grey matter are also shown. Values are reported as mean±sd.
a: Linear regression analyses with adjustments for age
DTI, diffusion tensor imaging; FA, fractional anisotropy; GCC, ganglion cell complex; MD, mean diffusivity; NGMV, normalised grey matter volume; NWMV, normalised white matter volume; OCT, optical coherence tomography; pRNFL; peripapillary retinal nerve fibre layer; RNFL, retinal nerve fibre layer; V1, primary visual cortex; V2, secondary visual cortex; V5, middle temporal visual area.

Bi-directional trans-synaptic degeneration in the visual system

Anterograde trans-synaptic degeneration

In patients with bilateral MSON, significant loss of integrity of the OR (measured by FA) was demonstrated, compared with patients with bilateral MSNON and HCs (Figure 2A, left graph). Consistent with these data, diffusivity (MD) was increased where anisotropy (FA) was decreased. Whereas MD was significantly lowest in HCs, followed by patients with MSNON and MSON, the difference between the MSON and MSNON groups was not statistically significant (Figure 2A, right graph).

Retrograde trans-synaptic degeneration

For the comparison of retinal pRNFL and GCC between MSON, MSNON and HCs, a clear trend was observed. Patients with MSON showed the most severe thinning of both retinal layers compared to patients with MSNON and HCs ($p<0.001$ for all comparisons). Importantly, patients with MSNON also showed significant thinning of both retinal layers, compared with HCs ($p<0.001$ for both comparisons, Figure 2B).

Additionally, the association between weighted lesion volume in the OR and retinal layer thickness was investigated. These analyses were stratified by MSON and MSNON. Increased lesion volume in the OR was related to a significant decrease of the pRNFL and

GCC (standardised ß -0.33, p=0.003 and standardised ß -0.32, p=0.005, respectively). This relationship disappeared when patients had experienced MSON, due to the severe damage in the retina (standardised ß -0.15, p=0.520 and standardised ß -0.10, p=0.686, respectively).

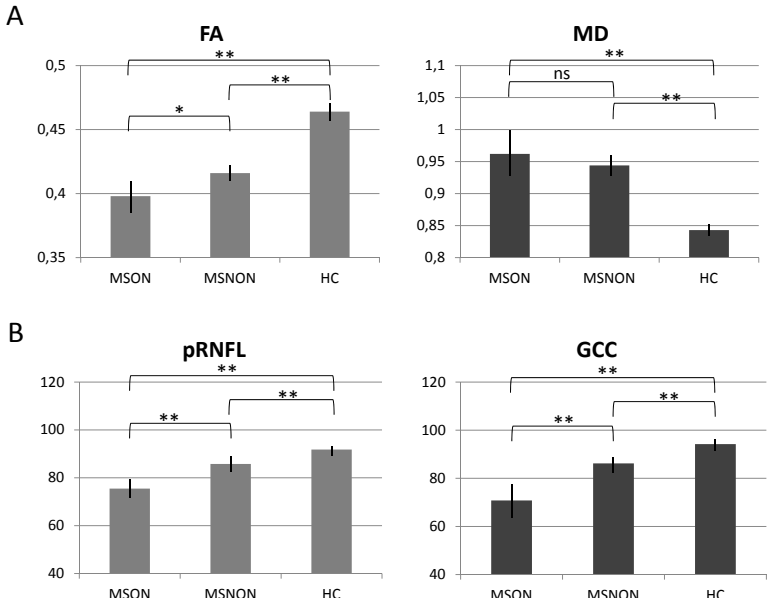

Figure 2. (A) Mean fractional anisotropy (FA) and mean diffusivity (MD) (grey bars) with 95% CIs (black bars) for patients with MSON, MSNON and healthy controls (HCs). In a single pathway model, integrity of the optic radiations (FA) was significantly impaired in patients with MSON compared with patients with MSNON and HC. For MD, this difference was significant for the comparison of patients with multiple sclerosis with HCs, irrespective of an episode of MSON. (B) Mean peripapillary retinal nerve fibre layer (pRNFL) and ganglion cell complex (GCC) (grey bars) with 95% CIs (black bars) for patients with MSON, MSNON and HCs. The pRNFL and GCC showed the most severe atrophy in MSON, followed by MSNON and then HC (p<0.001 for all comparisons). * p<0.05, ** p<0.001

Structurally related neurodegeneration in the visual pathway and the global brain

4.3

Atrophy of the visual pathway

Table 3 shows the results of the regression analyses with retinal layer thickness (pRNFL and GCC) and integrity of the OR (FA and MD) and visual cortex thickness (V1, V2 and V5). In patients with MSON, the retinal layer thickness was positively associated with FA and negatively associated with MD. The associations were, however, not statistically significant, due to reduced statistical power (n=38). The more substantial axonal loss from MSON was related to a significant degree of localised atrophy of V1. An anatomical relationship exists with V2, to which the OR projects as well, but the study was underpowered to show this. No associations with V5 were demonstrated.

In patients with MSNON, the GCC and, to a lesser extent, the pRNFL, were directly associated with the FA (standardised ß 0.72, p<0.001 and 0.42, p=0.064, respectively). Consistently, both were, although not statistically significant, inversely correlated with the MD (standardised ß -0.46, p=0.110 and standardised ß -0.11, p=0.715, respectively). In the visual pathway of HCs, there were no relationships observed between pRNFL or GCC thicknesses and MRI metrics of the OR, V1, V2 or V5 in HCs.

Table 3 Associations between structural damage in a single pathway model

	FA*	MD*	V1	V2	V5	NGMV	NWMV
MSON (N=38)							
GCC	0.58 (.205)	-0.76 (.145)	0.52 (.019)	0.34 (.155)	0.01 (.963)	0.36 (.109)	0.45 (.053)
pRNFL	0.52 (.180)	-1.01 (.043)	0.34 (.079)	0.11 (.606)	-0.27 (.221)	0.24 (.242)	0.33 (.122)
MSNON (N=103)							
GCC	0.72 (.001)	-0.46 (.110)	0.14 (.245)	0.15 (.217)	-0.05 (.657)	0.40 (<.001)	0.42 (<.001)
pRNFL	0.42 (.064)	-0.11 (.715)	0.10 (.414)	0.14 (.228)	-0.02 (.870)	0.30 (.005)	0.27 (.019)
HCs (N=62)							
GCC	0.21 (.092)	-0.22 (.087)	0.13 (.316)	0.14 (.283)	0.18 (.167)	0.06 (.640)	-0.03 (.829)
pRNFL	0.10 (.485)	-0.03 (.859)	0.06 (.663)	0.11 (.432)	0.06 (.667)	0.01 (.965)	-0.06 (.694)

In patients with MSON, retinal layer thickness was weakly associated with damage in the OR. The substantial axonal loss from MSON was related to a significant degree of localised atrophy of V1, to a lesser extent also V2, but not V5. In patients with MSNON, a significant relationship was demonstrated between damaged OR and atrophy of the pRNFL and GCC. In HCs, no significant associations were demonstrated. Values reported as standardised ß (p-value)
*Additionally adjusted for OR lesion volume in MSON and MSNON groups.
FA, fractional anisotropy; GCC, ganglion cell complex; HC, lateral nucleus; MD, mean diffusivity; NGMV, normalised grey matter volume; NWMV, normalised white matter volume; OR, optic radiation; pRNFL; peripapillary retinal nerve fibre layer.

Whole brain atrophy

The associations between retinal layer thickness and brain volume structures are illustrated in Table 3. In patients with MSON, the pRNFL and the GCC tended to be positively associated with NWMV and NGMV, but these relationships were not statistically significant, probably due to reduced statistical power. Interestingly, in the group of patients with MSNON, similar positive associations with both NWMV and NGMV were observed, all statistically significant. No such quantitative relationships were found for HCs.

DISCUSSION

This study provides evidence for the presence of bidirectional trans-synaptic axonal degeneration in the visual pathway of patients with MS. Degeneration of neurons and axons disseminates by means of both anterograde (towards the visual cortex) and retrograde (towards the retina) trans-synaptic axonal degeneration. Importantly, retinal layer thickness did also reflect global brain atrophy of both white and grey matter.

First, the present data shows that a history of MSON is associated with decreased integrity of the OR. This decrease in integrity of the OR is thought to be caused by anterograde trans-synaptic degeneration.

Second, besides decreased integrity of the OR, patients with MSON also showed significantly more thinning of the pRNFL and GCC compared with patients with MSNON or HCs. These findings showed that episodes of optic neuritis are not only suggestive of anterograde degeneration of the OR, but also of retrograde degeneration of the optic nerve and retinal layers. Importantly, whereas the presence of MSON was related to thinning of the retinal layers by retrograde degeneration, there was also significant retinal thinning observed in patients with MSNON. In these patients, with no history of lesions in the optic nerve, retinal layer thinning is most probably caused by retrograde trans-synaptic degeneration, caused by local damage
in other structures of the optic pathways.

Likewise, lesion volume in the OR was also related to retinal layer thickness, suggesting that lesions in the OR may lead to thinning of the retina by retrograde trans-synaptic degeneration. Interestingly, this relationship was less clear in patients with MSON, which was most probably caused by the fact that this subtle relationship was masked by the severe retinal thinning in patients with MSON.

Third, there were clear structural relationships between retinal layer thickness and other components of the visual pathway. Interestingly, the severe axonal loss in the optic nerve as a result from MSON, seemed to result in a significant degree of localised atrophy of V1. Although a weak relationship may still exist with V2, no relationship whatsoever was found with V5. In patients with MSNON however, retrograde trans-synaptic axonal degeneration is held responsible for the relationship between damaged OR and atrophy of the pRNFL and GCC. Importantly, in HCs there was no relationship whatsoever between pRNFL or GCC thicknesses and MRI metrics of the OR, V1, V2 or V5. This implies that the aforementioned relationships in patients with MS were atrophy based, and therefore, only present in case of neuroaxonal damage.

The presence of retrograde trans-synaptic degeneration in the visual pathway of MS has been described before.[7,10,11,23] In a previous study, we described the presence of retrograde trans-synaptic degeneration in the eyes of patients with MS. An episode

of MSON was strongly associated with severe atrophy of the inner layers of the retina, but not the outer layers. This suggested that retrograde (trans-synaptic) axonal degeneration is halted at an anatomical structure capable of neuroplasticity, the inner nuclear layer (INL) of the retina.[7] The present data suggest that the secondary visual cortex, like the INL, highly capable of plasticity,[24] may act as a physiological barrier to anterograde trans-synaptic degeneration, but this should be further investigated. In order to test this hypothesis, one would need to make use of detailed voxel-based morphometry of different areas of the higher visual cortex.

Consistent with the present study, others have found that in patients with optic neuritis, the OR,[25–27] but also the visual cortex,[28,29] revealed damage after episodes of MSON. A more recent study investigating multiple components of the visual pathway, reported that pRNFL thinning was associated with atrophy of the visual cortex, but this relationship disappeared when MSON and MSNON patients were analysed separately (N=100).[10] Gabilondo et al[10] also demonstrated a relationship between retinal layer thickness and lesion volume in the OR.

The present study extends on previous studies, by investigating individual retinal layers, the complete visual pathway and the global brain in a larger number of subjects. We observed a clear association between retinal layer thickness and global NWMV and NGMV, which is consistent with previous studies in MS[30,31] and NMO.[32] These data suggest that trans-synaptic degeneration might not be restricted to the visual pathway but could disseminate through the whole-brain. However, in our opinion, it is most unlikely that this process can be solely explained by trans-synaptic degeneration, as structures capable of plasticity act as a barrier to this process. Besides, if trans-synaptic degeneration would not be stopped, it would spread through the brain like a domino effect. Therefore, the observed damage to the global brain structures are more likely to be caused by a more global mechanism. In this systemic model, neuroaxonal degeneration is driven by a global mechanism, affecting the entire brain, including the visual system. Although hypothetical, a possible explanation for this systemic model could be mitochondrial failure, also known as the 'virtual hypoxia hypothesis' in MS research.[33]

An important limitation of this study was its cross-sectional nature. We were, therefore, unable to determine whether the degree of atrophy may already have reached a plateau after an average of 20 years of disease duration, or continues to progress. To address this question, longitudinal data is needed. Next, the HCs were significantly younger than our patient cohort. This was however taken into account by age-adjusted statistical tests. Finally, the assessment of history of MSON was based on clinically confirmed episodes and patient-reported history on earlier events during the disease. Although this approach is consistent with other studies in the field, it may have introduced a

bias towards more severe episodes of MSON and subclinical episodes may have gone unnoticed.

In summary, this study provides evidence for presence of bidirectional trans–synaptic axonal degeneration in the visual pathway of patients with MS. Additionally, thinning of the retinal pRNFL and GCC reflect visual pathway damage, and also global white and grey matter atrophy.

SUPPLEMENTARY MATERIAL

Magnetic resonance imaging

Structural magnetic resonance imaging (MRI) was performed on a 3T whole body scanner (GE Signa HDxt, Milwaukee, WI, USA). The protocol included a three-dimensional T1-weighted fast spoiled gradient echo sequence (FSPGR; repetition time [TR] 7.8 ms, echo time [TE] 3 ms, flip angle [FA] 12º, 240 x 240 mm^2 field of view [FOV], 176 sagittal slices of 1 mm thickness, 0.94 x 0.94 mm^2 in-plane resolution) for cortical thickness measurements, and a three-dimensional fluid attenuated inversion recovery image (FLAIR; TR 8000 ms, TE 125 ms, TI 2350 ms, 250 x 250 mm^2 FOV, 132 sagittal slices of 1.2 mm thickness, 0.98 x 0.98 mm^2 in-plane resolution) for lesion detection. Furthermore, 2D echo-planar diffusion tensor images (TR 13000 ms, TE 86 ms, 2.4 mm thick slices, 2.0 x 2.0 mm2 in-plane resolution) were acquired, including 30 volumes with noncollinear diffusion gradients (b value of 900 s/mm^2) and 5 volumes without diffusion weighting.

Brain lesion and atrophy measurements

White matter lesion segmentation was automatically performed using the FLAIR and FSPGR images.[Steenwijk, *Neuroimage Clin* 2013] The resulting lesion volume was corrected for head size, resulting in a normalised lesion volume (NLV). To minimize the impact of WM lesions on atrophy measurements, lesion filling was applied.[Chard, *J Magn Reson Imaging* 2010] Then, SIENAX (part of the FMRIB Software Library (FSL) 5.0.4, http://www.fmrib.ox.ac.uk/fsl) was used to measure GM and WM volumes (NGMV, and NWMV, respectively). Cortical thickness measurements were performed using the FreeSurfer pipeline (version 5.1) as previously described.[Dale, *Neuroimage* 1999 and Fischl, *Neuroimage* 1999] After running the FreeSurfer pipeline, the primary (V1), secondary (V2) and middle temporal (V5) visual cortex were segmented in each subject.[Fischl, *Cereb Cortex* 2008] The resulting cortical parcellations were then used to compute the average thickness of V1, V2 and V5.

DTI data processing and segmentation of the optic radiations

The DTI images were corrected for head movement and eddy current distortions using FMRIB's Diffusion Toolbox (FDT; also part of FSL). Subsequently the diffusion tensor was fitted, from which the fractional anisotropy (FA), mean diffusivity (MD) were calculated. The diffusion images were then used to segment the ORs and derive tract specific pathology measures. As tractography in the presence of MS pathology might lead to unreliable results, this was done by means of an atlas based on the healthy controls. The pipeline was as follows:

1. For each healthy control, subject-specific seed masks (i.e. the thalamus and V1) were derived for OR tractography. FIRST (also part of FSL) was used to obtain subject-specific masks of the thalami, whereas the FreeSurfer segmentation was used to obtain the subject-specific segmentations of V1.
2. For each healthy control and hemisphere separately, probabilistic tractography was run using the previously defined masks as a seed region. This involved bedpostx (part of FSL) to estimate the voxelwise diffusion parameter distributions and probabilistic tractography using FSL's probtrackx2 (5000 streamlines per voxel). Each probabilistic map was then binarised using 1.00% of the streamline total as a threshold to obtain a segmentation of the subjects' OR. This threshold was determined visually and led to consistent segmentation results throughout the healthy controls.
3. The binary maps were then non-linearly warped to MNI standard space, and averaged to construct a single probabilistic map with voxelwise values between zero and one forming the atlas of the ORs.
4. Then, to obtain a subject-specific segmentation, the probabilistic atlas was propagated to the individual space of each subject using non-linear registration. For patients, lesion voxels were masked out of the registration cost-function to enhance registration quality and minimize the influence of lesions.

For each subject and tract separately, the weighted average FA and MD values inside the tract, as well as the lesion volume in the tract, were computed using the atlas probability values as a weighting factor. Weighting was performed to emphasize integrity values in the centre of the tract. In order to include only WM, the weighting factors of voxels belonging to GM or CSF were set to zero using the earlier derived SIENAX segmentations. Also, the weighted lesion volume inside each tract was computed as described above. Note that the weighted lesion volume is a relative, instead of an absolute value, and cannot be compared with unweighted whole brain lesion volumes.

Supplementary Table 1 Quantification of the components of the visual pathway separately for MSON, MSNON and HCs. Quantitative structural measures are shown for the eye (OCT), optic radiations (DTI) and visual cortex (structural MRI). In addition to this single pathway data, global atrophy measures of white and gray matter are also shown. Values are reported as mean±sd.

	MSON	MSNON	Controls	p-value* MSON vs MSNON
N	38	103	62	
Eye				
pRNFL (µm)	75.5±10.3	85.8±10.2	91.8±6.7	<0.001
GCC (µm)	70.8±16.5	86.2±12.4	94.2±6.0	<0.001
Optic radiations				
FA	0.40±0.04	0.42±0.04	0.46±0.02	0.014
MD (10^{-3} mm^2/s)	0.96±0.10	0.94±0.09	0.84±0.03	0.248
Brain - visual cortex				
V1 (mm)	1.72±0.11	1.79±0.12	1.83±0.11	0.007
V2 (mm)	2.01±0.12	2.06±0.11	2.14±0.11	0.010
V5 (mm)	2.32±0.11	2.36±0.14	2.46±0.12	0.092
Brain - global				
NWMV (ml)	655.5±51.4	667.8±40.9	698.4±34.1	0.139
NGMV (ml)	754.4±63.6	751.1±56.6	795.8±51.9	0.865

* Linear regression analyses with adjustments for age
MSON: bilateral optic neuritis in MS, MSNON; no optic neuritis in MS, RNFL: retinal nerve fibre layer, GCC: ganglion cell complex, FA: fractional anisotropy, MD: mean diffusivity, V1: primary visual cortex, V2: secondary visual cortex, V5:middle temporal visual area, NWMV: normalized white matter volume, NGMV: normalized gray matter volume.

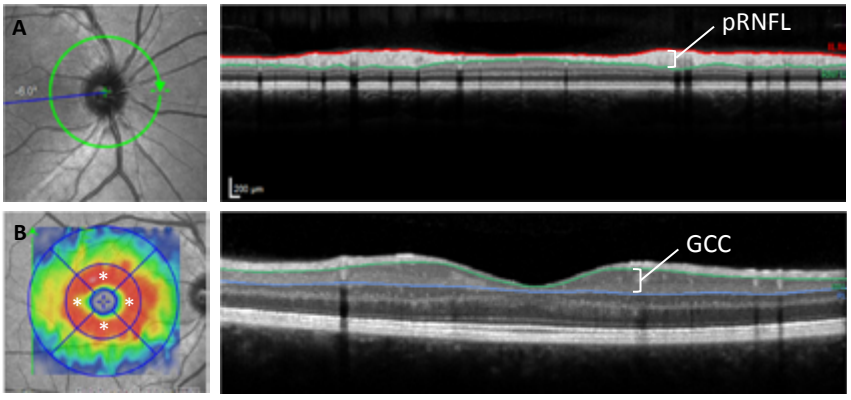

Supplementary Figure 1. Scan and segmentation protocol for the OCT scans used in this study. (A) The peripapillary ring scan was used to quantify the global mean retinal nerve fibre layer (pRNFL) thickness. (B) The macular volume scan (20 x 20 degrees field, 25 vertical B-scans) was used to assess thickness of the macular ganglion cell complex (GCC). The coloured map represents a GCC thickness map with a 1, 3 and 6 mm EDTRS grid of which only the perimacular rim (asterix) was used in this study.

REFERENCES

1. Stadelmann C, Albert M, Wegner C, Bruck W. Cortical pathology in multiple sclerosis. *Curr Opin Neurol* 2008;21:229-234.
2. Compston A, Coles A. Multiple sclerosis. *Lancet* 2008;372:1502-1517.
3. Trapp BD, Nave KA. Multiple sclerosis: an immune or neurodegenerative disorder? *Annu Rev Neurosci* 2008;31:247-269.
4. Petzold A. Neurodegeneration and multiple sclerosis. In: Galimberti D, Scarpini E. eds. Neurodegenerative diseases. Springer, 2014:227-45.
5. Albrecht P, Ringelstein M, Muller AK et al. Degeneration of retinal layers in multiple sclerosis subtypes quantified by optical coherence tomography. *Mult Scler* 2012;18:1422-1429.
6. Tatrai E, Simo M, Iljicsov A, Nemeth J, Debuc DC, Somfai GM. In vivo evaluation of retinal neurodegeneration in patients with multiple sclerosis. *PLoS One* 2012;7:e30922.
7. Balk LJ, Twisk JW, Steenwijk MD et al. A dam for retrograde axonal degeneration in multiple sclerosis? *J Neurol Neurosurg Psychiatry* 2014;85:782-9.
8. Petzold A, de Boer JF, Schippling S et al. Optical coherence tomography in multiple sclerosis: a systematic review and meta-analysis. *Lancet Neurol* 2010;9:921-932.
9. Jindahra P, Petrie A, Plant GT. Retrograde trans-synaptic retinal ganglion cell loss identified by optical coherence tomography. *Brain* 2009;132:628-634.
10. Gabilondo I, Martinez-Lapiscina EH, Martinez-Heras E et al. Trans-synaptic axonal degeneration in the visual pathway in multiple sclerosis. *Ann Neurol* 2014;75:98-107.
11. Klistorner A, Sriram P, Vootakuru N, et al. Axonal loss of retinal neurons in multiple sclerosis associated with optic radiation lesions. *Neurology* 2014;82:2165–72.
12. You Y, Gupta VK, Graham SL, Klistorner A. Anterograde degeneration along the visual pathway after optic nerve injury. *PLoS One* 2012;7:e52061.
13. Frisen L, Hoyt WF. Insidious atrophy of retinal nerve fibers in multiple sclerosis. Funduscopic identification in patients with and without visual complaints. *Arch Ophthalmol* 1974;92:91–3.
14. Balk L, Tewarie P, Killestein J, Polman C, Uitdehaag B, Petzold A. Disease course heterogeneity and OCT in multiple sclerosis. *Mult Scler* 2014.
15. Lublin FD, Reingold SC. Defining the clinical course of multiple sclerosis: results of an international survey. National Multiple Sclerosis Society (USA) Advisory Committee on Clinical Trials of New Agents in Multiple Sclerosis. *Neurology* 1996;46:907-911.
16. Balk LJ, Petzold A. Influence of the eye-tracking-based follow-up function in retinal nerve fiber layer thickness using fourier-domain optical coherence tomography. *Invest Ophthalmol Vis Sci* 2013;54:3045.
17. Tewarie P, Balk L, Costello F et al. The OSCAR-IB consensus criteria for retinal OCT quality assessment. *PLoS One* 2012;7:e34823.
18. Schippling S, Balk LJ, Costello F, et al. Quality control for retinal OCT in multiple sclerosis: validation of the OSCAR-IB criteria. Mult Scler 2014 Jun 16. [Epub ahead of print].
19. Petzold A, Plant GT. Diagnosis and classification of autoimmune optic neuropathy. *Autoimmun Rev* 2014;13:539–45.
20. Oberwahrenbrock T, Traber G, Gabilondo I, et al. Multicenter inter-rater reliability of retinal layer segmentation using spectral-domain OCT. ECTRIMS Meeting; Kopenhagen, Denmark, 2–5 October 2013, poster 480.
21. Steenwijk MD, Pouwels PJ, Daams M et al. Accurate white matter lesion segmentation by k nearest neighbor classification with tissue type priors (kNN-TTPs). *Neuroimage Clin* 2013;3:462-469.
22. Chard DT, Jackson JS, Miller DH, Wheeler-Kingshott CAM. Reducing the impact of white matter lesions on automated measures of brain gray and white matter volumes. *J Magn Reson Imaging* 2010;32:223-228.
23. Jindahra P, Petrie A, Plant GT. The time course of retrograde trans-synaptic degeneration following occipital lobe damage in humans. *Brain* 2012;135:534-541.
24. Jenkins TM, Toosy AT, Ciccarelli O, et al. Neuroplasticity predicts outcome of optic neuritis independent of tissue damage. *Ann Neurol* 2010;67:99–113.
25. Ciccarelli O, Toosy AT, Hickman SJ et al. Optic radiation changes after optic neuritis detected by tractography-based group mapping. *Hum Brain Mapp* 2005;25:308-316.

26. Kolbe S, Bajraszewski C, Chapman C et al. Diffusion tensor imaging of the optic radiations after optic neuritis. *Hum Brain Mapp* 2012;33:2047-2061.

27. Reich DS, Smith SA, Gordon-Lipkin EM et al. Damage to the optic radiation in multiple sclerosis is associated with retinal injury and visual disability. *Arch Neurol* 2009;66:998-1006.

28. Audoin B, Fernando KT, Swanton JK, Thompson AJ, Plant GT, Miller DH. Selective magnetization transfer ratio decrease in the visual cortex following optic neuritis. *Brain* 2006;129:1031-1039.

29. Pfueller CF, Brandt AU, Schubert F et al. Metabolic changes in the visual cortex are linked to retinal nerve fiber layer thinning in multiple sclerosis. *PLoS One* 2011;6:e18019.

30. Saidha S, Sotirchos E, Oh J et al. Relationships Between Retinal Axonal and Neuronal Measures and Global Central Nervous System Pathology in Multiple Sclerosis. *Arch Neurol* 2012;1-10.

31. Zimmermann H, Freing A, Kaufhold F et al. Optic neuritis interferes with optical coherence tomography and magnetic resonance imaging correlations. *Mult Scler* 2013;19:443-450.

32. von Glehn F, Jarius S, Cavalcanti Lira RP et al. Structural brain abnormalities are related to retinal nerve fiber layer thinning and disease duration in neuromyelitis optica spectrum disorders. *Mult Scler* 2014 Jan 29. [Epub ahead of print]

33. Trapp BD, Stys PK. Virtual hypoxia and chronic necrosis of demyelinated axons in multiple sclerosis. *Lancet Neurol* 2009;8:280-291.

Chapter 5

Summarising discussion and conclusions

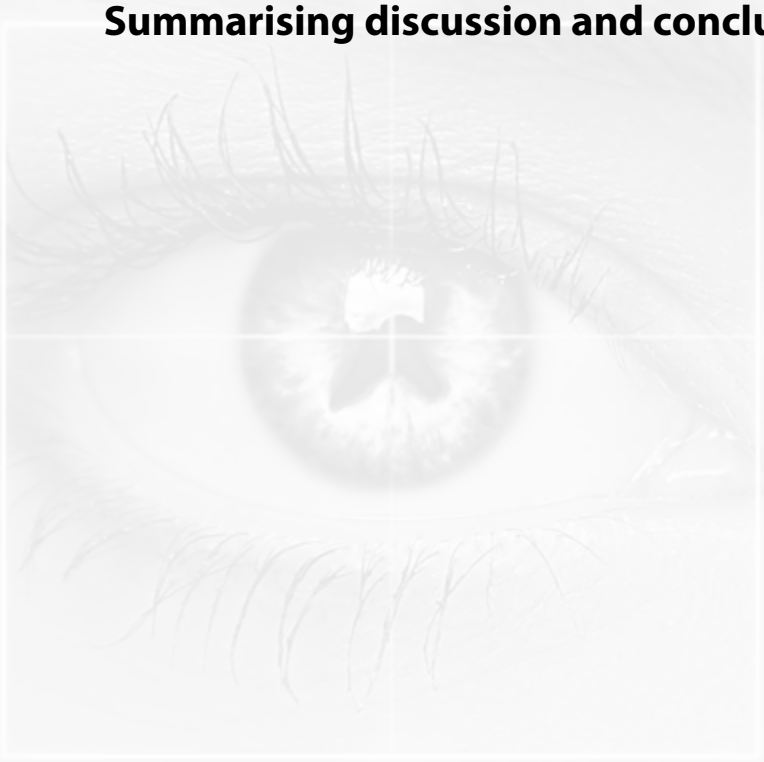

Parts of the introduction have also been published in a recent review on OCT in MS.

LJ Balk, A Petzold

A. Current and future potential of retinal OCT in Multiple Sclerosis
with and without optic neuritis

Neurodegener Dis Manag. **2014;4:165-76**

This thesis aimed to provide more insight in the mechanisms of neuroaxonal degeneration in longstanding MS by using OCT and to determine the added value of OCT in management of the disease. This final chapter summarises and critically discusses the results of the methodological and clinical data. Finally, we address the overall conclusions and the possible implications for future research.

METHODOLOGICAL CONSIDERATIONS

Physiological variation

During the past decade, OCT has been described as a promising method for imaging of neuroaxonal degeneration in MS.[1,2] Because OCT was suggested to be especially useful in longitudinal studies, the reliability of the technique is very important. This is even further underpinned by the fact that newer, high-resolution SD-OCT technology makes it possible to detect changes in the thickness of numerous retinal layers with a very high accuracy (12 µm). Aside from multiple other studies, we also have investigated the test-retest and inter-rater reliability of the SD-OCT machine. The results were consistent. All studies reported excellent inter- and intra-observer reliability for the assessment of the pRNFL using SD-OCT.[3-6] Additionally, a more recent study has shown that the newer segmentation algorithms, able to quantify more individual retinal layers, also show excellent reliability.[7]

Because the reliability of the technique is good, it is even more important to be aware of other potentially influencing factors, as the magnitude of these changes may exceed the degree of atrophy which can be reliably quantified in the eye of a patient suffering from MS. In chapter 2.1 we prospectively investigated whether physiological variation could cause detectable changes in pRNFL thickness and macular volume in healthy human subjects as measured by SDOCT.

The results of this study clearly demonstrated that the pRNFL thickness and the total macular volume (TMV) changed significantly under physiological conditions. Importantly, the degree of thickness changes were clearly above the level of measurement noise of the OCT machine.[4] Since no invasive physiological or laboratory measures were obtained during this study, it was not possible to identify the responsible mechanisms. Subjects who performed physical exercise in this study were requested to refrain from drinking during the exercise period, possibly leading to a mild state of dehydration. Whereas dehydration would be expected to cause thinning of the pRNFL and TMV due to decreasing cell volumes, an increase in thickness was observed. This could be explained by the runners' electrolyte status, which may influence the cellular volume in the retina. With the data available in this study however, such a theory

could not be tested. Multiple other studies have also reported a significant degree of variability of retinal layer thicknesses.[8-11] Several hypotheses have been put forward, such as changes in blood flow, retinal metabolism, standing position, and finally, disease related factors. Although all hypothesis are feasible to some extent, the first is a particularly realistic hypothesis and this was further investigated by a re-analysis of our data. In this study, described in chapter 2.2, we used new software to exclude all retinal blood vessel related segmentation artefacts and compared these data with the classical segmented data. The results showed however that these blood vessel artefacts masked, rather than caused, the observed physiological changes. Thus, as hyperaemia seemed a very unlikely explanation for the observed physiological changes, we explored whether oral hydration may be of importance in this matter. In the prospective study described in chapter 2.3, we investigated whether oral hydration could cause shortterm retinal changes and if so, if they would exceed what could be expected from normal ageing. Firstly, the randomised trial using a 2hour hydration escalation protocol with three consecutive SD-OCT assessments showed that there were no significant differences of retinal layer thicknesses between the three groups at any time-point. Secondly, the 18month follow up study with two SD-OCT assessments revealed significant ageing related changes of the GCL.

Taken together, there is significant short-term variability of retinal layers caused by physiological variation, as well as longitudinal ageing-related changes over time. The physiological variation can however not be explained by diurnal or exercise induced changes in retinal blood flow, or hydration status. The jury is still out on which of the many hypotheses put forward (see above) can explain this reproducible phenomenon. At presence, the practical advice from these studies is that in absence of strenuous physical exercise or dehydration retinal OCT can be reliably used in a routine clinical settings.

Scan quality: OSCAR-IB criteria

Evidently, in order to achieve the previously reported high accuracy and good reproducibility, an OCT scan has to be of sufficient quality. In chapter 3.1, the measurement artefact due to misplacement of the measurement beam was investigated. The results clearly showed that misplacement of the laser resulted in such a large measurement artefact (95%CI ±9µm, maximum size of error 42µm) that it may easily mask recognition of pRNFL loss due to neuroaxonal degeneration in MS. Importantly, the study describes a sign (regional heterogeneity of ONL/OPL reflectivity) by which retrospective identification of the error has become possible. Given the magnitude of the potential measurement artefact, we believe recognition of this artefact is relevant for multicentre studies using OCT. Using this sign will lead to rejection of these scans, preventing the use of incorrect, distorted data.

Before publication of the measurement artefact described in chapter 3.1, a small set of OCT quality control criteria were published by others.[12] Inter–rater agreement based on these (restricted) quality control criteria was not satisfactory. We therefore aimed to revise the consensus quality control criteria, including the sign described in chapter 3.1 and other published measurement artefacts. The development process of the 'OSCAR-IB' criteria is described in chapter 3.2. The set of seven criteria was tested by an international group of neuro(ophthalmo)logists and OCT experts. Using the criteria for evaluating scan quality increased the inter–rater agreement substantially, which is particularly important in a multi-centre setting. Improved agreement regarding the rejection of scans of insufficient quality will also be relevant for the overall success in detecting small degrees of neurodegeneration which may otherwise be masked by measurement noise. An important secondary advantage of the OSCAR-IB criteria is the increased awareness of pitfalls of the OCT operator. After an OCT scan is performed, measurement artefacts can be recognised, but most often can not be corrected retrospectively. Having knowledge of the potential pitfalls in advance, will lead to overall higher quality scans, as some artefacts (S, C, I, B) can be prevented at the moment of scanning.

The OSCAR-IB criteria were developed and validated in a large and heterogeneous cohort. In order to extend the use of these criteria, an external validation was needed. In chapter 3.3, we aimed to test the practicability and reliability of the OSCAR-IB criteria in a worldwide multi-centre setting. Twenty independent raters from thirteen international OCT expert centres participated in the study. The results showed that the OSCAR-IB criteria proved to work even better than in the pilot study (chapter 3.2). A substantial level of agreement was reached (inter-centre kappa of 0.7). In order to investigate the agreement between centres, a training- and test-set of OCT scans were composed. The trainingset was designed to ensure the researcher/OCT operator gets familiar with the use of the OSCAR-IB criteria. The test-set is used to perform an examination, in order to test whether the application of the criteria is used correctly. OCT experts participating in this study agreed that making these sets of scans with more broadly available would be helpful in order to increase quality of OCT scans in future clinical OCT trials. We have therefore made the training- and test-set of this manuscript available online (www.oscar-ib.org). This way, MS researchers, OCT operators and researchers at international OCT reading centres can get familiar with the OSCAR-IB criteria (trainingset), and perform an examination (testset) in order to obtain a OCT quality assessment certification.

To sum up, we believe that use of these validated quality control criteria is of major importance. Using the criteria will enhance reliability of the method, especially when used longitudinally and in multi-centre settings. Additionally, overall scan quality will increase due to awareness of pitfalls, reducing the amount of rejected scans.

CLINICAL CONSIDERATIONS: OCT IN LONGSTANDING MS

Retinal layer thickness and clinical disability

A consistent finding in patients with MS is thinning of the retina as assessed by OCT. Data on retinal layer thickness provides valuable information on the visual system in patients with MS. There are however good arguments that atrophy of certain retinal layers also reflects more global neuroaxonal degeneration of the CNS. Therefore, besides the relationships between visual function and OCT measures,[13] many studies have investigated the structure-function relationship between retinal layer thickness and clinical disability in MS. Although not part of this thesis, we also have investigated the relationship between retinal layer thickness and the expanded disability status scale (EDSS) score. Our findings showed that atrophy of the innermost retinal layers (pRNFL and GCC) was significantly and negatively associated with EDSS score, but only in eyes of MS patients without a history of ON. Consistent with our findings, many studies reported a significant negative correlation between pRNFL thickness and EDSS.[14-23] Yet, some studies did not confirm this finding in patients with progressive MS.[24,25] More recent reports including multiple retinal layers, reported significant inverse correlations between the mean pRNFL and macular thickness with EDSS, while the OPL thickness showed a significant positive correlation with EDSS score.[26] Likewise, Tatrai et al reported inverse correlations between the EDSS and the GCC and mean overall pRNFL.[27]

Overall, there is a clear structure-function association between clinical disability and retinal layer thickness in MS, suggesting that atrophy of especially the innermost retinal layers is indeed a reflection of global neuroaxonal degeneration of the CNS.

Retinal layer thicknesses and disease heterogeneity

The disease course in MS is very heterogeneous and mechanisms of pathology may differ between these types. We therefore investigated in chapter 4.1, the relationship between disease course heterogeneity, including benign MS, and retinal layer thicknesses in longstanding MS. This study demonstrated that retinal layer thicknesses, particularly of the innermost retinal layers (pRNFL, GCC), were significantly related to the heterogeneous disease course in MS, but only in MSNON eyes. We observed most severe atrophy of the innermost retinal layers in patients with SPMS. In PP and benign MS a relative preservation of these layers was observed, suggesting rather limited susceptibility to cerebral neuroaxonal degeneration in these disease types. This finding may be of relevance in future trials, using OCT as an outcome measure for neuroaxonal degeneration. The results of other previous studies exploring pRNFL thickness in different disease types were somewhat inconsistent. No differences in pRNFL thickness

were found between patients with PPMS and relapsing onset MS by some groups,[19,24,28,29] while others described significantly lower pRNFL thickness in progressive disease stages, compared with patients with RRMS or CIS.[30-32] The inconsistency of these results may be caused by the small sample sizes, especially of the progressive subgroups.
More recent studies comparing disease types using multiple retinal layers reported the most severe atrophy of the innermost layers in SPMS, followed by RRMS and PPMS,[33,34] although this trend was not reported by Albrecht et al, who reported that all MS subtypes had significant thinning of the pRNFL and the GCL and IPL.[26]
Besides the typical disease courses, 10 to 20% of all patient experience a relative mild clinical disease course, called benign MS (BMS). In our study, we observed significantly more thinning of the macular GCC and the pRNFL and pINL in typical MS, compared with BMS. Nevertheless, patients with BMS still revealed considerably more retinal atrophy than HC eyes. Finally, although retinal layer thickness of patients with BMS clearly differs from patients with typical MS, the data also revealed that OCT data should not be used solely to distinguish between a benign and a typical disease course.

Importance of (sub-)clinical episodes of optic neuritis

Clearly, the anterior visual pathway is a frequent target of the MS disease process. Some studies have shown with postmortem analysis, that almost all patients with MS are expected to have typical changes in the retinal structures and optic nerve. Importantly, this was observed in eyes with and without a history of MSON.[35] In eyes with a known history of MSON, a certain degree of axonal degeneration is expected.[24] A recent meta-analysis confirmed this finding, but the authors also reported considerable thinning of the pRNFL in eyes of MS patients without a history of MSON.[36] Petzold et al investigated the pRNFL thickness of patients with MSON, patients with MSNON and healthy controls. They reported a mean decrease of 20.38 µm (95% CI –22.86 to –17.91 µm) in MSON eyes, compared with HC eyes. Importantly, also in MSNON eyes a significant thinning of the pRNFL compared with HC (-7.08 µm, 95% CI –8.65 to –5.52) was observed. To illustrate this, figure 1 shows the peripapillary ring scans (1A) and the macular volume scans (1B) of both eyes of a female patient with RRMS, who experienced an episode of ON in OD multiple years before scanning. The pRNFL (1A) as well as the macular GCC (1B) show substantial thinning in the affected eye (OD), compared with the unaffected eye (OS).
In chapter 4.1, clear differences between MS disease types were observed in MSNON eyes, but not in MSON eyes. This lack of difference in MSON eyes is probably due to the large impact of the experienced episode of ON on the retinal layers. The damage caused by the inflammatory lesion in the optic nerve will most probably have superseded the more subtle effects of the disease subtype.

These reports, together with the findings from chapter 4.1 have important implications for the use of OCT as an outcome marker for neurodegeneration in MS trials or patient management. Especially when used cross-sectionally, it is of major importance to take into account the history of ON, as an episode of ON will mask the more subtle changes caused by global neuroaxonal degeneration. Consequently, sub-clinical atrophy of the retinal layers in MSNON eyes are probably a better reflection of global CNS damage than the retinal layers in severely damaged MSON eyes.

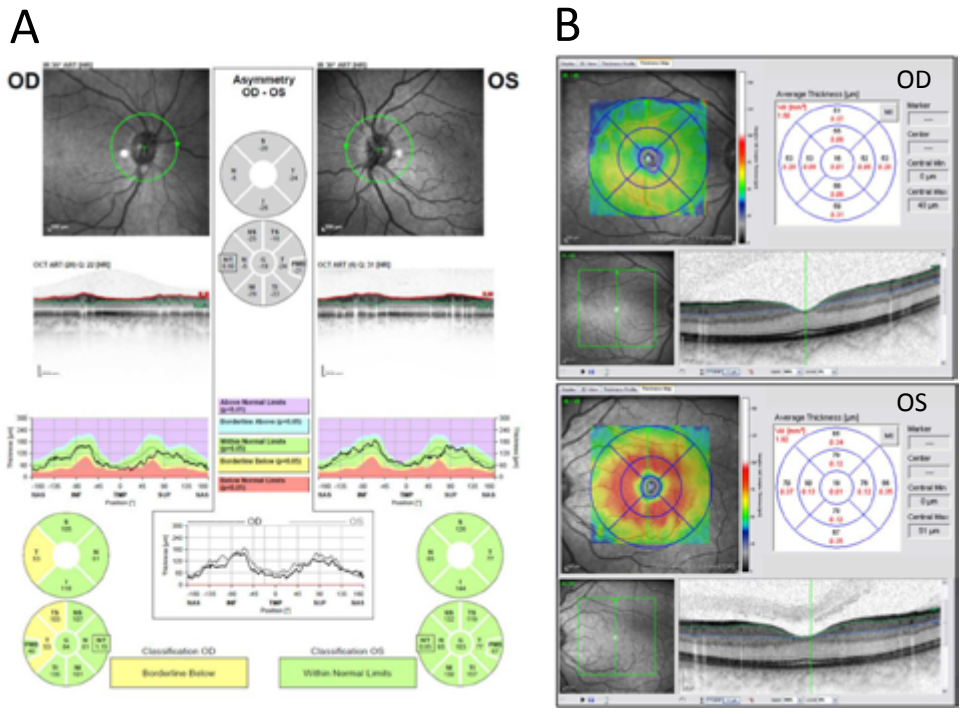

Figure 1. (A) Peripapillary ring scans (both eyes) of a female RRMS patient with a history of ON in OD, but not in OS. The global mean pRNFL thickness is clearly less in in the affected eye (OD, 84 µm) compared to the unaffected eye (OS, 103 µm). **(B)** Macular volume scan (both eyes, OD upper section, OS lower section) of a female RRMS patient with a history of ON in OD, but not in OS. The coloured thickness maps, together with the 1, 3, and 6 mm grids, show the thickness (µm) of the ganglion cell complex (GCC) for every retinal sector. The affected eye (OD) shows severe thinning of the GCC compared to the unaffected eye (OS).

Trans-synaptic axonal degeneration

Since the availability of newer segmentation software, it is possible to identify more individual retinal layers besides the pRNFL and TMV. Accordingly, new possibilities came up to investigate layer specific atrophy. Multiple studies have investigated this, and a consistent finding was the clear presence of atrophy of especially the innermost layers, the pRNFL and the macular GCL or GCC, in both eyes with and without history

of ON.[26,27,34,37] Data is however contradictory for the outermost layers which lie beyond the GCL, in particular the INL. In human retinal post-mortem samples, atrophy of the INL was demonstrated after about 20 years of disease duration.[38] Of the *in vivo* studies using OCT, only Saidha et al reported thinning of the INL and outer plexiform layer (OPL) in a subgroup of MSNON eyes and suggested this thinning was the results of a primary retinal process.[39] In contrast, several other studies reported preservation of the INL.[26,40,41]

Nevertheless, apart from the inconsistency regarding the retinal layers beyond the INL, multiple studies have shown that the innermost retinal layers are severely damaged in MSON eyes, but also, to a lesser extent, in MSNON eyes. In case of MSON eyes, it appears that the inflammatory lesion in the optic nerve causes chronic demyelination, eventually leading to axonal damage. This damage is then represented in the thickness of the pRNFL due to retrograde degeneration. The question is however, how it is possible that even MSNON eyes show, although less evident than in MSON eyes, significant thinning of the pRNFL and other inner retinal layers. Previous results from patients with a stroke suggest this thinning may be caused by retrograde *trans-synaptic* degeneration.[42,43]

The first experimental evidence for trans-synaptic axonal degeneration was first published by van Buren et al in 1963.[44] It is now understood that trans-synaptic axonal degeneration can occur following any damage to the CNS, and has therefore been suggested as a possible mechanisms of spreading of neuroaxonal degeneration in MS.[36,43] There is early experimental data showing thinning of the retinal layers following optic nerve axotomy.[45] Acquired transsynaptic retrograde axonal degeneration however, has only recently been demonstrated in humans in vivo.[42,43]

This hypothesis of trans-synaptic degeneration as a mechanism by which neurodegeneration spreads to the CNS in MS, is strengthened by the consistent findings reported in chapter 4.2 and other studies investigating the retinal layer atrophy in MS. All studies reported clear atrophy of the inner retinal layers (pRNFL, GCL), but a relative preservation of the more outer layers (OPL, ONL, ORLs) in MSNON eyes.[26,37,40] Chapter 4.2 reports extensive damage of the inner retinal layers, but almost no atrophy could be shown beyond the INL after an average disease duration of 20 years. This finding suggests that global damage in the CNS spreads towards the retina by retrograde trans-synaptic degeneration and that there may be a physiological barrier capable of halting this mechanism (the retinal INL). The rationale for such a physiological barrier might be that otherwise any form of trans-synaptic degeneration, if not stopped, could potentially spread through the human CNS, destroying all nerve cells eventually.

Chapter 4.2 describes the presence of retrograde trans-synaptic axonal degeneration, leading to retinal atrophy of the innermost layers. There is however also good evidence for this mechanism in the other direction; anterograde trans-synaptic

axonal degeneration. Interestingly, patients with a history of bilateral ON showed distinct, localised atrophy of the visual cortex, to a much larger extend than patients without any history of ON. This suggests that damage within the visual system causes not only retrograde (towards the retina), but also anterograde trans-synaptic axonal degeneration, leading to atrophy of at least V1 in the visual cortex.

Bi-directional trans-synaptic degeneration in the visual pathway

In order to further investigate the presence of bi-directional trans-synaptic degeneration, the visual system is a suitable model. In chapter 4.3 we have therefore explored the structure-structure relationship between damage to the posterior and anterior visual pathway, in order to explore the co-existence of antero- and retrograde trans-synaptic axonal degeneration in longstanding multiple sclerosis (MS). Besides, this study also investigated how damage of the visual system is associated with damage to the rest of the brain. Interestingly, this study provided evidence for the presence of both retrograde and anterograde transsynaptic axonal degeneration in the visual pathway of patients with MS. Additionally, it was demonstrated that thinning of the retinal pRNFL and GCC did not only reflect visual pathway damage, but was also related to global white and grey matter atrophy.

Regarding the visual pathway, the present findings are consistent with previous studies. Others have found that in patients with optic neuritis, the integrity of the optic radiations,[46-48] but also the visual cortex[49,50] revealed damage after episodes of ON. The present study extends on these studies however, by investigating individual retinal layers, the complete visual pathway *and* the global brain. Although no previous studies have explored these structures together, some studies have investigated the structurestructure relationship between retinal layer thickness and white and grey matter atrophy. Results were however inconsistent. In several studies, significant associations were found between pRNFL thickness and brain parenchymal fraction.[16,20,22,51] Associations with brain volume however, including multiple substructures, are still not entirely clear.[16,18,20,22,52] Two more recent studies using data on multiple segmented retinal layers showed the potential of this new segmented OCT as a measure for neuroaxonal degeneration, as they reported that retinal measures seem to reflect global central nervous system pathology in MS, with distinct retinal layers each associated with distinct CNS processes.[53] Additionally, Zimmermann et al described the pRNFL and GCL as parameters of neuroaxonal damage and were both linked to whole brain as well as white and grey matter atrophy.[54]

These data, together with the data from our study, suggest that trans-synaptic degeneration may not be restricted to the visual pathway and may disseminate through the whole brain. However, we believe that trans-synaptic degeneration is not solely

responsible for the observed relationships between retinal layer thickness and global brain atrophy. If it would be, a devastating 'domino-effect' would ensue affecting the entire brain. Therefore, the observed damage to the global brain might be more likely caused by a global mechanism affecting the entire brain, including the visual system.
Taken together, the thickness of the pRNFL and GCC reflect damage of multiple components of the visual pathway, suggesting co-existence of bi-directional (trans-synaptic) degeneration. Additionally, retinal layer thickness also reflects global white and grey matter atrophy. If bi-directional trans-synaptic degeneration is responsible for the latter, or a more global mechanism, remains to be elucidated.

MMO: a new MS phenotype, or a non-specific finding?

Recently, a potentially new sign in MS was described by Gelfland et al.[55] This new sign, microcystic macular oedema (MMO[a]), is characterised by the presence of cystic areas of hyporeflectivity in the INL of the retina, visible on the OCT scan (Figure 2). These microcysts are associated with increased INL thickness, are more common in MSON eyes than in MSNON eyes and are considered to indicate breakdown of the blood-retinal barrier.[55,56] The presence of MMO, and as a logical consequence also increased INL thickness, have shown to be associated with increased disability,[55,56] and some have even suggested MMO should be considered as a new MS phenotype.[56]

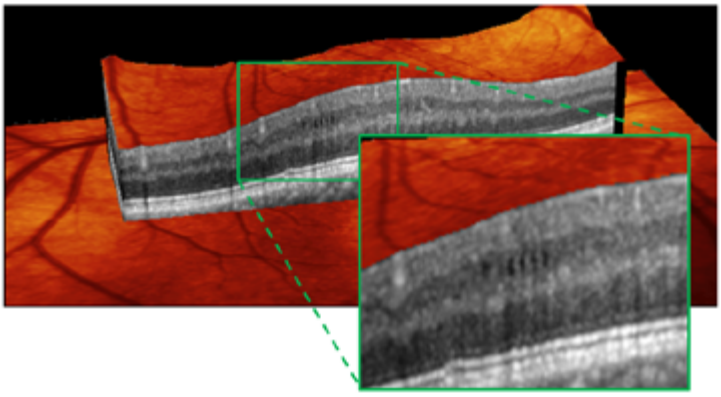

Figure 2. Microcystic macular oedema (MMO) in the left eye of an untreated male patient with RRMS. He had experienced an episode of ON in the affected eye 17 years ago. The MMO is characterised by several clear cystic areas of hyporeflectivity in the inner nuclear layer.

[a] Ironically, the American group who discovered this new sign published their first two papers in British Journals for which reason the most frequently used acronym has become MMO (from oedema) as opposed to MME (from edema). This linguistic prelude aside, MMO is a misnomer and the term "microcystic macular changes" has been suggested as an alternative [Kisimbi BRAIN 2013, Abegg BRAIN 2012].

Whereas the presence of MMO has shown to be related to disability in MS, it is important to note that it is not specific for MS. After evaluation of our own cohort of patients with longstanding MS (N=230), we found that the prevalence of MMO in longstanding MS (0.8%) was substantially lower than reported by others at an earlier disease phase.[57] More importantly however, we also reported a case of MMO in a patient with relapsing isolated optic neuritis, which indicates that MMO, although present in MS, is not specific for MS. This lack of specificity is further confirmed in a VUmc study by Burggraaff et al, where, besides refining and validating the diagnostic criteria for MMO, the clinical spectrum of MMO is discussed.[58] Burggraaff et al reported that the clinical spectrum of MMO is much broader than previously expected and that MMO was also present in age-related macular degeneration, epiretinal membranes, postoperative lesions, diabetic retinopathy, vascular occlusion, optic neuropathy, central serous chorioretinopathy, medication (interestingly not fingolimod) and miscellaneous causes.

Clearly, MMO is present in a broad range of diseases, but the aetiology remains unclear. The localisation of MMO is almost exclusively within the poorly vascularised INL of the perimacular rim, suggesting Müller cell pathology to be part of the cause of MMO, as Müller cells transverse through the entire retina with the bulk of their cell bodies in the INL. Moreover, the Müller cells are involved in maintaining the water homeostasis of the retina, possibly leading to formation of microcysts when dysfunctional. Experimental and clinical data however strongly suggest that MMO may be a result of neurodegeneration, through retrograde trans-synaptic degeneration.[59,60] If so, this would also explain the association between MMO and clinical disability and radiological disease activity.

Returning to the title of this paragraph, the presence of MMO has some predictive value in MS, but the precise cause and its clinical significance remain to be elucidated. We believe that one should be careful with considering MMO a new MS phenotype as MMO is clearly present in many other diseases besides MS, and clinical implications are still unknown. Longitudinal follow-up of patients with MMO may unravel the aetiology and clinical importance of this new clinical sign.

CONCLUSIONS

Chapters 2 and 3 of this thesis investigated the methodological issues of the SD-OCT technique, while Chapter 4 focused on the clinical application of OCT in patients with longstanding MS.

The main conclusions of this thesis are:

- Retinal OCT is a reliable and accurate tool to quantify the thickness of individual retinal layers, but there is significant short-term variability of retinal layers caused by physiological variation.
- The use of quality control criteria increases scan quality and consequently enhances the reliability of the method, especially for longitudinal studies and in multi-centre settings.
- Only the innermost retinal layer thicknesses are associated with clinical disability and were associated with visual pathway and global brain damage, expectedly as a result of retrograde and anterograde transsynaptic degeneration.
- The INL of the retina appears to act like a physiological barrier to retrograde transsynaptic degeneration.
- The interpretation of OCT data in MS is critically dependent on knowledge of prior episode(s) of optic neuritis, because any subtle changes will be masked by the severe atrophy caused by the inflammatory lesion in the optic nerve.
- Microcystic macular oedema (MMO) in MS is more frequent in MS patients with a history of optic neuritis and is related to disability. MMO is however not specific for MS and the aetiology remains unknown.
- There is a need for future longitudinal studies to further substantiate the functional and structural relationships suggested by the published, mainly cross-sectional data.

FUTURE PERSPECTIVE

In the past decade, retinal OCT has matured into a reliable and sensitive tool for assessing neuroaxonal degeneration in patients with MS and data on the subject is still rapidly accumulating. Especially with the development of new segmentation software, allowing segmentation of individual retinal layers, OCT is a promising tool for quantifying neuroaxonal degeneration in MS.

Currently, OCT is used in observational studies and clinical trials in MS. The most important future applications for OCT lie in monitoring disease progression over time in a clinical setting and assessing the degree of neuroaxonal degeneration in clinical trial settings. For the first, OCT can be of great value in monitoring subtle changes in neuroaxonal damage in patients with MS. The degree of neuroaxonal damage is not always in accordance with clinical outcomes, making a precise assessment tool more important. This assessment gives an objective impression of damage to the CNS, which can be of important predictive value regarding clinical disability in the future.

The fact that OCT can assess retinal layer thickness with a very high accuracy and reliability, is not painful or upsetting for the patient and is relatively quick, makes OCT a particularly useful tool to assess neuroaxonal degeneration in a clinical trial setting. In the coming years, many clinical trials with new neuro-protective, or even neuro-restorative agents will be performed. In these trials, QC controlled retinal OCT will enable the accurate and longitudinal assessment of the potential neuro-protective or neuro-restorative effect of these agents.

Future studies should focus on the collection of longitudinal OCT data. Whereas cross-sectional data on OCT has given important insights in structural differences between patients with MS and healthy controls and its relationship with clinical disability and brain pathology, longitudinal data is absolutely essential to explain the mechanisms underlying these relationships. Currently available longitudinal data is performed with the methodologically limited time-domain OCT and these data are not sufficient for demonstrating longitudinal associations between OCT and clinical disability. Therefore, longitudinal data with the more reliable SD-OCT, important because of the well recognised inter-eye and inter-subject differences, will help to investigate the predictive value of OCT on disease progression. Particularly the use of newer segmentation software enabling identification of the individual retinal layers, is a promising development and should be further investigated in larger and preferably longitudinal studies.

Besides the development of new software for SD-OCT machines, several improvements in OCT technology are being investigated. One of the promising new technologies is polarization-sensitive OCT (PS-OCT). PSOCT does not only detect the intensity, but also the polarization state of backscattered light from the retina. By detecting the birefringence and depolarisation of the different tissues, particularly highly structured ones, such as axons which are packed with a 9nm neuro-filament network, PSOCT yields depthresolved information of the order of these structures. Therefore, PS-OCT may be a promising tool to investigate axonal pathology early, prior to ensuing atrophy.

In summary, since the application of OCT in MS two decades ago, new data and insights regarding the usefulness of OCT in the management of MS have accumulated. The technology evolves and improves quickly and the acquired insights, with high quality longitudinal data being available in the near future, will likely open a window for the investigation and unravelling of the mechanisms underlying neuroaxonal degeneration and related disability in patient suffering from MS.

REFERENCES

1. Barkhof F, Calabresi PA, Miller DH, Reingold SC. Imaging outcomes for neuroprotection and repair in multiple sclerosis trials. *Nat Rev Neurol* 2009;5:256-266.
2. Frohman E, Costello F, Zivadinov R et al. Optical coherence tomography in multiple sclerosis. *Lancet Neurol* 2006;5:853-863.
3. Wolf-Schnurrbusch UEK, Ceklic L, Brinkmann CK et al. Macular thickness measurements in healthy eyes using six different optical coherence tomography instruments. *Invest Ophthalmol Vis Sci* 2009;50:34323437.
4. Balk LJ, Petzold A. Influence of the eye-tracking-based follow-up function in retinal nerve fiber layer thickness using fourier-domain optical coherence tomography. *Invest Ophthalmol Vis Sci* 2013;54:3045.
5. Huang JY, Pekmezci M, Yaplee S, Lin S. Intra-examiner repeatability and agreement of corneal pachymetry map measurement by time-domain and Fourier-domain optical coherence tomography. *Graefes Arch Clin Exp Ophthalmol* 2010;248:1647-1656.
6. Serbecic N, Beutelspacher SC, boul-Enein FC, Kircher K, Reitner A, Schmidt-Erfurth U. Reproducibility of high-resolution optical coherence tomography measurements of the nerve fibre layer with the new Heidelberg Spectralis optical coherence tomography. *Br J Ophthalmol* 2011;95:804-810.
7. Oberwahrenbrock T, Traber GL, Gabilondo I et al. Multicenter inter-rater reliability of retinal layer segmentation using spectral-domain OCT. *Submitted.*
8. Jo Y, Heo D, Shin Y, Kim J. Diurnal Variation of Retina Thickness measured with Time Domain and Spectral Domain Optical Coherence Tomography in Normal Subjects. *Invest Ophthalmol Vis Sci* 2011;52:6497-500.
9. Read SA, Collins MJ, onso-Caneiro D. Diurnal variation of retinal thickness with spectral domain OCT. *Optom Vis Sci* 2012;89:611-619.
10. Tan CSH, Ngo WK, Chew MC, Li KZ, Lim LW, Sadda SR. Diurnal variation of retinal thickness measured by optical coherence tomography in normal adults. *Invest Ophthalmol Vis Sci* 2012;53:1639-1640.
11. de Kinkelder R, Kalkman J, Faber DJ et al. Heartbeat-induced axial motion artifacts in optical coherence tomography measurements of the retina. *Invest Ophthalmol Vis Sci* 2011;52:3908-3913.
12. Domalpally A, Danis RP, Zhang B, Myers D, Kruse CN. Quality issues in interpretation of optical coherence tomograms in macular diseases. *Retina* 2009;29:775-781.
13. Sakai RE, Feller DJ, Galetta KM, Galetta SL, Balcer LJ. Vision in multiple sclerosis: the story, structure-function correlations, and models for neuroprotection. *J Neuroophthalmol* 2011;31:362-373.
14. Albrecht P, Frohlich R, Hartung HP, Kieseier BC, Methner A. Optical coherence tomography measures axonal loss in multiple sclerosis independently of optic neuritis. *J Neurol* 2007;254:1595-1596.
15. Fisher JB, Jacobs DA, Markowitz CE et al. Relation of visual function to retinal nerve fiber layer thickness in multiple sclerosis. *Ophthalmology* 2006;113:324-332.
16. Gordon-Lipkin E, Chodkowski B, Reich DS et al. Retinal nerve fiber layer is associated with brain atrophy in multiple sclerosis. *Neurology* 2007;69:1603-1609.
17. Merle H, Olindo S, Donnio A, Richer R, Smadja D, Cabre P. Retinal peripapillary nerve fiber layer thickness in neuromyelitis optica. *Invest Ophthalmol Vis Sci* 2008;49:4412-4417.
18. Sepulcre J, Murie-Fernandez M, Salinas-Alaman A, Garcia-Layana A, Bejarano B, Villoslada P. Diagnostic accuracy of retinal abnormalities in predicting disease activity in MS. *Neurology* 2007;68:1488-1494.
19. Siepman TAM, Bettink-Remeijer MW, Hintzen RQ. Retinal nerve fiber layer thickness in subgroups of multiple sclerosis, measured by optical coherence tomography and scanning laser polarimetry. *J Neurol* 2010;257:1654-1660.
20. Siger M, Dziegielewski K, Jasek L et al. Optical coherence tomography in multiple sclerosis: thickness of the retinal nerve fiber layer as a potential measure of axonal loss and brain atrophy. *J Neurol* 2008;255:1555-1560.
21. Toledo J, Sepulcre J, Salinas-Alaman A et al. Retinal nerve fiber layer atrophy is associated with physical and cognitive disability in multiple sclerosis. *Mult Scler* 2008;14:906-912.
22. Grazioli E, Zivadinov R, Weinstock-Guttman B et al. Retinal nerve fiber layer thickness is associated with brain MRI outcomes in multiple sclerosis. *J Neurol Sci* 2008;268:12-17.

23. Lange AP, Sadjadi R, Saeedi J, Lindley J, Costello F, Traboulsee AL. Time-Domain and Spectral-Domain Optical Coherence Tomography of Retinal Nerve Fiber Layer in MS Patients and Healthy Controls. *J Ophthalmol* 2012;2012:564627.

24. Henderson APD, Trip SA, Schlottmann PG et al. A preliminary longitudinal study of the retinal nerve fiber layer in progressive multiple sclerosis. *J Neurol* 2010;257:1083-1091.

25. Costello F, Hodge W, Pan YI, Eggenberger E, Freedman MS. Using retinal architecture to help characterize multiple sclerosis patients. *Can J Ophthalmol* 2010;45:520-526.

26. Albrecht P, Ringelstein M, Muller AK et al. Degeneration of retinal layers in multiple sclerosis subtypes quantified by optical coherence tomography. *Mult Scler* 2012;18:1422-1429.

27. Tatrai E, Simo M, Iljicsov A, Nemeth J, Debuc DC, Somfai GM. In vivo evaluation of retinal neurodegeneration in patients with multiple sclerosis. *PLoS One* 2012;7:e30922.

28. Henderson APD, Trip SA, Schlottmann PG et al. An investigation of the retinal nerve fibre layer in progressive multiple sclerosis using optical coherence tomography. *Brain* 2008;131:277-287.

29. Gelfand JM, Goodin DS, Boscardin WJ, Nolan R, Cuneo A, Green AJ. Retinal axonal loss begins early in the course of multiple sclerosis and is similar between progressive phenotypes. *PLoS One* 2012;7:e36847.

30. Oberwahrenbrock T, Schippling S, Ringelstein M et al. Retinal damage in multiple sclerosis disease subtypes measured by high-resolution optical coherence tomography. *Mult Scler Int* 2012;2012:530305.

31. Pulicken M, Gordon-Lipkin E, Balcer LJ, Frohman E, Cutter G, Calabresi PA. Optical coherence tomography and disease subtype in multiple sclerosis. *Neurology* 2007;69:2085-2092.

32. Costello F, Hodge W, Pan YI, Freedman M, DeMeulemeester C. Differences in retinal nerve fiber layer atrophy between multiple sclerosis subtypes. *J Neurol Sci* 2009;281:74-79.

33. Ratchford JN, Saidha S, Sotirchos ES et al. Active MS is associated with accelerated retinal ganglion cell/inner plexiform layer thinning. *Neurology* 2013;80:47-54.

34. Saidha S, Syc SB, Durbin MK et al. Visual dysfunction in multiple sclerosis correlates better with optical coherence tomography derived estimates of macular ganglion cell layer thickness than peripapillary retinal nerve fiber layer thickness. *Mult Scler* 2011;17:1449-1463.

35. Galetta KM, Calabresi PA, Frohman EM, Balcer LJ. Optical coherence tomography (OCT): imaging the visual pathway as a model for neurodegeneration. *Neurotherapeutics* 2011;8:117-132.

36. Petzold A, de Boer JF, Schippling S et al. Optical coherence tomography in multiple sclerosis: a systematic review and meta-analysis. *Lancet Neurol* 2010;9:921-932.

37. Balk LJ, Twisk JW, Steenwijk MD et al. A dam for retrograde axonal degeneration in multiple sclerosis? *J Neurol Neurosurg Psychiatry* 2014;85:782-9.

38. Green AJ, McQuaid S, Hauser SL, Allen IV, Lyness R. Ocular pathology in multiple sclerosis: retinal atrophy and inflammation irrespective of disease duration. *Brain* 2010;133:1591-1601.

39. Saidha S, Syc SB, Ibrahim MA et al. Primary retinal pathology in multiple sclerosis as detected by optical coherence tomography. *Brain* 2011;134:518-533.

40. Syc SB, Saidha S, Newsome SD et al. Optical coherence tomography segmentation reveals ganglion cell layer pathology after optic neuritis. *Brain* 2012;135:521-533.

41. Sriram P, Graham SL, Wang C, Yiannikas C, Garrick R, Klistorner A. Transsynaptic retinal degeneration in optic neuropathies: optical coherence tomography study. *Invest Ophthalmol Vis Sci* 2012;53:1271-1275.

42. Jindahra P, Petrie A, Plant GT. The time course of retrograde trans-synaptic degeneration following occipital lobe damage in humans. *Brain* 2012;135:534-541.

43. Jindahra P, Petrie A, Plant GT. Retrograde trans-synaptic retinal ganglion cell loss identified by optical coherence tomography. *Brain* 2009;132:628-634.

44. Van Buren JM. Trans-synaptic retrograde degeneration in the visual system of primates. *J Neurol Neurosurg Psychiatry* 1963;26:402-409.

45. Hollander H, Bisti S, Maffei L, Hebel R. Electroretinographic responses and retrograde changes of retinal morphology after intracranial optic nerve section. A quantitative analysis in the cat. *Exp Brain Res* 1984;55:483-493.

46. Ciccarelli O, Toosy AT, Hickman SJ et al. Optic radiation changes after optic neuritis detected by tractography-based group mapping. *Hum Brain Mapp* 2005;25:308-316.

47. Reich DS, Smith SA, Gordon-Lipkin EM et al. Damage to the optic radiation in multiple sclerosis is associated with retinal injury and visual disability. *Arch Neurol* 2009;66:998-1006.

48. Kolbe S, Bajraszewski C, Chapman C et al. Diffusion tensor imaging of the optic radiations after optic neuritis. *Hum Brain Mapp* 2012;33:2047-2061.

49. Audoin B, Fernando KT, Swanton JK, Thompson AJ, Plant GT, Miller DH. Selective magnetization transfer ratio decrease in the visual cortex following optic neuritis. *Brain* 2006;129:1031-1039.

50. Pfueller CF, Brandt AU, Schubert F et al. Metabolic changes in the visual cortex are linked to retinal nerve fiber layer thinning in multiple sclerosis. *PLoS One* 2011;6:e18019.

51. Dorr J, Wernecke KD, Bock M et al. Association of retinal and macular damage with brain atrophy in multiple sclerosis. *PLoS One* 2011;6:e18132.

52. Young KL, Brandt AU, Petzold A et al. Loss of retinal nerve fibre layer axons indicates white but not grey matter damage in early multiple sclerosis. *Eur J Neurol* 2013;20:803-811.

53. Saidha S, Sotirchos E, Oh J et al. Relationships Between Retinal Axonal and Neuronal Measures and Global Central Nervous System Pathology in Multiple Sclerosis. *Arch Neurol* 2012;1-10.

54. Zimmermann H, Freing A, Kaufhold F et al. Optic neuritis interferes with optical coherence tomography and magnetic resonance imaging correlations. *Mult Scler* 2013;19:443-450.

55. Gelfand JM, Nolan R, Schwartz DM, Graves J, Green AJ. Microcystic macular oedema in multiple sclerosis is associated with disease severity. *Brain* 2012;135:1786-1793.

56. Saidha S, Sotirchos ES, Ibrahim MA et al. Microcystic macular oedema, thickness of the inner nuclear layer of the retina, and disease characteristics in multiple sclerosis: a retrospective study. *Lancet Neurol* 2012;11:963-972.

57. Balk L, Killestein J, Polman C, Uitdehaag B, Petzold A. Microcystic macular oedema confirmed, but not specific for multiple sclerosis. *Brain* 2012;135:e226

58. Burggraaff MC, Trieu J, de Vries-Knoppert WA, Balk L, Petzold A. The clinical spectrum of microcystic macular oedema. *Invest Ophthalmol Vis Sci* 2014;55:952-61.

59. Abegg M, Dysli M, Wolf S, Kowal J, Dufour P, Zinkernagel M. Microcystic macular edema: retrograde maculopathy caused by optic neuropathy. *Ophthalmology* 2014;121:142-149.

60. Petzold A. Microcystic macular oedema in MS: T2 lesion or black hole? *Lancet Neurol* 2012;11:933-934.

Appendix

NEDERLANDSE SAMENVATTING

HET OOG ALS WEERSPIEGELING VAN HET BREIN
Optische coherentie tomografie in MS

Meer dan een eeuw geleden schreef een van de eerste neurologen die gebruik maakte van de oogspiegel, John Hughlings Jackson (Londen, UK, 1835-1911), het volgende: 'Het is niet teveel gezegd dat zonder uitgebreide kennis van het oog, het onderzoeken van ziektes van het zenuwstelsel niet alleen zeer lastig is, maar zelfs onmogelijk'.
Het oog, met meer dan een miljoen zenuwcellen, kan worden gezien als een 'weerspiegeling van het brein'. In dit proefschrift wordt beschreven op welke manier retinale optische coherentie tomografie (OCT) kan bijdragen aan het inzichtelijk maken van mechanismen die ten grondslag liggen aan de beschadiging van zenuwcellen bij de ziekte multiple sclerose.

ACHTERGROND

Multiple sclerose (MS) is een chronische ziekte van het centraal zenuwstelsel (de hersenen en het ruggenmerg), waarbij sprake is van schade aan de myeline schede (de isolerende laag om de zenuwceluitlopers) en de zenuwcellen zelf. Deze beschadigingen veroorzaken verstoringen in de signalen die deze zenuwcellen aan elkaar doorgeven, met zeer uiteenlopende verschijnselen als gevolg. Afhankelijk van de locatie van de schade kan de patiënt last krijgen van bijvoorbeeld krachtsverlies, gevoelsstoornissen, problemen met zien, blaasproblemen, maar ook problemen met het geheugen, concentratie en vermoeidheid. In Nederland heeft ongeveer 1 op de 1000 mensen MS. Het komt ongeveer 2 keer zo vaak voor bij vrouwen dan bij mannen en de eerste symptomen treden vaak op rond het 30^{e} levensjaar.
Het verloop van de ziekte varieert sterk per patiënt. In ongeveer 80% van de gevallen begint de ziekte met een episode van neurologische klachten (een relaps of schub), die meestal deels of volledig herstelt. Bij het merendeel van deze patiënten wordt deze eerste episode gevolgd door meerdere episodes. Deze vorm van MS heet 'relapsing remitting' MS (RRMS). Met de tijd zal ongeveer 50% van deze RRMS patiënten de secundaire progressieve fase (SPMS) ingaan, waarbij de episodes minder duidelijk aanwezig zijn en plaats maken voor een meer geleidelijke progressieve achteruitgang. Ongeveer 10-15% van de patiënten ervaart geen episodes in het begin van de ziekte, maar laten direct een progressieve achteruitgang zien (primair progressieve MS,

PPMS). In 10-20% van alle gevallen heeft de ziekte een relatief goedaardig beloop. Bij deze benigne vorm van MS, ervaren patiënten gedurende een lange tijd weinig fysieke klachten en blijven veelal mobiel.
Hoewel het gehele centrale zenuwstelsel is betrokken, is vooral het visuele systeem vaak aangetast bij MS. Ongeveer 20% van alle patiënten hebben oogproblemen als eerste klacht, terwijl uiteindelijk zelfs 50 tot 70% van de patiënten gedurende de ziekte een oogzenuwontsteking krijgt. Een oogzenuwontsteking veroorzaakt pijn aan een of beide ogen en het zicht is vaak slecht of zelfs helemaal weg. In de meeste gevallen begint het herstel binnen 3 tot 5 weken na de eerste klacht en is na enkele maanden het zicht volledig hersteld.

De ziekte MS kenmerkt zich door de aanwezigheid van ontstekingen in het centraal zenuwstelsel en de daarbij behorende schade aan de zenuwcellen (neurodegeneratie). Ondanks dat beide processen zelfs in het begin van het ziekteproces al duidelijk aanwezig zijn, is de precieze interactie tussen de ontstekingen en de schade nog niet duidelijk. Wel is duidelijk dat de schade aan de zenuwcellen (neuronen) en de uitlopers daarvan (axonen) onomkeerbare fysieke en cognitieve achteruitgang tot gevolg heeft. Het kunnen meten van deze schade is dus van groot belang om inzicht te krijgen in het onderliggende proces van de ziekte en daarnaast om het ziekteverloop van de patiënt in kaart te brengen en mogelijk zelfs te kunnen voorspellen.
Het meten van schade aan de zenuwcellen is lastig en wordt tot nu toe meestal gedaan met behulp van MRI. Het krijgen van een MRI is voor de meeste mensen niet prettig, en het meten van subtiele veranderingen in volume van het gehele brein met behulp van MRI scans is ook niet altijd even precies en betrouwbaar. Een relatief nieuwe techniek om schade aan de zenuwcellen te kunnen meten is optische coherentie tomografie (OCT). Met behulp van OCT kan men een scan maken van het netvlies van het oog, waarbij de dikte en de structuur van de verschillende lagen in kaart kunnen worden gebracht. Het grote voordeel van OCT is dat deze techniek op een niet-invasieve (dus niet pijnlijk) en snelle manier een uniek deel van het centraal zenuwstelsel (met zowel neuronen als axonen zonder myeline) kan weergeven.

DOEL VAN DIT PROEFSCHRIFT

Het doel van dit proefschrift is om met behulp van OCT, meer inzicht te krijgen in mechanismen die ten grondslag liggen aan de beschadiging van zenuwcellen bij de ziekte MS. Neurodegeneratie is een complex proces, met onomkeerbare invaliditeit bij de patiënt als gevolg. Het monitoren van dit proces is daarom belangrijk. Omdat

OCT pas sinds een aantal jaar wordt toegepast in de neurologie, beschrijven we in het eerste deel van dit proefschrift (hoofdstukken 2 en 3) de betrouwbaarheid van deze OCT techniek en de kwaliteitseisen waaraan een OCT scan moet voldoen. Het tweede deel van dit proefschrift (hoofdstuk 4) is gericht op de klinische toepassing en de bruikbaarheid van OCT bij patiënten met MS.

RESULTATEN

Betrouwbaarheid van de techniek

In *hoofdstuk 2* hebben we onderzocht of fysiologische veranderingen van invloed zijn op de resultaten van de OCT scans bij gezonde controles. In *hoofdstuk 2.1* zijn bij twee groepen gezonde controles meerdere OCT scans gemaakt. De deelnemers van de interventiegroep deden mee aan een 10 km. hardloopwedstrijd, terwijl de deelnemers van de controle groep geen fysieke inspanning leverden. Uit de resultaten van deze studie bleek dat de personen die intensieve inspanning hadden geleverd, een significante toename van de dikte van het netvlies lieten zien, terwijl in de controle personen geen verschil te zien was. Omdat bij een OCT scan ook de bloedvaten van het netvlies meegenomen worden in de meting, hebben we in *hoofdstuk 2.2* onderzocht of dit verschil tussen deelnemers die wel en geen fysieke inspanning hadden geleverd, wellicht te verklaren was door veranderingen van bloedtoevoer in het netvlies. Met behulp van nieuwe software konden we de invloed van de bloedvaten op een OCT scan minimaliseren. Hieruit bleek echter dat de verschillen bleven bestaan en dat veranderingen in bloedtoevoer in het netvlies het verschil tussen de twee groepen dus niet konden verklaren. In *hoofdstuk 2.3* hebben we daarom vervolgens onderzocht of (de-)hydratie korte-termijn veranderingen op de OCT scan teweeg kon brengen. Uit de resultaten van deze kleinschalige trial bleek dat het innemen/drinken van veel water vlak voor de scan geen verschil maakte voor de uitkomst van de scan. Kortom, het hoofdstuk laat zien dat er wel degelijk sprake is van korte-termijn veranderingen in het netvlies die worden veroorzaakt door fysiologische variatie. Deze veranderingen waren groter dan de meetfout van de machine (en daarom dus relevant), maar konden niet worden verklaard door veranderingen in bloedtoevoer van het netvlies, of door (de-) hydratie status. Wat deze variatie wel kan verklaren is nog niet duidelijk en wordt nog onderzocht.

In *hoofdstuk 3* van dit proefschrift hebben we een set kwaliteitscriteria beschreven; de 'OSCAR-IB criteria'. De OSCAR-IB criteria (waarbij elke letter voor een criterium staat) bestaan uit 7 criteria waaraan een OCT scan moet voldoen om van voldoende kwaliteit, en daarmee betrouwbaarheid, te zijn. In *hoofdstuk 3.1* is een van de 7 kwaliteitscriteria,

de juiste plaatsing van de laser, uitgebreid beschreven. In deze studie hebben we laten zien dat als niet aan dit criterium wordt voldaan, de meetfouten in de meest extreme gevallen kan oplopen tot wel 42 µm (bij een gemiddelde dikte van 100 µm). Het besef dat een dergelijke meetfout kan worden veroorzaakt door een relatief simpel te voorkomen fout, heeft mede geleid tot de ontwikkeling van de OSCAR-IB criteria. *In hoofdstuk 3.2 en 3.3* worden vervolgens het ontwikkelingsproces en de externe validatie van de OSCAR-IB criteria beschreven. Uit de resultaten van deze hoofdstukken bleek dat gebruik van deze criteria de gemiddelde kwaliteit van de scans, en daarmee de betrouwbaarheid, sterk verbetert. Met name bij herhaalde metingen en studies met meerdere deelnemende centra is dit erg belangrijk omdat het de precisie verhoogt en meetfouten kunnen worden voorkomen.

Toepassing van OCT bij patiënten met MS

Tot slot, in *hoofdstuk 4* zijn verschillende relaties tussen OCT metingen, klinische maten en MRI maten beschreven. Hoewel het niet direct onderdeel uitmaakt van dit proefschrift, hebben wij (en meerdere onderzoekers over de hele wereld) laten zien dat er een duidelijke relatie bestaat tussen het fysiek functioneren van patiënten met MS en de dikte van de lagen van het netvlies. Hoe dunner deze lagen waren, hoe slechter de patiënt functioneerde. Dit suggereert dat het dunner worden van deze lagen van het netvlies een reflectie is van meer globale neurodegeneratie in het gehele centrale zenuwstelsel.

In *hoofdstuk 4.1* hebben we vervolgens gekeken in hoeverre schade aan de zenuwcellen in het netvlies verschillen tussen de diverse ziektetypes.

De dikte van met name de binnenste lagen van het netvlies hing sterk samen met het verloop van de ziekte. Patiënten met SPMS, die al langere tijd in de progressieve fase zitten, lieten de meeste schade zien, gevolgd door RRMS en PPMS. Patiënten met een goedaardig verloop (benigne MS) lieten de minste schade zien. Belangrijk in deze studie was het duidelijke effect van een oogzenuwontsteking. De ogen van patiënten die dit ooit hadden gehad lieten duidelijk meer schade zien dan de ogen van patiënten die dit niet hadden gehad. Voor een juiste interpretatie van OCT data moet men dus rekening houden met eventuele doorgemaakte oogzenuwontstekingen in het verleden.

In *hoofdstuk 4.2* is het effect van een oogzenuwontsteking op de verschillende lagen van de retina in detail onderzocht. Een van de belangrijkste bevindingen van dit hoofdstuk was dat een oogzenuwontsteking niet alleen de desbetreffende axonen beschadigt, maar ook aangrenzende zenuwcellen in het netvlies (ganglion cellen). Een beschadigde zenuwcel kan dus zijn 'buurman' daardoor ook beschadigen. Daarnaast bleek dat ook in de ogen van patiënten die nooit een oogzenuwontsteking hadden gehad, duidelijke schade te zien was aan de uitlopers van de oogzenuw én aangrenzende zenuwcellen. Dit suggereert dat ook schade verderop in het brein zich 'verspreid' en op deze manier

'buurcellen' kan beschadigen. Deze manier van verspreiding van schade aan de zenuwcellen als gevolg van lokale ontsteking/schade, noemen we 'trans-synaptische degeneratie'.
Hoofdstuk 4.2 liet verder zien dat met name de dikte van de *binnenste lagen* van het netvlies schade laten zien. Dit komt mogelijk doordat de 'inner nucleaire laag' (INL), gelegen in het midden van het netvlies, bepaalde eigenschappen bezit waardoor hij deze trans-synaptische degeneratie kan stoppen. Lagen die achter de INL liggen, laten namelijk amper schade of veranderingen zien.
In *hoofdstuk 4.3* hebben we de aandacht gericht op deze trans-synaptische degeneratie om te zien of deze alleen van de oogzenuw richting het netvlies gaat, of ook andersom (vanaf de oogzenuw richting de hersenen). Uit deze studie, waarbij OCT en MRI data werden gecombineerd, bleek dat trans-synaptische degeneratie *beide* kanten op gaat en waarschijnlijk een belangrijk onderliggend mechanisme is voor het ontstaan van schade aan zenuwcellen bij patiënten met MS.

CONCLUSIE

Sinds de toepassing van OCT in het MS onderzoek is er veel onderzoek gedaan naar de bruikbaarheid van deze techniek. De resultaten van dit proefschrift laten zien dat het een zeer gebruiksvriendelijke en betrouwbare techniek betreft, die met hoge precisie schade aan de zenuwcellen in het netvlies kan meten. De beschreven studies in hoofdstuk 4 hebben een belangrijke bijdrage geleverd aan het inzicht in de mogelijke mechanismen (waaronder trans-synaptische degeneratie) die verantwoordelijk worden gehouden voor de schade aan de zenuwcellen bij patiënten met MS. Daarnaast is OCT een belangrijke techniek waarmee men de ziekteprogressie van individuele patiënten kan monitoren. In de nabije toekomst zal longitudinale data beschikbaar komen, waardoor we de voorspellende waarde van deze metingen nog beter kunnen onderzoeken. Tot slot zal OCT naar verwachting een belangrijke rol gaan spelen bij nieuwe medicijn studies, waarbij met behulp van OCT de neuro-protectieve effecten van nieuwe medicatie gemeten kan worden.

LIST OF PUBLICATIONS

Tewarie P, Steenwijk MD, Tijms BM, Daams M, Balk LJ, Stam CJ, Uitdehaag BMJ, Polman CH, Geurts JJG, Barkhof F, Pouwels PJW, Vrenken H, Hillebrand A. Disruption of structural and functional networks in long-standing multiple sclerosis. *Hum Brain Mapp.* 2014 Jul 22.

Balk LJ, Oberwahrenbrock T, Uitdehaag BMJ, Petzold A. Physiological variation of retinal layer thickness is not caused by hydration: A randomised trial. *J Neurol Sci*. 2014 Jun 30.

Sonder JM, Balk LJ, van der Linden FAH, Bosma LVAE, Polman CH, Uitdehaag BMJ. Towards the use of proxy reports for estimating long term patient reported outcomes in multiple sclerosis. *Mult Scler.* 2014. In press.

Balk LJ, Steenwijk MD, Tewarie P, Daams M, Killestein J, Barkhof F, Polman CH, Uitdehaag BM, Petzold A. Bidirectional trans-synaptic axonal degeneration in the visual pathway in multiple sclerosis. *J Neurol Neurosurg Psychiatry*. 2014 Jun 27.

Schippling S*,Balk LJ*, Costello F*, Albrecht P, Balcer L, Calabresi P, Frederiksen JL, Frohman E, Green AJ, Klistorner A, Outteryck O, Paul F, Plant GT, Traber G, Vermersch P, Villoslada P, Wolf S, Petzold A. Quality control for retinal OCT in Multiple Sclerosis: Validation of the OSCAR-IB criteria. *Mult Scler.* 2014 Jun 16.

Daams M, Weiler F, Steenwijk MD, Hahn HK, Geurts JJG, Vrenken H, van Schijndel RA, Balk LJ, Tewarie P, Tillema J, Killestein J, Uitdehaag BMJ, Barkhof F. Mean upper cervical cord area (MUCCA) measurement in long-standing MS: relation to brain findings and clinical disability. *Mult Scler.* 2014 May 8.

Steenwijk MD, Daams M, Pouwels PJW, Balk LJ, Tewarie PK, Killestein J, Uitdehaag BMJ, Geurts JJG, Barkhof F, Vrenken H. What explains gray matter atrophy in long-standing multiple sclerosis? *Radiology.* 2014 Apr 23.

Sonder JM, Balk LJ, Bosma LVAE, Polman CH, Uitdehaag BMJ. Do patient and proxy agree? Long term changes in Multiple Sclerosis physical impact and walking ability on patient reported outcome scales. *Mult Scler.* 2014 Apr 7.

Balk LJ, Tewarie P, Killestein J, Polman CH, Uitdehaag BMJ, Petzold A. Disease course heterogeneity and OCT in multiple sclerosis. *Mult Scler*. 2014;20:1198-1206.

Balk LJ, Petzold A. Current and future potential of retinal OCT in Multiple Sclerosis with and without optic neuritis. *Neurodegener Dis Manag*. 2014;4:165-76.

Balk LJ, Twisk JW, Steenwijk MD, Daams M, Tewarie P, Killestein J, Uitdehaag BM, Polman CH, Petzold A. A dam for retrograde axonal degeneration in multiple sclerosis? *J Neurol Neurosurg Psychiatry*. 2014;85:7829.

Burggraaff MC, Trieu J, de Vries-Knoppert WA, Balk LJ, Petzold A. The clinical spectrum of microcystic macular oedema. *Invest Ophthalmol Vis Sci*. 2014;55:952-61.

Balk LJ, Mayer M, Uitdehaag BM, Petzold A. Retinal hyperaemia-related blood vessel artifacts are relevant to automated OCT layer segmentation. *J Neurol*. 2014;261:511-7.

Balk LJ, Mayer M, Uitdehaag BM, Petzold A. Physiological variation of segmented OCT retinal layer thicknesses is short-lasting. *J Neurol.* 2013;260:3109-14.

van Rossum JA, Vennegoor A, Balk LJ, Uitdehaag BM, Polman CH, Killestein J. Safety, anxiety and natalizumab continuation in JC virus-seropositive MS patients. *Mult Scler*. 2014;20:108-11.

Kearney H, Rocca MA, Valsasina P, Balk LJ, Sastre-Garriga J, Reinhardt J, Ruggieri S, Rovira A, Stippich C, Kappos L, Sprenger T, Tortorella P, Rovaris M, Gasperini C, Montalban X, Geurts JJ, Polman CH, Barkhof F, Filippi M, Altmann DR, Ciccarelli O, Miller DH, Chard DT. Magnetic resonance imaging correlates of physical disability in relapse onset multiple sclerosis of long disease duration. *Mult Scler*. 2014;20:7280.

Balk LJ, Petzold A. Influence of the eye-tracking-based follow-up function in retinal nerve fiber layer thickness using fourier-domain optical coherence tomography. *Invest Ophthalmol Vis Sci*. 2013;54:3045.

Kruger HS, Balk LJ, Viljoen M, Meyers TM. Positive association between dietary iron intake and iron status in HIV-infected children in Johannesburg, South Africa. *Nutr Res.* 2013;33:50-8.

Sombekke MH, Wattjes MP, Balk LJ, Nielsen JM, Vrenken H, Uitdehaag BM, Polman CH, Barkhof F. Spinal cord lesions in patients with clinically isolated syndrome: a powerful tool in diagnosis and prognosis. *Neurology.* 2013;80:69-75.

Balk LJ, de Vries-Knoppert WA, Petzold A. A simple sign for recognizing off-axis OCT measurement beam placement in the context of multicentre studies. *PLoS One*. 2012;7:e48222.

Balk LJ, Killestein J, Polman CH, Uitdehaag BM, Petzold A. Microcystic macular oedema confirmed, but not specific for multiple sclerosis. *Brain*. 2012;135:e226.

Vennegoor A, Rispens T, Strijbis EM, Seewann A, Uitdehaag BM, Balk LJ, Barkhof F, Polman CH, Wolbink G, Killestein J. Clinical relevance of serum natalizumab concentration and anti-natalizumab antibodies in multiple sclerosis. *Mult Scler.* 2013;19:593-600.

Tewarie P, Teunissen CE, Dijkstra CD, Heijnen DA, Vogt M, Balk LJ, Vrenken H, Polman CH, Killestein J. Cerebrospinal fluid anti-whole myelin antibodies are not correlated to magnetic resonance imaging activity in multiple sclerosis. *J Neuroimmunol*. 2012;251:103-6.

Tewarie P, Balk LJ, Costello F, Green A, Martin R, Schippling S, Petzold A. The OSCAR-IB consensus criteria for retinal OCT quality assessment. *PLoS One*. 2012;7:e34823.

Balk LJ, Sonder JM, Strijbis EM, Twisk JW, Killestein J, Uitdehaag BM, Polman CH, Petzold A. The physiological variation of the retinal nerve fiber layer thickness and macular volume in humans as assessed by spectral domain-optical coherence tomography. *Invest Ophthalmol Vis Sci*. 2012;53:1251-7.

Balk LJ, Hoekstra T, Twisk JW. Relationship between long-term coffee consumption and components of the metabolic syndrome: the Amsterdam Growth and Health Longitudinal Study. *Eur J Epidemiol.* 2009;24:2039.

AUTHOR AFFILIATIONS

P Albrecht

Department of Neurology, Heinrich-Heine University, Düsseldorf, Germany

LJ Balcer

Department of Ophthalmology, New York University School of Medicine, New York, USA

F Barkhof

Department of Radiology and Nuclear Medicine, VU University Medical Centre, Amsterdam, the Netherlands

PA Calabresi

Department of Neurology Johns Hopkins Hospital, Baltimore, Maryland, USA

F Costello

University of Calgary, Departments of Clinical Neurosciences and Surgery, Calgary, Alberta, Canada

M Daams

Department of Radiology and Nuclear medicine, VU University Medical Centre, Amsterdam, the Netherlands

Department of Anatomy and Neurosciences, section of Clinical Neuroscience, VU University Medical Center, Amsterdam, The Netherlands

JL Frederiksen

Department of Neurology, Glostrup Hospital, Copenhagen, Denmark

E Frohman

Departments of Neurology and Ophthalmology, University of Texas Southwestern Medical Center, Dallas, Texas, USA

AJ Green

Department of Neurology, University of California San Francisco, San Francisco, California, USA

J Killestein

Department of Neurology, VU University Medical Centre, Amsterdam, the Netherlands

A Klistorner

Department of Ophthalmology, Save Sight Institute, University of Sydney, Sydney, Australia

R Martin

Institute for Neuroimmunology and Clinical Multiple Sclerosis Research, University Medical Center Hamburg Eppendorf, Hamburg, Germany

M Mayer

Pattern Recognition Laboratory, University of Erlangen-Nuremberg, Erlangen, Germany

T Oberwahrenbrock

Department of Neurology, Charité University Medicine Berlin, Berlin, Germany

O Outteryck

Department of Neurology, University of Lille Nord de France, Lille, France

F Paul

Department of Neurology, Charité University Medicine Berlin, Berlin, Germany

A Petzold

Department of Neurology, VU University Medical Centre, Amsterdam, the Netherlands

Department of Neuroimmunology, UCL Institute of Neurology, London, UK

GT Plant

Department of Neuro-Ophthalmology, The National Hospital for Neurology and Neurosurgery, London, United Kingdom

CH Polman

Department of Neurology, VU University Medical Centre, Amsterdam, the Netherlands

S Schippling

Department of Neurology, University Hospital Zurich, Zurich, Switzerland

JM Sonder

Department of Neurology, VU University Medical Centre, Amsterdam, the Netherlands

MD Steenwijk

Department of Radiology and Nuclear Medicine, VU University Medical Centre, Amsterdam, the Netherlands

EMM Strijbis

Department of Neurology, VU University Medical Centre, Amsterdam, the Netherlands

Department of Anatomy and Neuroscience, Section of Clinical Neuroscience, VU University Medical Centre, Amsterdam, The Netherlands

P Tewarie

Department of Neurology, VU University Medical Centre, Amsterdam, the Netherlands

G Traber

Department of Ophthalmology, University Hospital Zurich, Zurich, Switzerland

JWR Twisk

Department of Clinical Epidemiology and Biostatistics, VU University Medical Centre, Amsterdam, The Netherlands

BMJ Uitdehaag

Department of Neurology, VU University Medical Centre, Amsterdam, the Netherlands

P Vermersch

Department of Neurology, University of Lille Nord de France, Lille, France

P Villoslada

Center for Neuroimmunology, Institute of Biomedical Research August Pi Sunyer, Hospital Clinic of Barcelona, Barcelona, Spain

H Vrenken

Department of Radiology and Nuclear Medicine, VU University Medical Centre, Amsterdam, the Netherlands

Department of Physics and Medical Technology, VU University Medical Center, Amsterdam, The Netherlands

WAEJ de Vries–Knoppert

Dept. of Ophthalmology, VU University Medical Centre, Amsterdam, The Netherlands

MP Wattjes

Department of Radiology and Nuclear Medicine, VU University Medical Centre, Amsterdam, the Netherlands

S Wolf

Department of Ophthalmology, Bern University Hospital and University of Bern, Switzerland

BIOGRAPHY

Lisanne Johanna Balk is geboren op 15 februari 1987 in Heemskerk. Na het afronden van haar VWO aan het Jac. P. Thijsse college te Castricum, besloot zij haar carrière als professioneel tennisster voort te zetten. Na enkele jaren in het internationale tenniscircuit heeft ze deze tennis carrière beëindigd en is zij in 2005 begonnen aan de bachelor gezondheidswetenschappen aan de Vrije Universiteit Amsterdam. Na het behalen van haar bachelor is zij aansluitend begonnen met de 2-jarige researchmaster 'Lifestyle and chronic disorders'. Tijdens het 1e jaar van de masteropleiding heeft ze onderzoek gedaan naar de effecten van ijzerinname bij HIVbesmette kinderen in Potchefstroom, Zuid-Afrika. Tijdens het 2e jaar van de master kwam ze voor een onderzoeksstage terecht bij het MS centrum van het VUmc Amsterdam. In 2010 behaalde zij cum laude haar master bul, waarna ze is gestart met haar promotieonderzoek bij het MS centrum van het VUmc, onder leiding van prof. dr. Uitdehaag, prof. dr. Polman en dr. A. Petzold. Het onderzoek dat is verricht gedurende dit promotietraject staat beschreven in dit proefschrift. Na haar promotie heeft ze haar onderzoek voortgezet als post-doc bij het MS centrum van het VUmc.

Lisanne Johanna Balk was born on February 15th 1987, in Heemskerk, the Netherlands. After finishing high school at the Jac. P. Thijsse college in Castricum, she pursued her career as a full-time professional tennis player. After playing on the international tour for several years, she ended her international tennis career and started a Bachelor in Health Sciences at the Vrije Universiteit Amsterdam. After obtaining her Bachelor degree, she started the 2-year research Master 'Lifestyle and Chronic Disorders'. During the first year of her Masters, she investigated the effects of iron intake in HIV infected children in Potchefstroom, South Africa. For her second internship she did a reliability study at the MS Centre of the VU Medical Centre Amsterdam. After she obtained her Master degree (cum laude) in 2010, she started her PhD at the MS Centre under supervision of prof. dr. Uitdehaag, prof. dr. Polman en dr. A. Petzold. The research she performed during her PhD is described in this dissertation. After completing her PhD in 2014, she continued as a post-doctoral researcher at the MS centre of the VU Medical Centre Amsterdam.